5-1-2015

Yeast V-ATPase Regulation by Phosphofructokinase-1

Chun-Yuan Chan

Chun-Yuan Chan
Candidate

Biomedical Sciences
Department

This dissertation is approved, and it is acceptable in quality and form for publication:

Approved by the Dissertation Committee:

Karlett J. Parra, PhD, Chairperson

Mary Ann Osley, PhD

William S. Garver, PhD

Samuel A. Lee, PhD

Yeast V-ATPase Regulation by Phosphofructokinase-1

BY

Chun-Yuan Chan

B.S. Marine resource and Biotechnology, National Sun Yet-Sen University

M.S. Biomedical Science, National Sun Yet-Sen University

DISSERTATION

Submitted in partial fulfillment of the
Requirements for the Degree of

Doctor of Philosophy
Biomedical Sciences

The University of New Mexico
Albuquerque, New Mexico

May 2015

Acknowledgements

First, I would like to thank Dr. Karlett J. Parra, my advisor and dissertation chair, for her intellectual insight and for shaping core ideas of the approach to science. She is pleasure to work with and provided support throughout my dissertation work.

I also thank my committee members, Dr. Mary Ann Osley, Dr. Samuel A. Lee, Dr. Williams Sherman Garver and Dr. Jun Chen for their valuable guidance and ideas to this study and assistance in my professional development.

I extend my gratitude to Dr. Leyma De Haro, Dr. Vera Michael, Dr. Summer Hayek, Dr. Colleen Fordyce, Dr. Marth Gram, MS. Yamhilette Licon, Shaba, and Eli for being a wonderful group of labmates that help me complete my dissertation work.

Last, I would like to thank my friends and family, in particular my girl friend Flora Chuang who provided support and encouragement through my dissertation.

Yeast V-ATPase Regulation by Phosphofructokinase-1

BY

Chun-Yuan Chan

B.S. Marine resource and Biotechnology, National Sun Yet-Sen University
M.S. Biomedical Science, National Sun Yet-Sen University
Ph.D. Biomedical Sciences, University of New Mexico, 2015

Abstract

V-ATPase is a vacuolar (lysosome-like) ATPase-dependent proton pump necessary for maintaining pH homeostasis in the organelles of the endomembrane system. It also contributes to regulation of the cytosol pH and the extracellular pH. In specialized cells (renal intercalated cells, epididymis clear cells, and osteoclasts), V-ATPase proton transport supports urinary acidification, sperm maturation, and bone resorption. Genetic mutations of V-ATPase expressed in those tissue-specific cells cause distal renal tubular acidosis, infertility, and osteopetrosis.

V-ATPases are composed of a peripheral domain (V_1), which hydrolyzes ATP, and a membrane-bound domain (V_o), which transports proton. V-ATPase activity is tightly regulated *in vivo* by numbers of mechanisms, including reversible disassembly of the V_1 and V_o domains. Glucose, the nutrient oxidized in glycolysis, modulates reversible dissociation of V-ATPase. This dissertation was aimed at understanding how subunits of phosphofructokinase-1 (α subunit and β subunit) regulate V-ATPase function. Our

results showed that both subunits are important for V-ATPase activity, but β subunit displayed more significant phenotypes. Deletion of β subunit reduced glucose-dependent V_1V_o reassembly and altered V-ATPase binding to its assembly factor, RAVE. We additionally investigated the mechanisms by which phosphofructokinase-1 controls V-ATPase function. We concluded that glucose-dependent V_1V_o reassembly and V-ATPase function at steady state were controlled by the glycolytic flux, independently of phosphofructokinase-1. Notably, V-ATPase activation *in vivo* correlated with the presence of phosphoglycerate kinase at vacuolar membranes. These studies further advanced our understanding how glucose controls V-ATPase pumps *in vivo*.

Table of contents

List of Figures

List of Tables

Chapter I

Introduction to the Vacuolar ATPase (V-ATPase)

1.1 Structure and function of the V-ATPase enzyme complex

V-ATPase, a vacuolar (lysosomal-like) ATP-dependent proton pump, is a highly conserved multi-subunit complex that hydrolyzes ATP to transport protons across the membrane (Forgac 2007). V-ATPase is responsible for maintaining the differential acidic pH of organelles throughout the endomembrane system. Regulation of the pH of the extracellular space, cytoplasm, and intracellular compartments is tightly linked to V-ATPase function (Forgac 2007). Cellular processes that require normal V-ATPase activity include endocytosis, membrane trafficking, membrane fusion, protein processing, autophagy, and proton-coupled transport of diverse nutrients and ions (Forgac 2007).

V-ATPase pumps are composed of 14 different subunits that comprise two domains: V_1 and V_o. V_1, the ATP-hydrolytic domain, is makeup of subunits A, B, C, D, E, F, G and H. V_o, the proton-translocation domain is makeup of subunits a, d, e, c, c' and c'' (Fig. 1), the subunit c' is found exclusively in fungi (Kane 2006). In the V_1 domain, three copies of subunit A and B comprise a hexamer structure in alternating arrangement. The interface of A and B subunits form three catalytic sites to hydrolyze ATP and the subunit A is mainly responsible for ATP binding and hydrolysis. There are three ATP hydrolytic

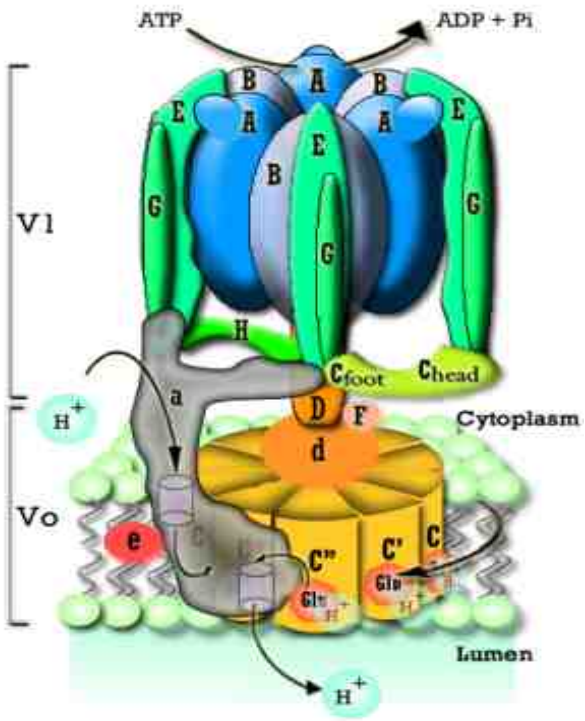

Figure 1. Structure of the yeast V-ATPase complex. The V-ATPase is composed of 14 different subunits and contains two major domains: The V_1 complex (A, B, C, D, E, F, G, H) is responsible for ATP hydrolysis and the V_o complex (c, c', c'', a, d, e) translocate protons across the lipid bilayer by a rotary mechanism. The mechanism of proton transport through V_o. Protons binds to an Arg residue of subunit a (shown in grey) that transfers the proton to a Glu residue of c, c' and c'' subunits in the proteolipid ring (shown in yellow) by passing through a hemi-channel of subunit a. After the V_1 domain hydrolyzes ATPs, the rotation of the c-ring releases protons into the lumen.

sites located in subunit A. Three noncatalytic nucleotide-binding sites (interacting with ATP but do not direct catalyze) in subunit B appear to play a regulatory role (Vasilyeva, Liu et al. 2000) (MacLeod, Vasilyeva et al. 1999). The subunits E and G form three peripheral stalks attached to subunit B that assist binding the hexamer to V_o. The subunits D and F are localized in the center of A_3B_3. Subunits D and F also connect the catalytic hexamer to V_o at the membrane by forming a central stalk. The central stalk not only connect the V_1 and V_o domains but also is involved in a rotary mechanism by which V-ATPase couples ATP hydrolysis and active proton transport. The V_1 subunits H and C have regulatory roles, as they modulate V-ATPase function by a mechanism involving V_1V_o reversible disassembly (see Chapter 1.2.3). There are two forms of V_1 in cells: cytosolic V_1 without V_o and V_1 attached to V_o at membranes.

In the V_o domain, the c, c' and c'' proteolipid subunits containing highly hydrophobic amino acids form a ring structure, which translocates protons through the membrane (Wilkens and Forgac 2001). A Glu residue at one transmembrane helix of each proteolipid subunit undergoes reversible protonation. Protonation and deprotonation involves a rotary mechanism that passes protons across the membrane (Nishi and Forgac 2002). Another important subunit, subunit a, interfaces with the c ring structure. It contains a highly hydrophilic N-terminal domain and a C-terminal transmembrane domain (Nishi and Forgac 2002). The N-terminal domain of subunit a faces the cytosolic space, while the C-terminal domain is mainly localized in the membrane. Subunit a has an Arg residue that participates in proton transport (Forgac 2007). Subunit d is the only soluble subunit of V_o. It sits on the top of the c ring structure and functions to connect the

central stalk of V_1 and the proteolipid c subunits of V_o (Drory, Frolow et al. 2004). There is another highly hydrophobic subunit, subunit e, that is localized in the membrane and the function of this subunit is still unclear (Sambade and Kane 2004). As showing Figure 1, V_1 contains three copies of the catalytic hexamer subunits A and B, and the stator (peripheral stalk) subunits E and G, one copy of the regulatory subunits C and H, and one copy of the central stator subunits D and F (Ohira, Smardon et al. 2006); Lee, Lee et al. (2014).

V-ATPase proton transport sustains pH homeostasis and energizes cellular membranes, because it activates secondary transport systems including nutrients and ions (Forgac 2007). V-ATPase-mediated pH homeostasis controls the pH of intracellular compartments, the cytoplasm, and the extracellular environment (Forgac 2007). The acidification of the Golgi Apparatus, endosomes and lysosomes by V-ATPase is required for fundamental cellular processes, including endocytosis, membrane trafficking and fusion, protein processing, and autophagy (Forgac 2007). Since V-ATPase transports cytosolic protons into the organelle lumen, and/or outside the cells, V-ATPase also sustains the cytosolic pH homeostasis. Proton secretion by plasma membrane associated V-ATPase pumps in specialized cells, such as the kidney α-intercalated cells and bone osteoclasts, maintain the systemic acid-base balance and bone resorption, respectively (Breton and Brown 2007).

1.2 Regulation of the V-ATPase complex

V-ATPase function is crucial for numerous and fundamental processes, and its activity is precisely and efficiently controlled by multiple stimuli and signaling pathways. V-ATPase activity is regulated by reversible disassembly of V_1 and V_o (Kane 1995), reversible disulfide-bond formation at the catalytic sites (Feng and Forgac 1992; Feng and Forgac 1994), modification of the number of protons transported per ATP hydrolyzed (coupling efficiency) (Muller, Jensen et al. 1999; Muller and Taiz 2002), changes in V-ATPase membrane localization (Toyomura, Murata et al. 2003), protein density (Hinton, Bond et al. 2009) and post-translational modifications (Kane 2006; Forgac 2007; Alzamora, Thali et al. 2010; Hughes and Gottschling 2012; Lee, Lee et al. 2014; Parra, Chan et al. 2014). In the following sections, the details of each regulatory mechanism will be discussed.

1.2.1 Control of V-ATPase coupling efficiency.

In order to transport protons the V-ATPase needs to hydrolyze ATP as energy**.** The coupling efficiency relates to each ATP per proton transport across the membrane**.** Various degrees of coupling efficiency between ATPase hydrolysis and proton transport have been proposed to regulate the acidification of intracellular compartments in mammalian cells (Nishi and Forgac 2002; Nelson 2003). Several biochemical studies support this idea (Moriyama and Nelson 1988; Arai, Pink et al. 1989; Owegi, Pappas et al.

2006; Ediger, Melman et al. 2009). This suggests that the coupling efficiency of V-ATPase acts an important regulatory model for cellular pH homeostasis.

It has been shown V-ATPase functional coupling can be controlled by the concentration of its substrate, ATP. In bovine clathrin-coated vesicles, the V-ATPase coupling rate is reduced at ATP concentrations greater than 0.3mM (Arai, Pink et al. 1989). The coupling efficiency in the lemon fruit is responsible for the steep vacuolar pH gradient, compared to other parts of the plant (Muller, Jensen et al. 1999). V-ATPase coupling efficiency is determined by citrate (stored in vacuolar lumen) and malate (in the vacuole) concentrations (high concentration increasing the coupling efficiency) in the lemon tree (Muller and Taiz 2002). The lemon fruit cells that generate more organic acids have higher levels of citrate and malate in the vacuole, suggesting that intracellular metabolites can modulate V-ATPase activity by modulating the number of protons transported per ATP hydrolyzed. Our studies (Chapter II) suggest that phsphofructokinase-1 can control V-ATPase proton transport *in vivo* in yeast, but whether it involves coupling alterations has yet to be determined.

Differences in coupling efficiency can be dictated by the V-ATPase subunit isoforms assembled in different membranes. In eukaryotic cells, different isoforms of V-ATPase subunits can be membrane-specific and cell-specific. Different combinations of subunit isforms may have different coupling capacity. In fungi, there are only two isoforms of subunit a (Vph1p at the vacuolar membrane and Stv1p at the Golgi Apparatus membrane).

The yeast Golgi V-ATPase pumps exhibit lower coupling ratios than the vacuolar V-ATPase pumps (Kawasaki-Nishi, Nishi et al. 2001). Thus, the two yeast V-ATPase subunit isoforms control coupling efficiency according to the pH requirement in different organelles. Higher eukaryotic cells have more isoforms of subunit a and various V-ATPase subunits that fulfill different functions in specific cells.

Structure and function studies are shedding light on the mechanism by which coupling efficiency may be changed. Site-directed mutations of conserved amino acids have revealed a coupling role a domain of the V_1 catalytic subunit A (non-homoloous domain (Shao, Nishi et al. 2003; Shao and Forgac 2004) and the central stalk V_o subunit d (Owegi, Pappas et al. 2006). While the mutations P217V in V_1 subunit A and F94A in V_o subunit d reduced coupling efficiency, other mutations in V_1 subunit A (P223V and P233V) and V_o subunit d (D217A, D261A E317A and E329A) increased the coupling ratio of proton transported per ATP hydrolyzed. These studies indicate that different coupling states may occur to adjust the proton transport by either up-regulating or down-regulating the ratio proton : ATP. Overexpression of the regulatory V_1 subunit H displays an uncoupling phenotype, which prevents proton transport without significantly decreasing ATP hydrolysis. These results suggest that subunit H is also involved in tuning the coupling efficiency, in addition to regulating the V-ATPase (Keenan Curtis and Kane 2002). However, the mechanism(s) involved in the regulation of coupling efficiency *in vivo* are still elusive.

1.2.2 Modulation of reversible disulfide bond formation at the catalytic site.

V-ATPase regulation by disulfide bond formation between conserved Cys residues in the catalytic sites of V_1 subunit A (Cys-261 and Cys-539) has been proposed in yeast. Formation of the disulfide bond inactivates V-ATPase by blocking ATP hydrolysis (Feng and Forgac 1992; Feng and Forgac 1992). The disulfide bond can be broken by changing other cysteine residue in the subunit A, suggesting that different pairs of disulfide bonds of subunit A control V-ATPase activity (Feng and Forgac 1994). It has also been shown that *cys4Δ* cells, which lack of the gene *CYS4* responsible for synthesis of cystathionine in the first step of cysteine biosynthesis, display a vacuolar membrane ATPase (*Vma-*) growth phenotype (sensitivity to alkaline pH), suggestive of malfunction of V-ATPase. It has been proposed that *cys4* mutant cells display a reduction in glutathione levels (redox state), which leads to a generalized more reduced cellular state and affects Cys-Cys formation in the catalytic sites. Accordingly, decreased glutathione levels and mutations at the conserved cysteine residue of the catalytic site of V_1 subunit A partially suppress the *Vma*$^-$ growth defects of *cys4Δ* cells (Oluwatosin and Kane 1997). This type of reversible disulfide bond formation in V_1 subunit A has also been found in other organisms. However, in plant cells the disulfide bridge (Cys 134 and Cys 186) is localized in the V_1 subunit E (Gruber, Radermacher et al. 2000). Together these studies suggest that the redox state of the cytoplasm can regulate V-ATPase activity via reversible disulfide bond formation in the catalytic sites of the yeast V-ATPase complex.

1.2.3 Regulation of V-ATPase activity by reversible V_1V_o dissociation.

An important mechanism that regulates V-ATPase is its reversible dissociation, which controls the level of V_1V_o assembly in a cell. This process was first described in yeast and insects (Kane 1995; Sumner, Dow et al. 1995). It also has been shown that V-ATPase activity is modulated through disassembly and reassembly in mammalian cells (Trombetta, Ebersold et al. 2003; Nakamura 2004), suggesting that reversible disassembly of V_1V_o is a conserved mechanism from yeast to mammals.

During disassembly, the peripheral domain V_1 (except subunit C) and V_1 subunit C detach from the integral membrane domain V_o. Disassembly adjusts the amount of functional V_1V_o complexes in response low glucose and other extracellular signals (Fig. 2). This response occurs in less than 5 minutes without new protein synthesis (Kane 1995). The V_1 subunit C, V_1 (in the cytosol) and V_o (at the membrane) stay intact during dissociation and re-associate upon glucose re-addition and other extracellular stimulations in less than 5 minutes. The V_1 subunit C, which localizes at the interface between the V_1 and V_o subcomplexes, is required for controlling the assembly of V-ATPase (Drory, Frolow et al. 2004; Inoue and Forgac 2005). However, overexpression of subunit C decreases V-ATPase activity without changing assembly of V-ATPase, suggesting that subunit C may also be involved in other regulatory mechanism (Keenan Curtis and Kane 2002). Additionally, to prevent unnecessary ATP hydrolysis and leakage of protons conformational changes in V_1 subunit H and V_o subunit a, respectively, silence free V_1

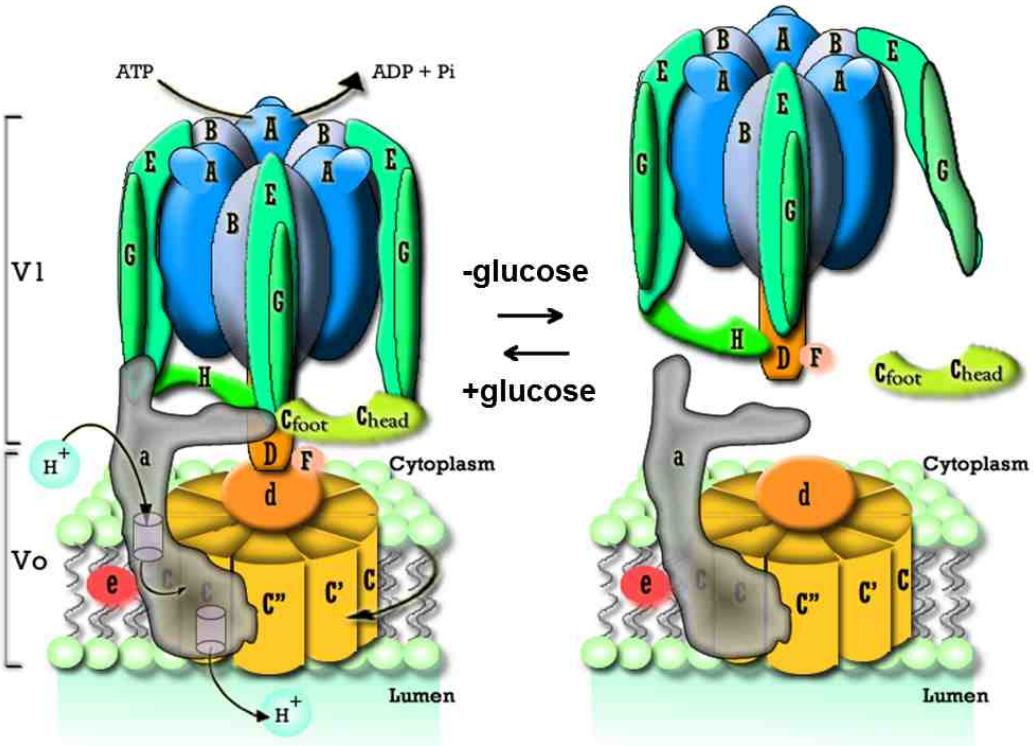

Figure 2. Glucose dependent reversible disassembly. V-ATPases can reversibly dissociate into V_1 (-C), V_o, and the C subunit. In yeast and kidney cells, glucose removal triggers dissociation, and this process is reversible upon glucose re-addition. This process does not require new protein to be synthesized and is a quick response to environmental changes. The dissociation of V-ATPase prevents proton transport and ATP hydrolysis under low glucose (energy) conditions preserving energy for cells. During dissociation, conformational changes occur in V_1H to avoid non-functional ATP hydrolysis and leakage of protons through the membrane.

and V_o (Parra, Keenan et al. 2000; Wilkens and Forgac 2001; Qi and Forgac 2008) (Figure 2).

Glucose changes constitute a major trigger of V_1V_o disassembly and reassembly (Toei, Saum et al. 2010; Kane 2012), which appears to involve diverse mechanisms and signaling pathways (described below). Disassembly is a fast and effective mechanism to regulate V-ATPase activity, which is crucial for preserving cellular ATP level when glucose is limiting. Free V_1 cannot hydrolyze ATP during glucose depletion (low energy status). The V_1V_o reversible disassembly is a response to acute and chronic changes in growth environments, assisting cells to adapt to stress. The PI3 Kinase activity that phosphorylates the hydroxyl group of phosphatidylinositols at membranes is also involved in glucose-induced V_1V_o reassembly in the kidney cells (Nakamura 2004; Sautin, Lu et al. 2005). This enzyme probably changes the lipid compositions of membrane, which affects the V_1V_o assembly state. In yeast cells, mutants of PI3 kinase or PI(3P) 5-kinase, Fab1, also increase the vacuolar pH, suggesting that reversible disassembly is also sensitive to the membrane composition (Weisman 2003).

Other extracellular stimuli, such as extracellular pH (Padilla-Lopez and Pearce 2006; Diakov and Kane 2010) and osmotic stress (Li, Diakov et al. 2012), also modulate V-ATPase assembly. In yeast, V_1V_o dissociation resulting from glucose depletion is suppressed at alkaline extracellular pH (higher than pH=7.0), which also enhances V-ATPase activity in isolated vacuolar membranes (Diakov and Kane 2010). An adaption

to hyperosmotic stress is an increase in V_1V_o assembly that in turn activates V-ATPase, because V-ATPase and the high-osmolarity glycerol (HOG) pathway work in parallel as cellular detoxification mechanisms (Li, Diakov et al. 2012). The signaling lipid phosphatidylinositol 3,5-bisphosphate (PI(3,5)P2) regulates salt-induced V_1V_o assembly (high osmotic stress). In general, the phosphoinositides act as signaling molecules by recruiting effectors from the cytosol to control assembly and/or activate nearby proteins (DeCamilli, Emr et al. 1996; Strahl and Thorner 2007). As more PI(3,5)P2 is present at the membrane, more Vph1p (subunit a) is recruited to the vacuolar membrane. The binding between Vph1 and PI(3,5)PI stabilizes V_1V_o assembly and enhances V-ATPase activity (Li, Diakov et al. 2014).

An assembly complex in yeast, RAVE (Regulator of ATPase of Vacuole and Endosome), is necessary for V_1V_o reassembly in response to glucose (Seol, Shevchenko et al. 2001; Smardon, Tarsio et al. 2002; Smardon and Kane 2007; Smardon, Diab et al. 2014). The RAVE complex is composed of three proteins, Rav1p, Rav2p and Skp1p (Seol, Shevchenko et al. 2001). The Rav1p and Rav2p subunits are essential for glucose-induced V_1V_o reassembly and for biosynthetic assembly of V_1V_o (Smardon, Tarsio et al. 2002; Smardon and Kane 2007). Deletion of *RAV1* and *RAV2* prevented growth on alkaline pH media containing calcium at millimolar concentrations when exposed to 37°C (Seol, Shevchenko et al. 2001). However, this *Vma*$^-$ phenotype was partial because the cells grew on pH 7.5 plates. Partial *Vma*$^-$ growth phenotype suggests that the RAVE complex may cooperate with other regulatory factors to control V-ATPase or another parallel pathway may be involved. However, a later study showed that RAVE is a

chaperone exclusive for Vph1p-containing V-ATPase complexes (Smardon, Diab et al. 2014). As a result V_1V_o complexes containing Stv1p remained intact in the RAVE mutants, which caused the partial *Vma*⁻ growth defect.

As expected, non-acidic vacuoles were present in RAVE deficient cells. Vacuolar staining by the pH sensitive dye, quinacrine was absence at 37ºC (Seol, Shevchenko et al. 2001), suggesting that loss of function of V-ATPase happened after *RAV1* and *RAV2* deletion. The roles of the subunit Skp1p in RAVE function are not clear. Skp1p is best known for its function as a component of the SCF (Skp1-cullin-F-box) E3 ubiquitin ligase, but the RAVE complex containing Skp1 does not function as ubiquitin ligase (Seol, Shevchenko et al. 2001).

The RAVE complex most likely functions as a chaperone that facilitates V_1V_o assembly (Kane 2012). RAVE not only binds to cytosolic V_1, through interactions with V_1 subunits E and G (Smardon and Kane 2007) but also the N-terminal domain of Vph1 (Smardon, Diab et al. 2014). However, RAVE is not the glucose sensor because the interaction between V_1 and RAVE is not glucose dependent; stable V_1-RAVE complexes are formed if V_1 is constitutively present in the cytosol. The *vma3Δ* strain, which lacks V_o complexes and only contains cytosolic V_1 has stable cytosolic V_1-RAVE complexes independent of the extracellular glucose levels (Smardon and Kane 2007).

The V_1 subunit C, which dissociates from V_1 and V_o upon disassembly, also binds to the RAVE complex (Smardon and Kane 2007). The crystal structure of the C subunit reveals two globular domains, C_{head} and $C_{foot,}$ connected by a flexible helix structure (Drory, Frolow et al. 2004). During reassembly, these two domains bind to different EG heterodimers with different affinity (Oot and Wilkens 2010), as V_1 subunit C re-associates with V_1 and V_o to form active V_1V_o complexes (Kane 1995). Deletion of V_1 subunit C resembles the assembly phenotype of RAVE mutants (Smardon and Kane 2007), suggesting that V_1 subunit C-RAVE binding may also be involved in RAVE-dependent regulation of V_1V_o biosynthetic assembly. The deletion of RAVE complexes, like the deletion of V_1 subunit C, leads to unstable and inactive V_1V_o structures (Smardon and Kane 2007). RAVE bound to V_1 and V_1 subunit C may play a docking role to assist the peripheral stalk to re-attach onto V_o domain at the vacuolar membrane. In order to reassemble subunit C into V_1V_o, structural stress between C and one of the three EG dimers occurs (Fig. 1) (Oot, Huang et al. 2012). Meanwhile, the RAVE complex appears to be the only assembly factor in V_1V_o reassembly (Parra, Chan et al. 2014).

Glucose regulation of V_1V_o is intertwined with glycolysis. There is evidence that glucose-dependent reversible disassembly is not an all-or-none response. In yeast, the level of V_1V_o assembly is dictated by the concentration of glucose in the media (Parra and Kane 1998) with increasing concentrations of glucose gradually increasing V_1V_o reassembly. Thus, the glucose level fine-tunes V-ATPase activity by changing the V_1V_o assembly state. A phosphoglucose isomerase (*pgi1*) deficient mutant strain, which cannot convert glucose-6-phosphate into fructose-6-phosphate fails to reassemble V_1V_o in response to

glucose. However, *pgi1* supports V_1V_o reassembly after addition of fructose (Parra and Kane 1998). This suggests that glucose metabolism through glycolysis is required for reversible disassembly.

Some glycolytic enzymes are involved in V_1V_o reassembly. The V_1V_o complexes interact with the glycolytic enzymes aldolase, phosphofructokinase-1 and GAPDH (Lu, Holliday et al. 2001; Su, Zhou et al. 2003; Lu, Sautin et al. 2004; Lu, Ammar et al. 2007; Su, Blake-Palmer et al. 2008; Chan and Parra 2014). The binding between aldolase and V_1 subunits B and E and V_o subunit a is glucose-dependent; disruption of these interactions causes V_1V_o dissociation. Aldolase mutants (R303W and H108A) that abolish its catalytic function *in vitro* do not affect V-ATPase assembly and function (Lu, Ammar et al. 2007), suggesting that aldolase-V-ATPase binding is required for V-ATPase function but not aldolase enzymatic activity. Notably, those experiemnts were performed *in vitro* in isolated vacuolar membranes in which excess ATP was added to the reactions. *In vivo,* decreased glycolytic-ATP in the aldolase mutants may affect V-ATPase function. Lu et al. have shown that V_1 subunit B and GAPDH co-immunoprecipitate from purified yeast vacuolar membranes, suggesting that GAPDH interacts with the V-ATPase complex as well.

The human phosphofructokinase-1 enzyme interacts with C-terminus of the V_o subunit isoform a4 (isoform experessed in α-intercalated cells) and a1 (ubiquitously expressed isoform) in kidney cells (Su, Zhou et al. 2003). Mutations of the renal V-ATPase V_o

subunit a isoform a4 (G820R) alter its interactions with human phosphofructokinase-1and caused distal renal tubular acidosis (dRTA) in human. Phosphofructokinase-1 catalyzes a rate-limiting reaction in glycolysis and constitutes an important regulatory step that integrates main energy metabolic pathways (glycolysis, Krebs Cycle, and lipid metabolism). Together these studies support the concept that glycolytic enzymes can form a super-complex with V-ATPase at the vacuolar membrane. It is possible that this super-complex plays a role as the glucose sensor. Another possibility is that the super-complex locally makes glycolytic-ATP for use in proton transport by V-ATPase. However, to make glycolytic ATP, the phosphoglycerate kinase enzyme has to be present at the vacuolar membrane to activate V-ATPase. Chapter III describes Pgk1p presence at vacuolar membranes, suggestive of the concept that locally made glycolytic-ATP may be coupled to V-ATPase proton transport.

Protein kinase A (PKA) modulates various cellular functions, including energy metabolism, glucose sensing and osmotic shock tolerance (Estruch 2000; Norbeck and Blomberg 2000; Santangelo 2006). PKA is involved also in V_1V_o reversible disassembly in yeast and insects (Bond and Forgac 2008; Tiburcy, Beyenbach et al. 2013). In this glucose-sensing pathway, glucose induces PKA to hyperphosphorylate the RGT1 gene, which represses the genes HXTs (glucose transporters) and HXK2 (hexokinase that phosphorylates glucose in the first step of glycolysis. Yeast mutants that stimulate PKA activity and increase cAMP levels (*ira1Δ*, *ira2Δ*, and $RAS2^{val19}$) result in defective disassembly of the V-ATPase under glucose starvation (Bond and Forgac 2008). This suggests that the PKA pathway regulates glucose-dependent V_1V_o assembly in yeast. An

independent study indicates that glucose-dependent V_1V_o reassembly functions upstream of the PKA pathway (Dechant, Binda et al. 2010). Although at first these two studies appear contradictory, we have considered the possibility that the PKA pathway and V_1V_o reassembly could influence each other by a positive feedback mechanism (Parra, Chan et al. 2014).

Lastly, cytosolic pH changes has been shown to modulate V_1V_o assembly in response to glucose (Dechant, Binda et al. 2010). It has been proposed that cytosolic pH could act as a second messenger that controls glucose-dependent reversible disassembly (Dechant, Binda et al. 2010; Dechant and Peter 2011). The authors believe that rapid changes in the cytosol pH are caused by glucose metabolism and that V-ATPase senses the level of protons in the cytosol to control the levels of V_1V_o assembly. In this model, glucose depletion leads to low cytosol pH that triggers V_1 dissociation from V_o; increased cytosol pH caused by glucose re-addition leads V_1V_o reassembly (Dechant, Binda et al. 2010).

1.3 Rationale for dissertation studies.

Glucose-dependent V_1V_o disassembly is an universal mechanism to rapidly and efficiently control V-ATPase function in different cells types and organisms (Kane 2012). Independent studies have shown that glycolysis controls V-ATPase assembly (Parra and Kane 1998). The glycolytic enzyme phosphofructokinase-1 catalyzes an important regulatory step in the glycolytic pathway, suggesting that phosphofructokinase-1 function may influence V-ATPase function. Additionally, human phosphofructokinase-1 binds to

the C-terminal domain of the V_o subunit a4 of V-ATPase, and mutants of a4 that block this interaction cause dRTA. Perhaps binding of phosphofructokinase-1 to V-ATPase, is required for V-ATPase function (Su, Zhou et al. 2003; Su, Blake-Palmer et al. 2008). Chapters II and III provided new insights into the mechanisms by which organisms regulate V-ATPase in response to glucose.

We studied the role of the yeast phosphofructokinase-1 subunits separately, Pfk1p (α subunit) and Pfk2p (β subunit). The reasons why we analyzed the interrelation of individual subunits of yeast phosphofructokinase-1 and V-ATPase function are based on several results from previous studies. First, Su et al. showed that human phosphofructokinase-1 (muscle isoform) interacts with V-ATPase and that yeast phosphofructokinase-1 co-immunoprecipitated with V-ATPase (Su, Blake-Palmer et al. 2008). However, the authors did not specify which phosphofructokinase-1 subunit binds to V-ATPase. We asked whether both subunits of the yeast phosphofructokinase-1 enzyme interact with V-ATPase and play the same role in controlling V-ATPase function. Second, the double deletion strain, *pfk1Δ pfk2Δ,* was used in those studies. The *pfk1Δ pfk2Δ* strain cannot utilize glucose or grow on media containing glucose as the sole carbon source (Arvanitidis and Heinisch 1994). The blockage of glycolysis and several glucose-dependent signals may mask the effects of Pfk1p and Pfk2p in regulating V-ATPase activity in this strain. However, strains carrying individual deletions of the yeast genes encoding phosphofructokinase-1 subunits can metabolize glucose, which makes the single deletion strains suitable for our studies. Third, the authors maintained the

pfk1Δ pfk2Δ strain in 0.2% glucose media instead of 2% glucose, but at this low level of glucose only 20~30% V_1V_o assembly could be sustained (Parra and Kane 1998). This low level of assembly at steady state makes difficult to determine whether defective V-ATPase function is caused by reduced assembly or defective interactions between phosphofructokinase-1 and V-ATPase. Finally, the human a4 subunit mutants (G820R and G807) lack V-ATPase activity (Su, Blake-Palmer et al. 2008). Those mutants may not only block phosphofructokinase-1 and V-ATPase binding but also affect V-ATPase structure and activity, independently of phosphofructokinase-1. This dissertation examined the phenotypes of phosphofructokinase subunit single deletion yeast strains (*pfk1Δ* and *pfk2Δ*); they are appropriate for studying the interplay between phosphofructokinase-1 and V-ATPase.

The first part of this dissertation describes *in vivo* and *in vitro* studies designed to evaluate how each subunit of the yeast phosphofructokinase-1 enzyme regulates V-ATPase function and assembly. The results of this work indicated that subunits Pfk1p and Pfk2p are necessary for V-ATPase –mediated vacuolar acidification and pH homeostasis *in vivo*. Only Pfk2p is necessary for glucose-dependent V_1V_o reassembly and normal Rav1p-V_1 interaction. The details of this work are described in Chapter II and in a published reference (Chan and Parra 2014).

The second part of this dissertation characterizes the mechanism by which yeast phosphofrctokinase-1 subunit Pfk2p controls V-ATPase function and V_1V_o reassembly in

response to glucose. We showed that defective V_1V_o reassembly in cells lacking the *PFK2* gene (*pfk2Δ*) can be rescued by increasing the concentration of glucose in the growth media from 2% (normal yeast media concentration) to 4% glucose. Since our studies also suggested that the glycolytic flow was increased in *pfk2Δ* cells exposed to 4% glucose, we proposed that V-ATPase reassembly is controlled by glycolytic flow *in vivo*. Notably, these results showed that the phosphofructokinase-1 subunits *PFK1* or *PFK2* are dispensable for V_1V_o reversible disassembly. These studies also suggest that glucose-dependent V-ATPase-mediated vacuolar acidification (no reassembly) can be controlled by additional factors such as the level of Pgk1 at the vacuolar membrane. Thus, we concluded that reassembly and reactivation are independently controlled events. The details of this work are described in Chapter III. In Chapter IV, conclusions and future directions are presented.

Chapter II

*Yeast Phosphofructokinase-1 Subunit Pfk2p is Necessary for pH Homeostasis and Glucose-Dependent V-ATPase Reassembly**

Chun-Yuan Chan[1] and Karlett J. Parra[1§]

From the [1]Department of Biochemistry and Molecular Biology of the School of Medicine, University of New Mexico Health Sciences Center, Albuquerque, New Mexico 87131

*Running title**:** *Phosphofructokinase-1 Subunits and V-ATPase Function*

[§]To whom correspondence should be addressed: Karlett J. Parra, Department of Biochemistry and Molecular Biology, University of New Mexico, MSC08 4670, Albuquerque, NM 87131. Tel: (505) 272-1633; Fax: (505) 272-6587; Email: kjparra@salud.unm.edu

Keywords: vacuolar ATPase, V-ATPase, V_1V_o-ATPase, yeast, *Saccharomyces cerevisiae,* vacuole, vacuolar acidification; phosphofructokinase-1, RAVE, glucose.

Published in The *Journal of Biological Chemistry*

May, 2014

2.1 Introduction

The vacuolar ATP-dependent proton pump, V- ATPase[2], is a highly conserved protein complex that maintains pH homeostasis and energizes membranes in all eukaryotic cells (Kane 2006); Forgac (2007). V-ATPase is distributed throughout the endomembrane system and V-ATPase mediated proton transport is required for receptor-mediated endocytosis, protein sorting and processing, and vacuolar and lysosomal functions (Kane 2006; Forgac 2007). Cells specialized for active proton secretion such as kidney-intercalated cells, clear cells of the epididymis, and bone osteoclasts, also have V-ATPase pumps on the plasma membrane. Plasma membrane associated V-ATPases lower the extracellular pH and are necessary for maintenance (Breton and Brown 2013), sperm maturation (Breton and Brown 2013), and bone resorption (Sobacchi, Frattini et al. 2001), respectively.

V-ATPases operate as molecular motors that use mechanical rotation of subunits to couple ATP hydrolysis and proton transport. Composed of 14 different subunits, V-ATPases are organized into two domains, V_1 and V_o. Eight subunits (named A-H) form the ATP-hydrolyzing domain (V_1) that is peripherally attached to the cytosolic side of the membrane. Six subunits (named a, c, c', c" d, and e) form the proton-translocating domain (V_o), which is embedded in the membrane (Sun-Wada, Wada et al. 2003; Forgac 2007; Muench, Trinick et al. 2011).

An important regulatory mechanism that controls V-ATPase activity *in vivo* is its reversible disassembly. Yeast (Kane 1995; Sumner, Dow et al. 1995; Kane 2006), insects (Sumner, Dow et al. 1995; Voss, Vitavska et al. 2007; Tiburcy, Beyenbach et al. 2013), and mammalian (Trombetta, Ebersold et al. 2003; Liberman, Bond et al. 2014) cells disassemble and reassemble V_1V_o complexes to reversibly inhibit V-ATPase proton transport. Disassembly stops ATP hydrolysis and ceases organelle acidification. The V-ATPase complexes separate into three parts: V_1 subunit C, V_1 (without subunit C), and V_o (Kane 1995; Kane and Parra 2000). Reassembly, which entails rapid re-association of these three components, restores V-ATPase catalytic activity.

At steady state, when glucose is abundant, cells contain assembled and disassembled V-ATPase pumps (Kane 1995; Parra and Kane 1998); about 70% of the pumps are assembled into V_1V_o complexes. The ratio of assembled to disassembled V-ATPases is dynamic and responds to variations in glucose concentration. Glucose removal leads to V_1V_o disassembly, which helps reserve energy when glucose is limiting. Once energy is restored, after glucose re-addition, V_1V_o reassembles (PM. 2006).

It has been proposed that V-ATPase pumps are structurally primed to disassemble, so that disassembly occurs easily and promptly when energy is low (Oot, Huang et al. 2012; Stewart and Stock 2012). However, V_1V_o reassembly may require some form of energy (e.g., ATP) to introduce structural changes necessary to reform the subunit-subunit interactions in V_1V_o complexes.

Reassembly is facilitated by a V-ATPase exclusive assembly factor in yeast, the Regulator of ATPase of Vacuoles and Endosomes (RAVE) complex (Seol, Shevchenko et al. 2001; Kane and Smardon 2003). The RAVE complex consists of three subunits, Skp1p, Rav1p, and Rav2p; Rav1p aids in the re-association of cytosolic V_1 with V_o at the membrane (Smardon, Tarsio et al. 2002; Smardon and Kane 2007; Smardon, Diab et al. 2014). Although the mechanisms involved in yeast reversible disassembly remain elusive, components of the glycolytic pathway and Ras/cAMP/PKA pathway are involved (Parra and Kane 1998; Bond and Forgac 2008). The cytosol and extracellular pH also have been shown to affect yeast V-ATPase reassembly in response to glucose (Dechant, Binda et al. 2010; Diakov and Kane 2010).

Glycolytic enzymes interact with V-ATPase and may functionally couple glycolytic ATP production and V-ATPase proton transport (Lu, Holliday et al. 2001; Peters, Bayer et al. 2001; Su, Zhou et al. 2003; Lu, Ammar et al. 2007; Su, Blake-Palmer et al. 2008). There is evidence that glycolysis itself could regulate yeast V_1V_o reassembly and/or V-ATPase activity (Parra and Kane 1998). First, reassembly can be triggered by fructose and mannose that are rapidly fermentable sugars like glucose. Second, glucose oxidation beyond glucose-6 phosphate formation is required for reassembly. Third, the ratio of assembled to disassembled V-ATPase pumps gradually increases as the glucose concentration increases, indicating that reversible disassembly is not an all-or-none response.

The interplay between glycolysis and V-ATPase is conserved; it has been described in renal epithelial cells (Sautin, Lu et al. 2005), viral infections (Kohio and Adamson 2013), and the metabolic switch in cancers (Avnet, Di Pompo et al. 2013; Fogarty, O'Keeffe et al. 2013). Two glycolytic enzymes can modulate the V-ATPase function, aldolase and phosphofructokinase-1. Aldolase associates with yeast (Lu, Holliday et al. 2001; Lu, Sautin et al. 2004; Lu, Ammar et al. 2007), plant (Konishi, Yamane et al. 2004), and mammalian (Merkulova, Hurtado-Lorenzo et al. 2011) V-ATPases. The interaction with aldolase is glucose-dependent in yeast and necessary for stable V_1V_o assembly. Phosphofructokinase-1 interacts with V-ATPase in vacuolar membranes and directly binds to V-ATPase V_o subunit a *in vitro* (Su, Zhou et al. 2003; Su, Blake-Palmer et al. 2008). Phosphofructokinase-1 also co-localizes with the V-ATPase V_o subunit a isoform a4 (V_oa4) in the a-intercalated cells of the cortical collecting duct. This interaction may be physiologically relevant. A genetic mutation in the human subunit V_oa4 that causes hereditary distal renal tubular acidosis also prevents V_oa4 binding to phosphofructokinase-1 (Su, Blake-Palmer et al. 2008).

The yeast ortholog of human phosphofructokinase-1 consists of two tetramers, each made of two subunits, Pfk1p (α subunit) and Pfk2p (β subunit) (Banaszak, Mechin et al. 2011). Deletion of both subunits prevents yeast growth on glucose, but the single deletion strains metabolize glucose (Heinisch 1986). They are therefore suitable to study the interplay between phosphofructokinase-1 and V-ATPase; we anticipated V_1V_o complexes to be assembled in *pfk1Δ* and *pfk2Δ* mutants.

This study examined V-ATPase functions at steady state and under disassembly and reassembly conditions in the *pfk1Δ* and *pfk2Δ* mutants. Each mutant failed to acidify vacuoles, even though V-ATPases were catalytically active *in vitro*. Overall V-ATPase function was significantly more affected in *pfk2Δ* than *pfk1Δ*. The *pfk2Δ* cells exhibited a partial *Vma*$^-$ growth phenotype, enhanced Rav1p-V_1 binding, and abnormal V_1V_o reassembly after re-addition of glucose to cells briefly deprived of glucose.

2.2 Materials and Methods

Materials and strains. Zymolase 100T was purchased from Seikagaku (Tokyo, Japan), Concanamycin A from Wako Biochemicals (Richmond, VA), and Ficoll from United Stated Biologicals (Swampscott, MA). The antibody to the Myc antigen was from Invitrogen (Carlsbad, CA). DSP was purchased from Pierce (Rockford, IL), and Tran[^{35}S]-label from MP Biomedicals (Santa Ana, CA). Alkaline phosphatase-conjugated secondary antibodies from Promega (Madison, WI) and horseradish peroxidase secondary antibodies from Invitrogen (Carlsbad, CA). All other reagents were from Sigma (St. Louis, MO). The *Saccharomyces cerevisiae* strains referred to throughout are listed in Table 1. The mutant strains were verified by PCR. The primers used in this study are listed in Table 2.

Construction of the pfk2Δ Rav1p-Myc strain. The *pfk2Δ* Rav1p-Myc mutant was made by disrupting the *PFK2* gene using PCR based homologous recombination, in which LEU2-containing cassettes were generated using the PFK2D primers (Table 2) and pRS315 as template. The Rav1p-Myc strain (Smardon, Tarsio et al. 2002) was transformed directly with the PCR product using the lithium acetate method. Transformants were selected on fully supplemented synthetic complete (SC) medium lacking leucine (SC-Leu) plates. The mutant was tested for integration by PCR.

Growth phenotype. Overnight cell cultures were grown to stationary phase, diluted to 0.1 OD Abs_{600}/mL in fresh YEPD or selective medium buffered to pH 5.0, and cells grew for 4-6 hours. Cultures were washed twice with sterile ddH_2O and 2.5 OD Abs_{600} cells resuspended into 1 mL sterile ddH_2O. Ten-fold serial dilutions were stamped onto YEPD or SC plates lacking uracil (SC-Ura) buffered to pH 5.0 with 50 mM, succinic acid 50 mM, sodium phosphate pH 7.5 with 50 mM MES, 50 mM MOPS, or pH 7.5 with 100 mM calcium chloride added. The plates were incubated for three days at 30 ^{o}C and 37 ^{o}C.

Table 1. ***S. cerevisiae*** **strains used in this study**

Strain (Ref)	***Parent***	***Relevant Phenotype***
WT	*BY4742*	MATα ; his3Δ 1; leu2Δ 0; lys2Δ 0; ura3Δ 0
*pfk1*Δ	*BY4742*	MATα ; his3Δ 1; leu2Δ 0; lys2Δ 0; ura3Δ 0 pfk1 Δ:: KanMX6
*pfk2*D	*BY4742*	MATα ; his3Δ 1; leu2Δ 0; lys2Δ 0; ura3Δ 0 pfk2 Δ:: KanMX6
*vma6*Δ	*BY4742*	MATα ; his3Δ 1; leu2Δ 0; lys2Δ 0; ura3Δ 0 vma6 Δ:: KanMX6
*vma2*Δ	*BY4742*	MATα ; his3Δ 1; leu2Δ 0; lys2Δ 0; ura3Δ 0 vma2 Δ:: KanMX6
*vma3*Δ	*BY4742*	MATα ; his3Δ 1; leu2Δ 0; lys2Δ 0; ura3Δ 0 vma3 Δ:: KanMX6
Rav1-Myc (Smardon, Tarsio et al. 2002)	*SF838-5A*	Matα ; ura3-52 ; leu2-3,112 ; his4-519 ade6 ; RAV1-Myc13:: kanMX6
*pfk2*Δ Rav1-Myc	*SF838-5A*	Matα ura3-52 leu2-3,112 his4-519 ade6 RAV1-Myc13:: kanMX6 pfk2 Δ:: Leu2

Table 2. Primers used in this study

Primer	***Sequence (5'-3')***	***Purpose***
pfk2Δ-5'	GAC ATT AAT A AT AGA AAG TG T AAT AAA AGG TCA TTT TCT T TTA AGC AAG GAT TTT CTT AAC	Generate Rav1-13myc, *pfk2*Δ
pfk2Δ-3'	AGAGACTAGT TTAGCATTGG CCAAGAACTA ACCATACGCAATG TCT GCC CCT ATG TCT GC	Generate Rav1-13myc, *pfk2*Δ
PFK2-XhoI	GGG CTC GAG CTC ATG TTT CTT ATT AGG	*Clone pRS316-PFK2*
PFK2-XmaI	GGG CCC GGG TTA ATC AAC TCT CTT TCT TCC	*Clone pRS316-PFK2*

Cytosol and vacuolar pH measurements. For cytosol pH measurements, the lithium acetate method (Elble 1992) was used to transform the cells with a 2μ pHLuorin plasmid under control of the phosphoglycerate kinase promoter (Tarsio, Zheng et al. 2011; Chan, Prudom et al. 2012). Cells were maintained in SC-Ura medium buffered to pH 5.0. Fluorescence (ex 405, ex 485; em 508) was monitored and the cytosol pH measured as described before using a FluoroMax 4 spectrofluorometer (Horiba Jobin Yvon Inc., NJ) (Chan, Prudom et al. 2012). The pHLuorin plasmid was created by Dr. Rajini Rao (Department of Physiology, Johns Hopkins University) and was a generous gift from Patricia Kane (SUNY Upstate Medical University, Syracuse).

Vacuolar pH was measured using the ratiometric fluorescent dye BCECF-AM (Brett, Tukaye et al. 2005; Martinez-Munoz and Kane 2008; Johnson, Allen et al. 2010). Glucose-dependent vacuolar pH changes were continuously monitored 20 min after addition of 2% glucose (final concentration) to cells briefly (10 min) depleted of glucose. The fluorescence intensity (490nm/450nm) was measured in a FluoroMax 4 spectrofluorometer (Horiba Jobin Yvon Inc., NJ).

Immuniprecipitations. Non-denaturing immunoprecipitations from whole cell lysates were performed as described previously (Ediger, Melman et al. 2009), except that the monoclonal antibodies 13D11 (anti V_1 subunit B) and 10D7 (anti V_o subunit a, Vph1p isoform) were used. To conduct immunoprecipitations from the cytosol, cytosolic fractions were isolated by high-speed centrifugation (100,000 xg for 1hr in a Beckman optima L-100 XP) and 4 μg total protein was used per immunoprecipitation. Protein was separated in 10% SDS-PAGE and analyzed by Western blots. The nitrocellulose membranes were scanned using a Bio-Rad ChemiDoc XRS+ and the intensity of protein bands quantified using the Multi Gauge and GraphPad Prism 5 software. Protocols previously described were followed (Parra and Kane 1998) to conduct the immunoprecipitations from whole cell lysates and biosynthetically radiolabeled cells. Except that the chases were performed at the indicated times and the antibodies 13D11 and 10D7 were used. The SDS-PAGE gels (13% acrylamide) were dried, scanned in a Fuji Scanner FLA-5100, and analyzed using the Multi Gauge and GraphPad Prism 5 software.

Other methods. Vacuolar membrane vesicles were isolated by Ficoll density gradient centrifugation (Owegi, Carenbauer et al. 2005; Ediger, Melman et al. 2009; Chan, Prudom et al. 2012). ATP hydrolysis was measured by monitoring NADH oxidation spectrophotometrically (Owegi, Carenbauer et al. 2005; Ediger, Melman et al. 2009; Chan, Prudom et al. 2012) using 5mg of total vacuolar membrane protein in the presence and absence of 100 nM concanamycin-A. Proton transport was measured by monitoring 9-amino-6-chloro-2-methoxyacridin (ACMA) quenching after addition of MgATP (Forgac, Cantley et al. 1983; Chan, Prudom et al. 2012). Protein concentration was measured by the Bradford assay (Bradford 1976).

2.3 Results

Studying V-ATPase functions in a phosphofructokinase-1 null mutant strain (*pfk1Δ pfk2Δ*) is not straightforward because *pfk1Δpfk2Δ* cells cannot metabolize glucose (Heinisch 1986), which causes V_1V_o disassembly (Parra and Kane 1998). The single deletion strains *pfk1Δ* and *pfk2Δ* are suitable for these studies. They grow on glucose as the only carbon source, because each phosphofructokinase-1 subunit Pfk1p and Pfk2p (a and b, respectively) has catalytic and regulatory functions (Heinisch 1986; Arvanitidis and Heinisch 1994). Thus, upon deletion of one subunit, the other subunit retains catalytic activity sufficient to support glycolysis. We examined the roles of individual phosphofructokinase-1 subunits for V-ATPase activity, assembly, and regulation.

Phosphofructokinase-1 subunits Pfk1p and Pfk2p co-precipitate with V-ATPase. First, we asked if the individual phosphofructokinase-1 subunits retain binding to V-ATPase in the single deletion mutants. We immunoprecipitated V-ATPase and conducted immunoblots using a polyclonal antibody that recognizes both phosphofructokinase-1 subunits. Yeast *pfk1Δ* and *pfk2Δ* cells and an isogenic wild-type strain were grown in rich media in the presence of 2% glucose (YEPD, normal yeast growth media). The cells were lysed and the V-ATPase complex immunoprecipitated under nondenaturing conditions using the monoclonal antibody 13D11 to the V-ATPase V_1 subunit B (anti-B) (Ediger, Melman et al. 2009).

As expected, both phosphofructokinase-1 subunits co-precipitated with V-ATPase in wild-type cells (Fig. 1A). So did each individual subunit in *pfk1Δ* and *pfk2Δ*. Deletion of one phosphofructokinase-1 subunit did not prevent interaction of the other subunit with V-ATPase. The subunit expressed in *pfk1Δ* cells (subunit Pfk2p) and *pfk2Δ* cells (subunit Pfk1p) can associate with V-ATPase.

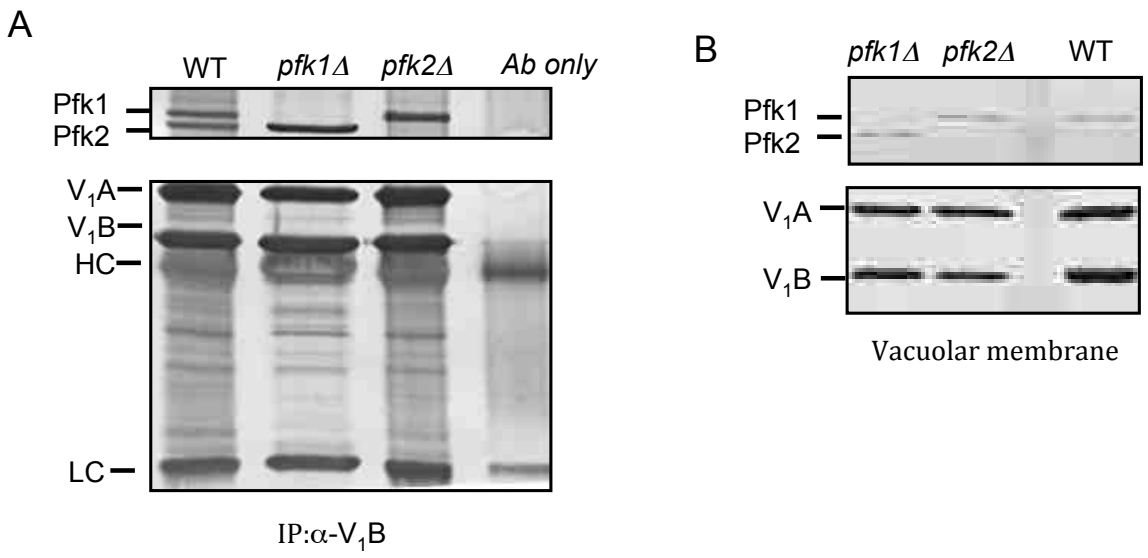

Figure 1. **V-ATPase associates with phosphofructokinase subunits Pfk1p and Pfk2p.** *A. V-ATPase co-immunoprecipitates with Pfk1p and Pfk2p from whole cell lysates*. Isogenic wild-type, *pfk1Δ* and *pfk2Δ* cells were grown overnight to mid-log phase (0.8 -1.0 OD Abs_{600}/ml). Cells were converted to sheroplast by zymolase treatment and V-ATPase immunoprecipitated under non-denaturing conditions using the monoclonal antibody 13D11 to subunit B of V_1 and protein A sepharose. The immunoprecitated protein was separated by 10% SDS-PAGE and immunoblotted with antibodies to phosphofructokinase and V_1 subunits A and B using horseradish peroxidase secondary antibodies. HC: antibody heavy chain; LC: antibody light chain. *B. Pfk1p and Pfk2p subunits co-purify with vacuolar membrane fractions*. Vacuolar membrane vesicles (0.25 mg total membrane protein) were purified from *pfk1Δ, pfk2Δ* , and wild-type cells by density gradient centrifugation. Membranes were immunoblotted as described above.

Next, we asked if the subunit expressed in the *pfk1Δ* and *pfk2Δ* mutants was present at the vacuolar membrane. We purified vacuolar membrane fractions from *pfk1Δ, pfk2Δ*, and wild-type cells by density gradient centrifugation and conducted Western blots (Fig. 1B). Both subunits were detected in wild-type membranes. The subunit Pfk1p was in *pfk2Δ* membranes and Pfk2p in *pfk1Δ* membranes. Given that individual phosphofructokinase subunits retained binding to V-ATPase and that *pfk1Δ* and *pfk2Δ* cells metabolize glucose (Heinisch 1986), we asked if V-ATPase was functional in *pfk1Δ* and *pfk2Δ*.

The pfk2Δ mutants exhibit partial Vma⁻ growth phenotype. V-ATPase inactivation leads to a conditionally lethal growth phenotype that is pH-dependent in yeast, the vacuolar membrane ATPase (*Vma⁻*) phenotype. The *vma* mutants grow at pH 5.0, but cannot grow at either pH 7.5 or at pH 7.5 in the presence of high concentrations of calcium chloride (Kane 2006).

We plated *pfk1Δ* and *pfk2Δ* cells on YEPD media buffered to pH 5.0, pH 7.5, and pH 7.5 plus calcium chloride to determine whether deletion of one subunit altered normal V-ATPase function (Fig. 2). For reference, we compared *pfk1Δ* and *pfk2Δ* growth to V-ATPase mutants (*vma2Δ* and *vma6Δ*). The *vma2Δ* and *vma6Δ* mutants lack all V-ATPase activity because the structural genes *VMA2* and *VMA6* that encode subunits B of V_1 and d of V_o, respectively, were deleted (Bauerle, Ho et al. 1993; Doherty and Kane 1993). As expected, *vma2Δ* (Fig. 2A) and *vma6Δ* (Fig. 2B) did not grow at pH 7.5 and pH 7.5 plus calcium chloride.

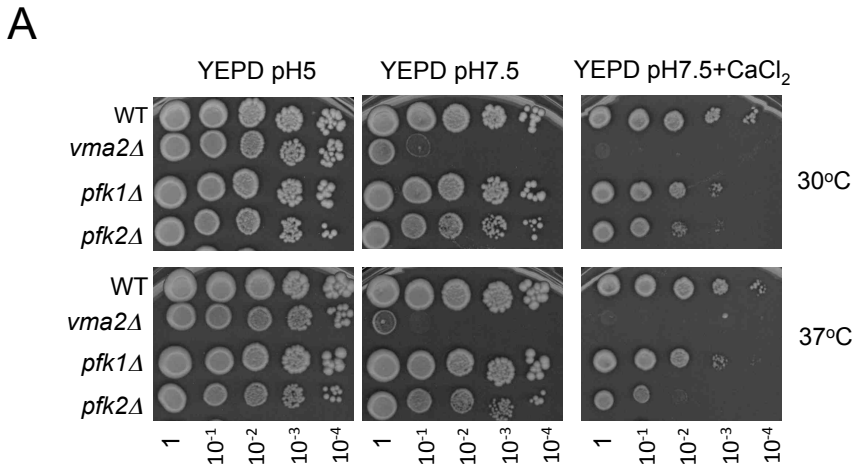

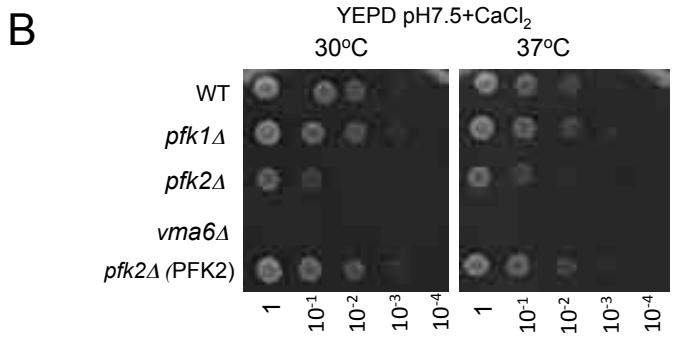

Figure 2. **The *pfk2Δ* mutant exhibits partial *Vma*⁻ growth phenotype.** *A.* *Growth of the pfk2Δ strain is sensitive to pH 7.5 with calcium chloride.* Cell cultures were grown overnight to mid-log phase and ten-fold serial dilutions stamped onto YEPD plates adjusted to pH 5.0, pH 7.5, and pH 7.5 plus 100 mM $CaCl_2$. Cell growth was monitored for 3 days at 30°C and 37°C. *B.* *PFK2 rescues the Vma⁻ growth phenotype of pfk2Δ*. The wild-type strain and the mutant strains *pfk1Δ*, *pfk2Δ* and *vma6Δ* were transformed with the empty CEN plasmid pRS316. The *pfk2Δ and vma6Δ* were transformed with the gene *PFK2* expressed from the same plasmid under control of its endogenous promoter (*pfk2Δ* (PFK2)). Serial dilutions of the cells were stamped onto SC-Ura plates adjusted to pH 7.5 plus 100 mM $CaCl_2$ and allowed to grow for 3 days at 30°C and 37°C. Shown are representative plates of triplicates.

The *pfk2Δ* cells exhibited a partial *Vma*$^-$ growth phenotype, in which the growth defect was evident at pH 7.5 plus calcium chloride and accentuated at 37^{o}C (Fig. 2A, right panel). This growth defect was much subtler in the *pfk1Δ* mutant. At the less stringent growth condition, pH 7.5, the *pfk2Δ* cells grew normally, as did *pfk1Δ* and the isogenic wild type strain. To address if *Vma*$^-$ growth defects in *pfk2Δ* were specific to *PFK2*, we expressed the *PFK2* gene from a CEN plasmid in *pfk2Δ* cells. As expected, the empty vector did not rescue growth on pH 7.5 plus calcium chloride plates (*vma6Δ*, Fig. 2B). Exogenously expressed *PFK2* rescued *pfk2Δ* growth (*pfk2Δ* (*PFK2*), Fig 2B), indicating that the *Vma*$^-$ growth phenotype of *pfk2Δ* was caused by lack of *PFK2 e*xpression. These results suggest that the phosphofructokinase-1 subunit Pfk2p is necessary for normal V-ATPase function.

Vacuolar and cytosolic pH are significantly altered in pfk2Δ cells. Having shown that lack of *PFK2* leads to growth defects typical of cells with impaired V-ATPase activity (*Vma*$^-$ phenotype), we asked if pH homeostasis was altered. V-ATPase mutants have alkalinized vacuoles and acidified cytosol, because V-ATPase proton transport is necessary to sustain yeast vacuolar and cytosolic pH homeostasis (Martinez-Munoz and Kane 2008).

We used fluorometric assays and pH-sensitive fluorescent dyes to measure vacuolar (BCECF) and cytosolic (pHLuorin) pH (Johnson, Allen et al. 2010; Tarsio, Zheng et al. 2011; Chan, Prudom et al. 2012) in *pfk1Δ* and *pfk2Δ* cells *in vivo* (Fig. 3). As expected,

pH homeostasis was aberrant in a control strain that lacks all V-ATPase function (*vma2Δ*). The vacuolar pH of *vma2Δ* cells was considerably more alkaline and its cytosol more acidic than wild-type cells.

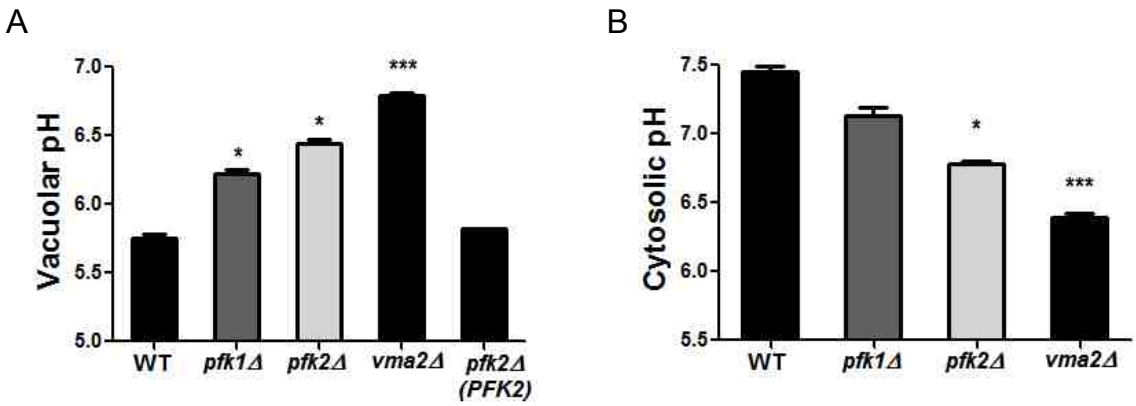

Figure 3. ***pfk1Δ* and *pfk2Δ* mutants have altered vacuolar and cytosol pH homeostasis at steady state.** *A. The vacuolar lumen is alkalinized in live pfk1Δ* and *pfk2Δ cells.* Overnight mid-log phase cultures from wild-type cells, mutant cells (*pfk1Δ*, *pfk2Δ, vma2Δ*), and the mutant *pfk2Δ* expressing exogenous *PFK2* from the CEN plasmid pRS316 (*pfk2Δ* (*PFK2*)) were stained with 50mM BCECF-AM for 30 minutes at 30°C. The ratio of fluorescent emission (535 nm) excited at 490 and 450 nm was measured in a fluorometer to quantitatively assess vacuolar pH. The average fluorescence over 6 minutes was compared to a standard curve to generate absolute pH values. *B. The cytosol pH is acidified in live pfk1Δ and pfk2Δ cells.* The wild-type, *pfk1Δ*, *pfk2Δ,* and *vma2Δ* cells expressing cytosolic pHLuorin were grown overnight to mid-log phase (0.4-0.6 OD Abs_{600}/mL). The cells were transferred to 1 mM HEPES/MES buffer pH 5.0 containing 2% glucose at a cell density of 5.0 OD Abs_{600}/mL. The ratio of fluorescent emission (508 nm) excited at 405 nm and 485 nm was measured for 6 min at 1 min intervals. The average fluorescence was estimated and calibration curves made in parallel used to calculate pH values in a fluorometer. Vacuolar and cytosol data is presented as average pH values from three independent experiments, error bars= +/- standard deviation, * $p<0.05$, *** $p<0.001$ compared to wild-type control as measured by two-tailed unpaired *t*-test.

We detected vacuolar and cytosolic pH alterations suggestive of V-ATPase dysfunction in the *pfk1Δ* and *pfk2Δ* cells. The vacuolar lumen was alkalinized and the cytosol acidified. Vacuolar pH increased by 0.4 pH units in *pfk1Δ* (pH=6.2 +/-0.04) and 0.6 pH units in *pfk2Δ* (pH=6.4 +/-0.06), compared to wild-type cells (pH=5.8+/-0.05) (Fig. 3A). Reciprocally, the cytosol pH decreased. It dropped from pH 7.4 (+/-0.06) in wild-type cells to pH 7.1 (+/-0.10) in *pfk2Δ* , and pH 6.8 (+/-0.03) in *pfk2Δ* (Fig. 3B). Vacuolar acidification, which is a direct indicator of V-ATPase activity, was rescued by expression of exogenous *PFK2* (*pfk2Δ* (*PFK2)*). Together, these results indicate that the pH defects in *pfk2Δ* are specific to V-ATPase malfunction caused by lack of *PFK2*.

The fact that pH alterations were milder in *pfk1Δ* than *pfk2Δ*, and more severe in the *vma2*Δ mutant is consistent with the extent of the growth defects observed in these strains (Fig. 2). Together these phenotypes suggest that subunit Pfk2p is more critical than Pfk1p to sustain optimal V-ATPase proton transport at steady state *in vivo*.

V-ATPase is catalytically competent in pfk2Δ. To directly address the effect that deletion of *PFK1* and *PFK2* has on V-ATPase catalytic activity, we purified vacuolar membrane fractions by density gradient centrifugation. We measured ATP hydrolysis and proton transport *in vitro* in the presence and absence of the V-ATPase inhibitor conanamycin A (Chan, Prudom et al. 2012).

The V-ATPase pumps at *pfk1Δ* than *pfk2Δ* membranes were significantly active. The conanamycin A-sensitive ATP hydrolysis and proton transport were partially reduced by about 35% in the *pfk2Δ* membranes (Fig. 4A). They were normal in *pfk1Δ*. Comparative membrane protein titrations in Western blots showed equivalent amounts of V_1 (subunits A and B) and V_o (subunit a) subunits in wild-type, *pfk1Δ*, and *pfk2Δ* membranes (Fig. 4B), suggesting that V_1V_o assembly is normal at the vacuolar membrane.

Subtle alterations of the V_1V_o assembly level may not be detected by Western blots. We further examined if loss of Pfk1p or Pfk2p affected V_1V_o assembly by using a more sensitive approach. We biosynthetically radiolabeled the cells with S^{35} to estimate the total fraction of V_1V_o complexes assembled in *pfk1Δ* and *pfk2Δ*. The radiolabeled V-ATPase pumps were immunoprecipitated from whole cell lysates with the antibodies 13D11 (anti-B, recognizes V_1 and V_1V_o) and 10D7 (anti-a, recognizes V_o) and the total fraction of assembled V-ATPase complexes calculated as described before (Parra and Kane 1998).

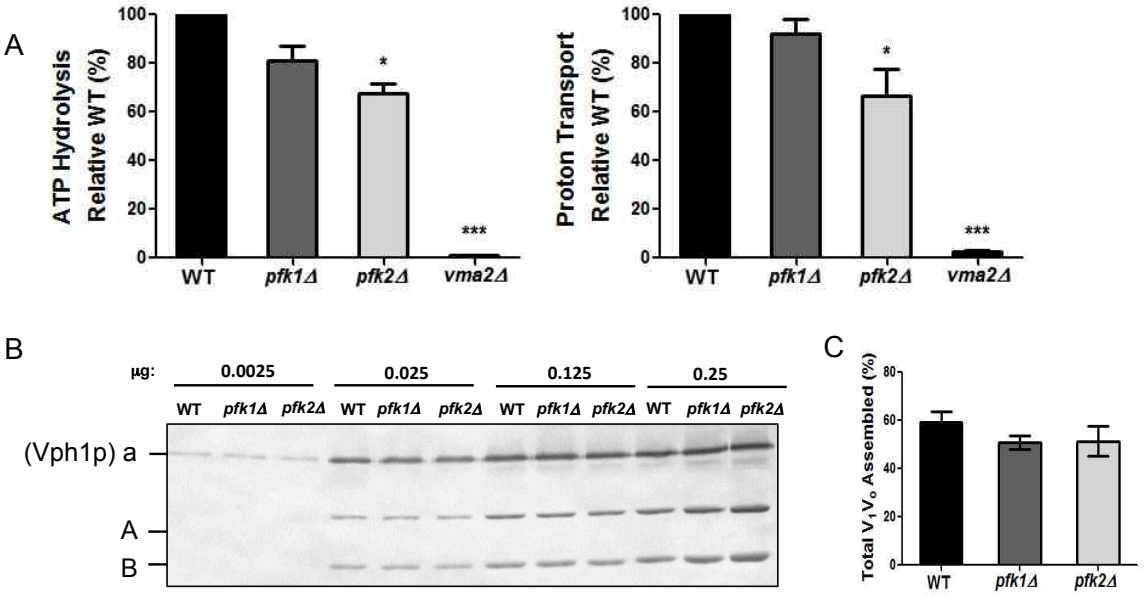

Figure 4. **V-ATPase activity is partially reduced at *pfk2Δ* vacuolar membrane vesicles.** *A. ATP hydrolysis and proton transport are differentially affected in pfk1Δ and pfk2Δ cells.* Vacuolar membrane fractions were purified from the isogenic wild-type, *pfk1Δ*, *pfk2Δ*, and *vma2Δ* cells. ATP hydrolysis (*left*) was assayed spectrophotometrically in the presence and absence of the V-ATPase inhibitor concanamycin A by using an enzymatic coupled assay that measures NADH oxidation at 340 nm. The wild-type specific activity of the concanamycin A-sensitive ATP hydrolysis was 2.5 - 4 µmol of ATP/min/mg of protein. The strains showing significant activity (wild-type, *pfk1Δ* and *pfk2Δ*) were equally inhibited (~80%) by 100 nM concanamycin-A. ATP-dependent proton transport (*right*) was measured via fluorescence quenching of 1µM 9-amino-6-chloro-2-methoxyacridin (ACMA)(Ex 410 nm; Em 490 nm) upon the addition of 0.5mM ATP/1mM $MgSO_4$ to 5µg of total protein in vacuolar membranes vesicles. Initial velocities were calculated for 15 seconds following MgATP addition. The average wild-type slope was -1320.32 fluorescence units/15 seconds. Data represent three independent vacuolar preps; * $p<0.05$, *** $p<0.001$ decreased ATPase activity compared to wild-type membranes as measured by two-tailed unpaired *t*-test. *B. Wild-type levels of V_oV_1 complexes are assembled at the vacuolar membrane of pfk1Δ and pfk2Δ mutants*. The purified vacuolar membrane vesicles were analyzed by quantitative immunoblotting using antibodies against V_1 subunits B and A and the V_o subunit a (Vph1p isoform) and alkaline phosphatase-conjugated secondary antibodies. Serial dilutions of wild-type and mutant membrane fractions were prepared and the indicated amounts of vacuolar protein loaded per well and separated on 10% SDS-PAGE gels. A representative gel of three independent vacuolar preps is shown. *C. Pfk1Δ and pfk2Δ assemble wild-type levels of V_1V_o complexes at steady state*. An isogenic wild-type, *pfk1Δ*, and *pfk2Δ* cells were biosynthetically radiolabeled with Tran^{35}S for 60 minutes and V-ATPase immunoprecipitated from whole cell lysates under non-denaturing conditions using the antibodies anti-B (recognizes V_1 and V_1V_o) and anti-a (recognizes V_o). The protein was separated in 13% SDS-PAGE gels and assembled V_1V_o estimated as the fraction of V_o immunoprecipitated with anti-B relative to the total immunoprecipitated with both antibodies. Gels from three independent experiments were analyzed in a Fuji Scanner FLA-5100, and analyzed using the Multi Gauge and GraphPad Prism 5 software.

Consistent with previous studies (Parra and Kane 1998; PM. 2006), about 60% of the V-ATPase pumps were assembled in wild-type cells at steady state (Fig. 4C). A comparable fraction of assembled V-ATPases was detected in *pfk2Δ* and *pfk1Δ* cells, consistent with the Western blots (Fig. 4B) and further suggesting that absence of either phosphosfructokinase-1 subunit does not disturb biosynthetic V_1V_o assembly. Next, we asked whether V-ATPase reversible disassembly was normal.

Glucose-dependent V-ATPase reassembly is defective in pfk2Δ mutants. Until now our studies have been conducted at steady state, in the presence of abundant glucose (2% glucose). We determined whether the phosphofructokinase-1 subunits were necessary for V_1V_o reversible disassembly in response to glucose depletion and re-addition. It is known that under disassembly and reassembly conditions the equilibrium [V_1V_o] to [V_1+V_o] is changed (PM. 2006); lack of glucose favors disassembly, glucose re-addition promotes reassembly and restores steady state equilibrium.

The wild-type, *pfk1Δ*, and *pfk2Δ* cells were biosynthetically radiolabeled and chased in the presence (assembly condition) and absence (disassembly condition) of 2% glucose, and after re-addition of 2% glucose following a brief glucose depletion period (reassembly condition). We estimated the fraction of assembled V_1V_o by nondenaturing immunoprecipitation experiments using the anti-B and anti-a antibodies (Parra and Kane 1998).

The *pfk1Δ* cells disassembled and reassembled V_1V_o normally, as wild-type cells (Fig. 5A). Approximately 70-80% of the total V_1V_o complexes disassembled upon glucose depletion. An equivalent proportion of V_1V_o complexes reassembled after glucose re-addition to *pfk1Δ*. Notably, disassembly was normal in the *pfk2Δ* strain but reassembly was significantly reduced (Fig. 5B). Only 50% reassembly was detected relative to wild-type cells. Maximum reassembly is achieved within 5 minutes in wild-type cells; an increase of the incubation time from 5 minutes to up to 15 minutes did not lead to an increase of *pfk2Δ* assembly after glucose re-addition. These results suggest that the mechanism(s) of reassembly are defective in *pfk2Δ*, while the kinetics of reassembly remains similar to wild type cells.

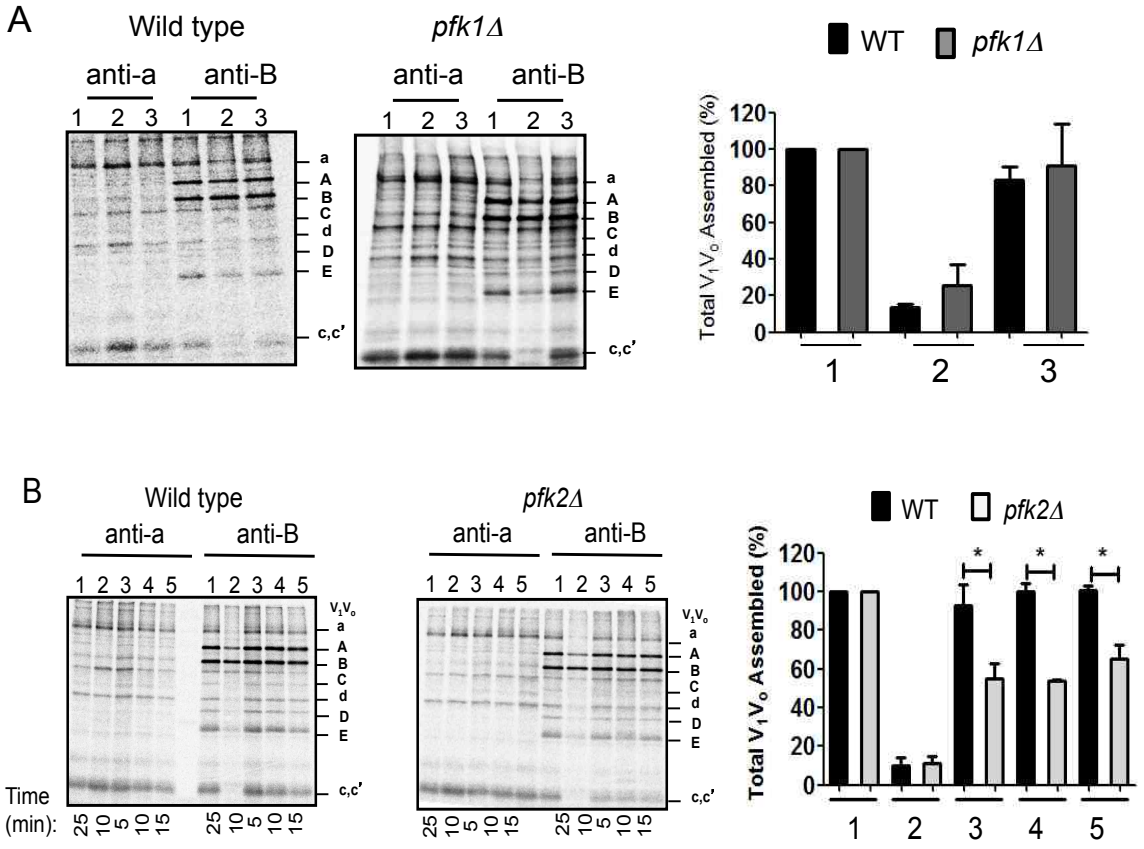

Figure 5. **Glucose dependent V_1V_o reassembly is defective in *pfk2Δ*.** *A. Glucose-dependent disassembly and reassembly is normal in pfk1Δ cells.* Biosynthetically radiolabeled wild-type and *pfk1Δ* cells were chased in YEP media containing 2% glucose (YEPD) for 20 minutes (1), lacking glucose for 10 minutes (2), and in medium lacking glucose for 10 minutes followed by an additional 10 minutes chase after re-addition of glucose to a final concentration of 2% glucose (3). The cells were lysated, immunoprecipitated, and gels from four independent experiments analyzed as described for Figure 4C. A representative gel is shown (*left*). Analyzed results are expressed as the average ± standard deviation relative to wild-type (*right*). *B. Glucose-dependent disassembly and reassembly is defective in pfk1Δ cells.* Wild-type and *pfk2Δ* cells were radiolabeled, chased, immunoprecipitated, and V_1V_o assembly levels analyzed as described for Figures 4C and 5A. Sample (1) was chased in YEPD for 25 minutes, (2) in YEP for 10 minutes, and (3), (4), and (5) were chased respectively for 5 minutes, 10 minutes, and 15 minutes after glucose re-addition (2% final concentration). The data is expressed as the average ± standard deviation relative to wild-type (*right*). * $p<0.05$compared to wild-type as measured by two-tailed unpaired *t*-test.

V-ATPase-Rav1p interaction is enhanced in the pfk2Δ strain. Reassembly requires the RAVE complex, particularly the RAVE subunit Rav1p that connects RAVE with V_1, subunit C, and V_o (Smardon, Tarsio et al. 2002; Smardon and Kane 2007; Smardon, Diab et al. 2014). Since these interactions are necessary for reassembly of V-ATPase pumps at the vacuolar membrane, we asked whether the Rav1p-V_1 binding was affected in *pfk2Δ*. We deleted *PFK2* in cells expressing Myc epitope tagged genomic *RAV1* (Rav1p-Myc). It has been shown that wild-type Rav1p-Myc cells retain normal growth and assemble functional V_1V_o complexes at vacuolar membranes (Smardon, Tarsio et al. 2002). Thus, the Myc tag does not interfere with steady state V-ATPase assembly and activity.

To address if Rav1p binding to V_1 was affected in *pfk2Δ* we immunoprecipitated V_1 from a cytosolic fraction isolated from the *pfk2Δ* Rav1p-Myc strain. We estimated about 5-fold more Rav1p bound to V_1 subunits A and B in *pfk2Δ* than wild-type cells (Fig. 6A). This increase in Rav1p-V_1 binding was not caused by enhanced expression of cytosolic Rav1p and/or V_1 subunits, since these proteins were comparable in whole cell lysates from *pfk2Δ* and wild-type cells (input, Fig. 6A). Rather, Rav1p-V_1 binding was increased in the cytosol of *pfk2Δ*, suggesting an enhanced Rav1p-V_1 affinity.

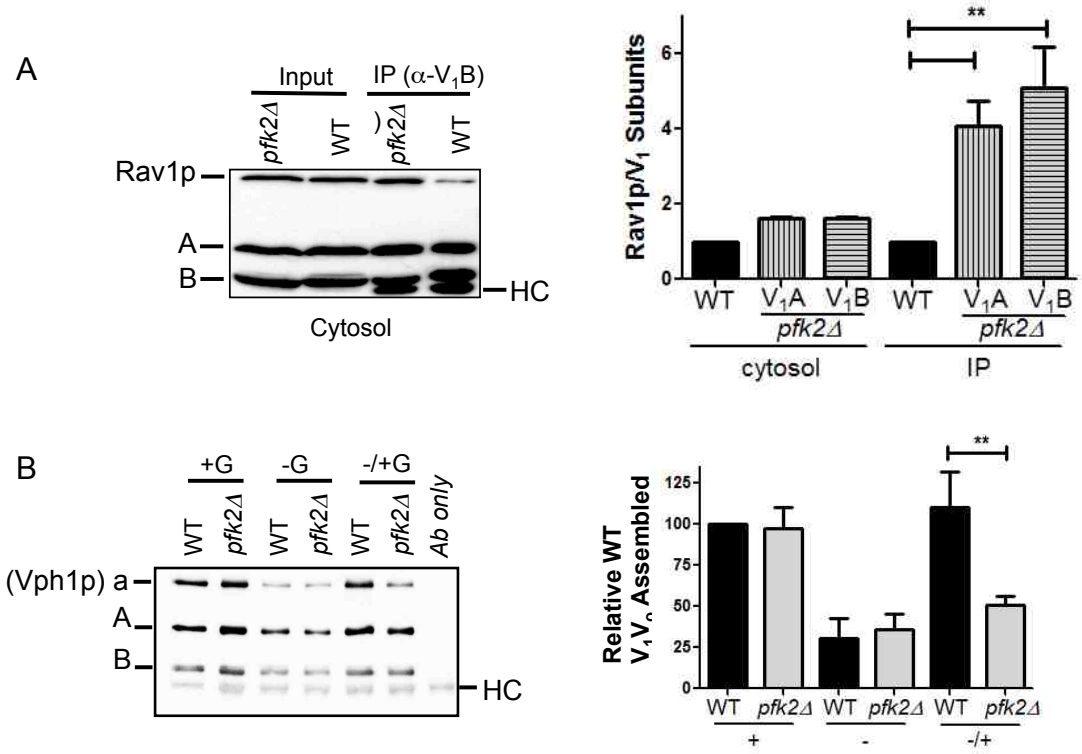

Figure 6. **The interaction between Rav1p and cytosolic V_1 is increased in *pfk2Δ* cells.** *A. Cytosolic fractions from pfk2Δ cells contain more Rav1p-V_1 than wild-type cells*. Overnight mid-log phase cultures (0.8~1.0 OD Abs_{600}/ml) of wild-type and *pfk2Δ* cells expressing Rav1p-Myc were lysated and the cytosolic fraction prepared by centrifugation (100,000xg for 1 hour). Cytosolic V_1 complexes were immunoprecipited with anti-B antibody. Immunoprecitated protein (*IP*) and total cytosolic protein (*Input*) were loaded on 10% SDS-PAGE gels. Rav1p and V_1 (subunits A and B) were detected by immunoblots with anti-Myc, anti-B and anti-A monoclonal antibodies respectively. A representative gel is shown (*left*). Gels from three independent experiments were scanned using a Bio-Rad ChemiDoc XRS+ and data analyzed using Multi Gauge V3.0 and GraphPad Prism 5 software. Data was expressed as fold-increase Rav1p:V_1-subunit ratio ± standard deviation relative to wild-type (*right*). *B. Glucose-dependent V_1V_o reassembly is defective in Rav1p-Myc pfk2Δ cells*. Isogenic wild-type and *pfk2Δ* mutant cells expressing genomic Rav1p-Myc were grown overnight to mid-log phase. Cells were converted to sheroplast incubated in YEPD media (2% glucose) for 20 minutes (+G), deprived of glucose for 10 minutes (-G), and deprived of glucose for 10 minutes followed by an additional 10 minutes after glucose re-addition to a final concentration of 2% glucose (-/+G). V-ATPase was immunoprecipitated (200 OD Abs_{600}/IP) as described for Figure 1A and immunoblots analyzed with antibodies to V_o subunit a (vacuolar isoform Vph1p) and V_1 subunits A and B. One representative gel is shown (*left*). Gels from three independent experiments were analyzed, and total V_1V_o estimated as for Figure 4C. The data is expressed as the average ± standard deviation relative to wild-type. ** $p<0.01$ compared to wild-type as measured by two-tailed unpaired *t*-test.

To eliminate the possibility that the Myc tag itself affected Rav1p-V_1 binding, we also immunoprecipitated V-ATPase complexes from whole cell lysates after brief glucose depletion and re-addition. As expected for wild-type Rav1p-Myc cells, about 70 % of the V_1V_o disassembled and reassembled after glucose removal and its re-addition, respectively (Fig. 6B). Only half of the V_1V_o complexes reassembled after re-addition of glucose to *pfk2Δ* Rav1p-Myc cells. We concluded that tagged Myc did not interfere with V-ATPase reversible disassembly. Thus, the increased level of RAVE-V_1 in the cytosol of *pfk2Δ* is a phenotypic trait of the phosphofructokinase-1 mutant *pfk2Δ*.

Rav1p also interacts with V_o subunit a at the membrane, specifically the subunit a isoform Vph1p (vacuolar isoform) (Smardon, Diab et al. 2014). We isolated membrane fractions to determine whether binding of Rav1p to V_o subunit a was also enhanced in *pfk2Δ*. We detected similar levels of Rav1p in *pfk2Δ* and wild-type vacuolar membranes (not shown). These results suggest that the binding of RAVE to V_o was not altered in *pfk2Δ*. A greater affinity of Rav1p-V_1 binding could lead to reassembly defects of *pfk2Δ*.

Glucose-dependent V_1V_o reassembly fails to acidify pfk2Δ vacuoles. In wild-type cells, glucose depletion alkalinizes the vacuoles and glucose re-addition acidifies the vacuolar lumen (Martinez-Munoz and Kane 2008). These pH changes are V-ATPase-dependent, because V_1V_o reassembly restores ATP hydrolysis and proton transport (Kane 2006; Martinez-Munoz and Kane 2008). We monitored vacuolar pH in the phosphofructokinase-1 mutants under reassembly conditions. The vacuoles were loaded

with the pH sensitive fluorophore BCECF-AM and deprived of glucose for 10 minutes, after which glucose was re-added and the pH continuously measured (Fig. 7).

The wild-type and *pfk1Δ* cells acidified the vacuolar lumen after glucose re-addition, indicating that reassembled V_1V_o resumed proton transport. Glucose re-addition to *pfk2Δ* did not result in vacuolar acidification. Instead the vacuolar pH gradually increased until reaching approximately pH 6.5, the same pH measured at steady state (Fig. 3). A similar alkalinization of the vacuolar lumen is obvious in the V-ATPase mutant *vma2Δ* (Fig. 7) and other yeast mutants lacking V-ATPase activity. Although the vacuolar pH increased abruptly in *vma2Δ* and gradually in *pfk2Δ*, these results indicate that reassembled V-ATPase pumps are inactive in the *pfk2Δ* strain.

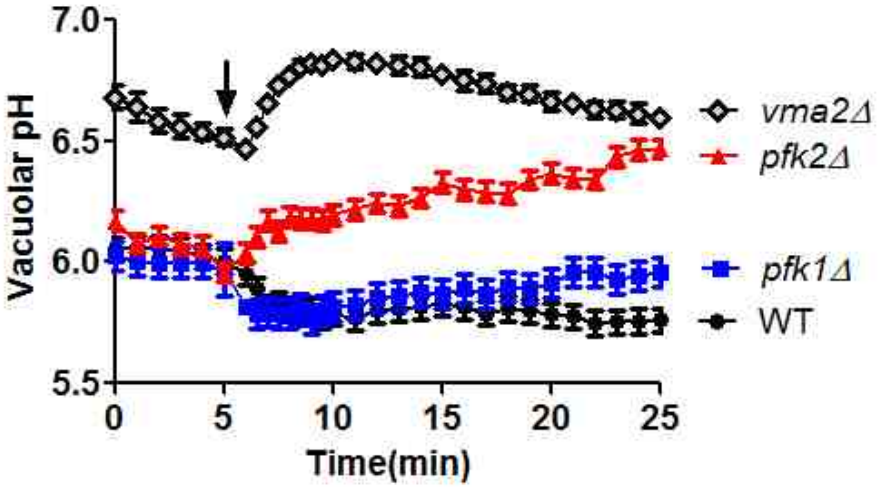

Figure 7. **Glucose-dependent vacuolar acidification is impaired in *pfk2Δ* cells.** The *pfk1Δ*, *pfk2Δ*, *vma2Δ* mutants and a wild-type strain were stained with 50mM BCECF-AM for 30 minutes at 30°C. The cells were depleted glucose for 10 min, after which glucose (2% final concentration) was added (*arrow*) and fluorescence monitored for an additional 20 minutes. The ratio of fluorescent emission (535 nm) excited at 490 and 450 nm was measured as for Figure 3A. The vacuolar pH was estimated using calibration curves made in parallel

2.4 Discussion

We studied V-ATPase assembly, activity and regulation in phosphofructokinase-1 single deletion mutants lacking the phosphofructokinase-1 structural genes *PFK1* and *PFK2*. Whereas both phosphofructokinase-1 subunits make contributions to V-ATPase activity, the most critical subunit is Pfk2p.

The pfk1Δ and pfk2Δ mutants are suitable to study V-ATPase. V-ATPase studies using *pfk1Δ pfk2Δ* cells are difficult to interpret because the double deletion mutant cannot metabolize glucose. Although *pfk1Δ pfk2Δ* tolerates 0.2% glucose (Su, Zhou et al. 2003), suppression of glycolysis and glucose-dependent signals promotes V_1V_o disassembly. Only 30-40% of the V_1V_o complexes are assembled at 0.2% glucose in wild-type cells (Parra and Kane 1998).

Because there is an equal contribution of Pfk1p (subunit α) and Pfk2p (subunit β) in the wild-type phosphofructokinase-1 heteromeric complex, each individual subunit can assemble to an unknown structure that is partially active *in vivo* (Arvanitidis and Heinisch 1994; Klinder, Kirchberger et al. 1998). Each single deletion strain grows on glucose, indicating that *pfk1Δ* and *pfk2Δ* have phosphofructokinase-1 activity above a threshold level that supports sufficient glycolytic flow.

The phosphofructokinase-1 subunit Pfk2p is necessary for cellular pH homeostasis and V-ATPase regulation. Heteromeric (wild-type) and homomeric (*pfk1Δ* and *pfk2Δ* cells) phosphofructokinase-1 complexes co-precipitate with V-ATPase. Our study suggests that phosphofructokinase-1 interacts with V_1V_o because Pfk1p and Pfk2 were detected in vacuolar membrane fractions and co-immunoprecipitated with the anti-B antibody (13D11). However, we cannot exclude the possibility that it binds to cytosolic V_1 as well because the antibody 13D11 recognizes both $V_1V_o$and V_1. Additional studies will be necessary to determine whether the interactions between Pfk2p and V-ATPase are direct or indirect, for example, involving other glycolytic enzymes.

Pfk2p could bridge interactions involving phosphofructokinase-1 and V-ATPase. Yeast phosphofructokinase-1 forms stable $\alpha_4\beta_4$ complexes in which β subunits (Pfk2p) are at the periphery (Banaszak, Mechin et al. 2011), more readily available to form intermolecular interactions with other proteins, including V-ATPase.

The subunit a is not critical for V-ATPase function, although the vacuole and cytosol pH homeostasis are altered *in vivo*. The *pfk1Δ* strain exhibits wild-type levels of V-ATPase activity in membrane fractions and V_1V_o assembly at steady state. They also disassemble and reassemble V_1V_o normally and resume vacuolar acidification after glucose readdition.

At steady state, V-ATPase proton transport is somewhat inhibited *in vivo*; *pfk1*Δ has more alkaline vacuoles and acidic cytosol than wild-type cells. Together with the fact that *pfk1*Δ growth is slightly reduced on plates buffered to pH 7.5 containing calcium chloride, these results indicate that V-ATPase proton transport is suppressed in *pfk1*Δ vacuolar membranes *in vivo* at steady state.

The subunit β is critical for V-ATPase function. V-ATPase function and its regulation are more severely impaired in the *pfk2Δ* mutant strain. Vacuolar and cytosol pH alterations are more pronounced in *pfk2*Δ than *pfk1*Δ at steady state. The vacuolar and cytosol pH, respectively, increased and decreased by 0.75 pH unit each. For reference, complete lack of V-ATPase activity in *vma2*Δ changes the vacuole and cytosol pH by about 1.0 pH unit.

V-ATPase reversible disassembly is also defective in *pfk2Δ*. Only half of the V-ATPase complexes reassemble after glucose readdition compared with wild-type cells. Notably, *pfk2Δ* does not acidify the vacuolar lumen after glucose readdition. Because glucose-triggered vacuolar acidification is a direct outcome of V-ATPase reassembly and reactivation (Martinez-Munoz and Kane 2008), these results suggest that V_1V_o complexes do not pump protons after reassembly occurs in *pfk2Δ*.

One explanation is that *pfk2Δ* does not acidify the vacuoles because 50% of V_1V_oreassembles and those pumps are ~35% less active. However, wild-type yeast

vacuoles are acidified when 30–40% of the V-ATPase pumps reassemble after addition of 0.2% glucose. Another explanation is that RAVE-mediated reassembly is defective in *pfk2Δ*.

*Enhanced Rav1p-V_1 Interaction May Impair pfk2Δ Glucose-dependent Reassembly*The The chaperone activity of RAVE directly involves its subunit Rav1p, which binds to cytosolic V_1 and subunit C and connects RAVE and V-ATPase subunits (Smardon, Tarsio et al. 2002; Smardon and Kane 2007; Smardon, Diab et al. 2014). We estimated about 5-fold more Rav1p-V_1 complexes in the cytosol of *pfk2Δ* than wild-type cells (Fig. 6). Because these experiments were conducted at steady state, excess Rav1p-V_1 complexes are not a byproduct of failure to reassemble V_1V_o.

RAVE likely facilitates the structural changes necessary to properly reform V_1V_o subunit interactions (Oot, Huang et al. 2012; Parra, Chan et al. 2014). Reassembled V_1V_o complexes can be inactive if reassociation of V_1 and/or subunit C with V_o is structurally flawed or "loose." Structurally loose complexes will not acidify vacuoles; they could also break apart V_1 and V_o during the immunoprecipitation experiments (Fig. 5).

RAVE exclusively controls assembly of Vph1p-containing V-ATPases, which reside in the vacuole (Smardon, Diab et al. 2014). Thus, Vph1p-containing V-ATPases are likely

defective in *pfk2Δ*. In agreement with this notion, vacuolar pH and glucose-dependent reassembly are altered in *pfk2Δ*. In addition, *pfk2Δ* and *rav1Δ* mutants share common growth characteristics, a partial *Vma*$^-$ growth phenotype (Smardon, Diab et al. 2014). This phenotype suggests that non-vacuolar V-ATPase pumps at other cellular compartments probably are functional. Like *rav1Δ*, *pfk2Δ* may retain normal V-ATPase function at Golgi and endosomes, which house the second V_o subunit a isoform Stv1p (Smardon, Diab et al. 2014).

A difference between *pfk2Δ* and *rav1Δ* is that biosynthetic V_1V_o assembly is normal in *pfk2Δ*, but the glucose-triggered re-assembly is partially reduced. Both mechanisms, biosynthetic assembly and reassembly, are severely defective in *rav1Δ* cells which also lacks V-ATPase activity at the vacuolar membrane (Smardon, Tarsio et al. 2002). Our interpretation of these results is that RAVE activity is partially compromised in *pfk2*Δ. Only its function at mediating glucose-triggered reassembly is defective.

Are V-ATPase and glycolysis directly coupled in vivo? Glycolysis is necessary to reassemble V_1V_o complexes (Parra and Kane 1998). This study suggests that glycolysis may also modulate V-ATPase activity under steady-state conditions. *In vivo* vacuolar acidification is defective in *pfk1*Δ and *pfk2*Δ, although the V-ATPase pumps are active *in vitro*. Reactivation *in vitro* could be explained if the mechanism that inhibits proton transport *in vivo* is lost during the purification of membrane vesicles.

Glycolysis is necessary to reassemble V_1V_o complexes (Parra and Kane 1998). Glycolysis may also modulate V-ATPase activity under steady state conditions. *In vivo* proton transport is inhibited in *pfk1Δ* and *pfk2Δ*, although the V-ATPase pumps are active *in vitro*. This discrepancy could be explained if V-ATPase proton transport is inhibited in the phosphofructokinase-1 mutants *in vivo* by a mechanism lose during the purification of membrane vesicles.

Recent crystallographic data of the yeast V-ATPase complex suggest that V_1V_oreassembly may require some energy input in addition to RAVE (Oot, Huang et al. 2012; Parra, Chan et al. 2014). It is conceivable that reduced glycolytic flow and therefore lower energy (**e.g.** ATP) production contribute to the V_1V_o reassembly defects in *pfk2Δ*.

There is evidence that the glycolytic flow is reduced in the *pfk1Δ* and *pfk2Δ* mutants compared to wild-type cells (Heinisch 1986). Homomeric complexes consisting of subunit β (*pfk1Δ* cells) are more active than the subunit a-containing complexes (*pfk2Δ* cells) (Heinisch 1986) The concentration of phosphofructokinase-1 reaction product is 10- to 15-fold lower in the *pfk2Δ* mutant as compared to wild-type cells; it is only 2-fold lower in *pfk1Δ* (Heinisch 1986). In addition, the NADH spike triggered by readdition of glucose is reduced or absent in *pfk2Δ*, but not in *pfk1Δ* (Williamson, Adiamah et al. 2012; Schroder, Ozalp et al. 2013).

Additional studies will be necessary to understand the interplay between V-ATPase and glycolysis. It likely involves additional glycolytic enzymes. A super-complex consisting of V-ATPase and glycolytic enzymes has been proposed before (Su, Zhou et al. 2003; Konishi, Yamane et al. 2004; Lu, Sautin et al. 2004; Lu, Ammar et al. 2007; Su, Blake-Palmer et al. 2008). It also could directly provide glycolytic ATP to drive proton transport. Other rapid energy-consuming processes rely on glycolysis-derived ATP locally made by glycolytic enzymes at the site where the energy supply is needed. These processes include, glutamate uptake in synaptic vesicles (Ikemoto, Bole et al. 2003), regulation of ATP-sensitive K+ channels in cardiac myocytes (Weiss and Lamp 1987; Dhar-Chowdhury, Harrell et al. 2005), and phototransduction at rod and cone cells (Hsu and Molday 1991).

In summary, deletion of the structural genes encoding subunits of the glycolytic enzyme phosphofructokinase-1 interferes with yeast V-ATPase function and regulation *in vivo*, despite the fact that V-ATPases are catalytically competent and the cells can metabolize glucose. V-ATPase proton transport at the vacuole is inhibited by unknown cellular mechanisms; a reduction of the glycolytic flow is an attractive candidate. Given that RAVE-V_1 binding is enhanced and V_1V_o reassembly reduced in *pfk2*Δ, we concluded that Pfk2p is necessary for normal RAVE functions

Chapter III

Glycolysis controls glucose-dependent V-ATPase reassembly and vacuolar acidification by different mechanisms

Chun-Yuan Chan[1] and Karlett J. Parra[1*]

From the [1]Department of Biochemistry and Molecular Biology of the School of Medicine, University of New Mexico Health Sciences Center, Albuquerque, New Mexico 87131

3.1 Introduction

The vacuolar proton ATPase pump (V-ATPase) is a highly conserved multi-subunit complex present throughout the endomembrane system. V-ATPase is responsible for acidification of the Golgi Apparatus and vacuolar/lysosomal and endosomal compartments in all eukaryotic cells. V-ATPases are also present at the plasma membrane of certain cells specialized for active proton secretion. These cells include osteoclasts, intercalated cells of the kidney, and clear cells of the epididymis where V-ATPases sustain an acidic pH at the extracellular lumen (Nelson 2003; Wagner, Finberg et al. 2004; Kane 2006; Forgac 2007).

V-ATPase pumps are necessary for a broad spectrum of cellular processes. Intracellular V-ATPase proton transport generates and maintains the acidic luminal pH necessary for receptor-mediated endocytosis, membrane trafficking, protein sorting and processing, zymogen activation, and amino acid sensing in lysosomes (Forgac 2007; Mijaljica, Prescott et al. 2011; Efeyan, Zoncu et al. 2012). Plasma membrane associated V-ATPase proton transport at the apical membrane of the kidney proximal tubule cells and intercalated cells maintain the systemic acid-base balance (Stehberger, Schulz et al. 2003). At the bone osteoclasts, V-ATPases are essential for bone resorption (Yang, Feng et al. 2012). At the clear cells of the epididymis, V-ATPase-mediated acidification of the epididymal lumen sustains the low pH necessary for sperm maturation (Brown and Breton 2000). Mutations of subunit isoforms of the human V-ATPase have been described in patients with distal renal tubular acidosis (Stehberger, Schulz et al. 2003; Ochotny, Van Vliet et al. 2006) and osteopetrosis (Stehberger, Schulz et al. 2003;

Ochotny, Van Vliet et al. 2006; Su, Blake-Palmer et al. 2008). Some human conditions, including cancers (Fan, Niu et al. 2012; Michel, Licon-Munoz et al. 2013), viral infections (Kohio and Adamson 2013), and fungal infections (Kohio and Adamson 2013; Rane, Bernardo et al. 2013; Hayek, Lee et al. 2014) rely on V-ATPase normal or enhanced proton transport. This collection of studies have made V-ATPase pumps attractive therapeutic targets.

V-ATPases operate as molecular motors that couple active transport of protons to ATP hydrolysis by a rotational mechanism (Yokoyama, Nakano et al. 2003; Owegi, Pappas et al. 2006; Toei, Gerle et al. 2007; Jefferies and Forgac 2008; Lau and Rubinstein 2010). V-ATPases consist of fourteen different subunits. Eight peripheral subunits (A-H) form the V_1 domain assembled at the cytosolic side of the membrane. ATP binds and is hydrolyzed in V_1. Six subunits (a, d, e, c, c', c'') form the membrane V_o domain that binds the cytosolic protons and forms the path for proton transport (Kane 2006).

An important mechanism that regulates V-ATPase *in vivo* involves physical separation or disassembly of the V_1V_o complex into three components: V_1 subunit C, the V_1 domain without subunit C (V_1-C), and the V_o domain (Kane 1995). Disassembly occurs when glucose is absent (Kane 1995). It inactivates the pumps and alkalinizes the vacuolar lumen . Since the V_1-C sub-complexes cannot hydrolyze ATP (Zhang, Myers et al. 1992; Parra, Keenan et al. 2000; Kane 2012; Parra, Chan et al. 2014), it also prevents energy depletion (e.g., ATP) when the main energy source for most organisms, glucose, is absent. Glucose is the main and strongest external stimulus for reassembly in yeast (Kane 1995).

Glucose re-addition after a brief period of glucose-depletion triggers V_1V_o reassembly, which can be detected within 2-5 min. Reassembly resumes ATP hydrolysis and proton transport (Kane 1995; Parra and Kane 1998) and restores the acidic vacuolar pH (Nakamura 2004; Tarsio, Zheng et al. 2011). Thus, reassembly restores energy utilization by V-ATPase when glucose is available and metabolism resumes.

Reversible disassembly has been described in yeast (Kane 1995), insects (Sumner, Dow et al. 1995) and mammalian cells (Trombetta, Ebersold et al. 2003; Sautin, Lu et al. 2005). However, what is the glucose sensor and the mechanism(s) communicating the presence of glucose (or its absence) to V-ATPase remains unanswered (Kane 2012). In yeast, reversible disassembly is intertwined with glycolysis (Kane 1995; Parra and Kane 1998) and the RAS/cAMP/ PKA pathway (Bond and Forgac 2008), and involves a V-ATPase-dedicated chaperone complex (the Regulator of the (proton)-ATPase of the Vacuolar and Endosomal Membranes, RAVE) (Seol, Shevchenko et al. 2001; Smardon, Tarsio et al. 2002; Smardon and Kane 2007; Smardon, Diab et al. 2014).

Several lines of evidence suggest that glycolysis could control V_1V_o reassembly: 1) Only rapidly fermentable carbon sources such as mannose and fructose can substitute for glucose in triggering reassembly of V-ATPase complexes (Parra and Kane 1998). 2) Addition of less efficiently fermented carbon sources such as raffinose and galactose, or non-fermentable carbon sources such as glycerol and ethanol, do not trigger reassembly (Wick, Drury et al. 1957; Kane 1995; Parra and Kane 1998). 3) Glucose-dependent V_1V_o reassembly is impaired in a phosphoglucose isomerase glycolytic mutant that

accumulates glucose 6-phosphate and blocks glycolysis; only fructose, which bypasses the phosphoglucose isomerase step and resumes glycolysis, can trigger V_1V_o reassembly (Parra and Kane 1998). And lastly, 4) Pharmacologic inhibition of glycolysis with 2-deoxyglucose causes V_1V_o disassembly and 2-deoxyglucose cannot trigger reassembly. (Parra and Kane 1998).

Glucose-triggered reversible disassembly is not an all-or-none response (Parra and Kane 1998); under steady state conditions, the level of assembled V_1V_o is proportional to the concentration of glucose in the media (Parra and Kane 1998). In addition, cells contain pools of cytosolic V_1 and membrane bound V_o domains that co-exist with fully assembled V_1V_o complexes at the vacuolar membrane (Doherty and Kane 1993; Myers and Forgac 1993; Sumner, Dow et al. 1995). When glucose is abundant, yeast cells contain about 70% of the V_o domains assembled and the remaining 30% disassembled. The equilibrium $V_1 + V_o : V_1V_o$ is switched in response to glucose. It favors disassembly ($V_1 + V_o$) if the glucose level drops; it favors assembly (V_1V_o) if the glucose level raises (Parra and Kane 1998). The fact that complete removal of glucose leads to about 75%-80% disassembly (Kane 1995), suggests that 20-25% of assembled V_1V_o is sufficient to maintain basal levels of V-ATPase function necessary for survival during nutrient scarcity (Kane 1995).

An interplay between V-ATPase and the glycolytic enzymes aldolase and phosphofructokinase-1 has been described and appears to be important for V-ATPase function (Lu, Holliday et al. 2001; Su, Zhou et al. 2003; Lu, Sautin et al. 2004; Lu, Ammar et al. 2007; Su, Blake-Palmer et al. 2008). Aldolase interacts with several V-

ATPase subunits (subunits B and E from V_1 and subunit a from V_o). Aldolase is necessary for V_1V_o assembly (Lu, Ammar et al. 2007) and its overexpression prevents disassembly in yeast (Lu, Ammar et al. 2007). Human phosphofructokinase-1 binds the V_o subunit a (isoform a4), and associates with V-ATPase pumps in human kidney cells (Su, Zhou et al. 2003; Su, Blake-Palmer et al. 2008). Notably, mutations in subunit a4 that prevent V-ATPase binding to phosphofructokinase-1 cause distal renal tubular acidosis (Su, Blake-Palmer et al. 2008). Phosphofructokinase-1 catalyzes the phosphorylation of fructose 6-phosphate into fructose 1,6 -bisphosphate, the substrate for aldolase.

The yeast phosphofructokinase-1 enzyme has two subunits, Pfk1p (α subunit) and Pfk2p (β subunit), that form a hetero-octameric complex ($\alpha_4\beta_4$) (Banaszak, Mechin et al. 2011). Although both subunits have catalytic and regulatory functions, the *PFK2* deletion has much more significant metabolic implications. The *pfk2Δ* cells do not have detectable glycolytic oscillations (Williamson, Adiamah et al. 2012) and Pfk2p binds the glycolytic activator, fructose-2,6-bisphosphate (F2,6BP) that is made by *PFK26* and *PFK27*. The triple deletion strain *pfk1Δ pfk26Δ pfk27Δ* strain cannot grow on glucose, but *pfk26Δ pfk27Δ* metabolizes glucose (Muller, Zimmermann et al. 1997), suggesting the F2,6BP-Pfk2p binding is essential for Pfk2p activity. In addition, *pfk2Δ* cells have 5 - 7.5 fold lower concentration of the phosphfructokinase-1 reaction product, fructose 1,6 biphosphate than *pfk1Δ* cells.

Chapter II studied the functional interrelation between phosphofructokinase-1 and V-ATPase in yeast (Chan and Parra 2014). We characterized the yeast mutant strains *pfk1Δ* and *pfk2Δ*. The *pfk2Δ* mutant exhibits a number of traits indicative of V-ATPase functional defects *in vivo*, despite that V-ATPase pumps are functionally competent in *pfk2Δ* vacuolar membrane fractions *in vitro* (Chan and Parra 2014). In addition, the *pfk2Δ* cells have alkalinized vacuoles, reduced glucose-dependent V_1V_o reassembly, and growth sensitivity to pH 7.5 in the presence of calcium (Chan and Parra 2014).

Chapter III investigated the factors that suppress V-ATPase function in the *pfk2Δ* strain *in vivo*. Phosphofructokinase-1 is a rate-limiting step in glycolysis and an allosteric control point that senses the energetic state of the cell (Farooqui, Kim et al. 1980; Simonis, Wodak et al. 2004). Thus, we hypothesized that a reduction of the glycolytic flow in *pfk2Δ* suppressed V-ATPase function. We examined V-ATPase, Pfk2p, and glycolysis at steady state and under reversible disassembly conditions in *pfk2Δ* cells and cells overexpressing Pfk2p (Pfk2-ov). V-ATPase functions were rescued by increasing the amount of glucose available from 2% to 4%. Restoration of vacuolar acidification, V_1V_o reassembly, and growth correlated with an increase in the glucose-dependent rate of NADH formation (metabolic reactivation) and the concentration of ethanol produced. These results are the first direct evidence that stimulation of the glycolytic flow itself is sufficient to induce V_1V_o reassembly after glucose readdition. Expression of phosphofructokinase-1 subunits is not essential for reassembly and V_1V_o reactivation. Notably, reactivation after reassembly correlated with an increased level of the ATP

producing glycolytic enzyme, phosphoglucose isomerase (Pgk1p), at vacuolar membranes.

3.2 Materials and Methods

Materials and strains. The antibody to the Myc antigen was from Invitrogen (Carlsbad, CA). DSP was purchased from Pierce (Rockford, IL), and Tran [35S]-label from MP Biomedicals (Santa Ana, CA). The 10D7 and 13D11 antibodies were from Invitrogen (Carlsbad, CA). The anti-phosphoglycerate kinase antibody 22C5D8 was from Invitrogen (Carlsbad, CA). Alkaline phosphatase-conjugated secondary antibody was from Promega (Madison, WI) and horseradish peroxidase secondary antibody was purchased from Invitrogen (Carlsbad, CA). Zymolase 100T was purchased from Seikagaku (Tokyo, Japan), Concanamycin A from Wako Biochemicals (Richmond, VA), and Ficoll and carbonyl cyanide m-chlorophenyl hydrazone from United States Biologicals (Swampscott, MA). All other reagents were from Sigma (St. Louis, MO). The ATP assay kit was purchase from Biovision (K354-100)(Milpitas, CA) and ethanol assay kit was purchased from Abcam (ab65343)(Cambridge, MA). The *Saccharomyces cerevisiae* strains referred to throughout are listed in Table 1. The mutant strains were verified by PCR using primers to amplify the *PFK2* gene with promoter sequences, Xho I and Xma I cutting site. We cloned the *PFK2* gene into the 2μ vector (pRS426) to overexpress the *PFK2* gene; the primers used are listed in Table 2.

Growth phenotype. Cells were grown overnight to 0.4 - 0.6 OD A_{600}/mL in YEPD (1% yeast extract, 2% peptone and 2% glucose) medium buffered to pH 5.0. Cultures were washed twice with sterile ddH_2O and 2.5 OD A_{600} cells were resuspended into 1 mL sterile ddH_2O. Ten-fold serial dilutions were spotted onto YEP containing 2% or 4% glucose. Plates were buffered to pH 5.0 with 50 mM succinic acid/ sodium phosphate, pH 7.5 with 50 mM MES/ MOPS, or pH 7.5 with 100 mM calcium chloride added. The plates were incubated for three days at 30 ^{o}C and 37 ^{o}C.

Vacuolar pH measurements. Vacuolar pH was measured using the ratiometric fluorescent dye BCECF-AM (Martinez-Munoz and Kane 2008). Cells were grown to A_{600} 0.4 - 0.8 and stained with 50 µM BCECF-AM for 30 minutes at 30^{o}C. To generate a pH calibration curve for each strain, A_{600} 5 OD unit cells were added to 2 ml of buffer pH = 5.5, 5.75, 6.0, 6.25, 6.5, 7.0. Calibration buffers consisted of 50 mM MES, 50 mM HEPES, 50 mM KCl, 50 mM NaCl, 200 mM ammonium acetate, 10 mM sodium azide, 10 mM 2-deoxyglucose, 50 µM and carbonyl cyanide m-chlorophenyl hydrazone (CCCP). Cells were incubated in calibration buffer 30 - 45 minutes at 30^{o}C. For steady state studies, the cells were stained with BCECF and transferred to 1 mM HEPE/MES pH 5.0 buffer with 2% or 4% glucose (final concentration). The BCECF fluorescence was measured for 10 minutes at 30^{o}C. Vacuolar pH was calculated according to the standard curve. For studies under reassembly conditions, the vacuolar pH was monitored for 20 minutest after 2% or 4% glucose (final concentration) re-addition to cells deprived of

glucose for 10 minutest. The BCECF fluorescence intensity (emission 525 nm, excitation 490 nm/450 nm) was measured in a FluoroMax 4 spectrofluorometer (Horiba Jobin Yvon Inc., NJ).

Immuniprecipitations. *Biosynthetically radiolabeled cells.* Pulse-chase experiments followed by nondenaturing immunoprecipitations of V-ATPase complexes were performed as described previously with the monoclonal antibodies 13D11 (anti V_1 subunit B) and 10D7 (anti V_o subunit a, Vph1p isoform), except that the chases were performed at the indicated glucose concentrations and times. The immunoprecipitated protein was separated by SDS-PAGE (13% acrylamide gels), the gels were dried, scanned in a Fuji Scanner FLA-5100, and analyzed using the Multi Gauge and GraphPad Prism 5 software as previously described (Ediger, Melman et al. 2009; Parra, Chan et al. 2014). *Non-radiolabeled immunoprecipitations*. Immunoprecipitations were as described before (Chan and Parra 2014). The immunoprecipitated protein was separated by SDS-PAGE in 10% gels and analyzed by Western blots. The nitrocellulose membranes were scanned using a Bio-Rad ChemiDoc XRS+ and the intensity of protein bands quantified using the Multi Gauge and GraphPad Prism 5 software.

NADH fluorescence measurement. NADH fluorescence was measured as described by Poulsen et al with the following modifications (Poulsen, Andersen et al. 2008). Briefly, cells were grown overnight to A_{600} 0.6 - 0.8 OD in 200 ml YEP+2% glucose, harvested and 100 OD units resuspended in 50 mM potassium phosphate buffer pH 6.8 up to a

density of 10% by weight. The cells were starved of glucose by incubation in phosphate buffer for 3 hours on a rotary shaker at 30°C and placed on ice for 10 minutes before the NADH measurements were intiated. The NADH fluorescence intensity (excitation at 366 nm; emission at 450nm) was monitored without glucose for 60 seconds and then continuously recorded for another 90 seconds after re-addition of 2% or 4% glucose at 25°C in a FluoroMax 4 spectrofluorometer (Horiba Jobin Yvon Inc., NJ).

Ethanol conditions assay. For steady state analyses, the cells were cultured overnight to A_{600} 0.4 - 0.6 OD in YEP pH 5.0 media or in SC-Ura pH 5.0 media containing 2% or 4% glucose. 2 OD units (per condition) were harvested and the cells were converted to sheroplasts by zymolase treatment. The spheroplasts were incubated in YEP (containing 2% or 4% glucose) pH 5.0 plus 1.2 M sorbitol for 10 minutes at 30°C and the ethanol concentration was measured using the Ethanol Assay Kit (Abcam, Cambridge, MA, US) according to the manufacturer's instructions. Briefly, spheroplasts were lysed and an ethanol standard curve with 0, 2, 4, 6, 8, 10 nmol/well in a 96 well plate was prepared. The reaction mix was contained 94 µl ethanol assay buffer plus 2 µl ethanol probe, 2 µl ethanol enzyme mix and 2 µl of the cell lysis to final 100 µl/reaction. The reaction was incubated for 30 minutes at 37°C protected from light and the absorbance (A_{570}) measured in a micro-plate reader. The ethanol concentration was calculated according to the standard curve. For glucose-depletion and re-addition analyses, the cells were grown in media containing 2% glucose overnight and converted to spheroplasts as described above. The spheroplasts were incubated in YEP pH 5.0 plus 1.2 M sorbitol in the presence of 2% glucose for 20 minutes (+G), in YEP plus 1.2M sorbital for 10 minutes (-

G), and in YEP plus 1.2M sorbital for 10 minutes followed by re-addition of 2% glucose, 4% glucose or 2% 2-deoxyglucose for 10 minutes at 30°C (-/+G). The cells were lysed and the ethanol concentration measured as described above.

ATP concentration assay. Cells were grown overnight to A_{600} 0.4 to 0.6 OD in YEP pH 5.0 media containing 2% glucose and converted to spheroplasts as described in the ethanol concentration assay. The spheroplasts were incubated in YEP pH 5.0 plus 1.2 M sorbitol media with 2% glucose for 20 minutes (+G), in YEP plus 1.2M sorbital for 10 minutes (-G), and in YEP plus 1.2 M sorbital for 10 minutes followed by addition of 2% glucose or 4% glucose for 10 minutes at 30°C (-/+G). ATP concentration was measured by using the ATP Assay Kit according to the manufacturer instructions.

Other methods. Vacuolar membranes fractions were purified by Ficoll density gradient centrifugation as described (Owegi, Pappas et al. 2006; Ediger, Melman et al. 2009; Chan and Parra 2014). Protein concentration was measured by the Bradford assay (Parra, Chan et al. 2014).

Table 1. S. cerevisiae strains used in this study

Strain	Parent	Relevant phenotype
WT	BY4742	*MAT_α; his3 Δ 1; leu2 Δ _0; lys2 Δ 0; ura3 Δ 0*
pfk1Δ	BY4742	*MAT_α; his3 Δ 1; leu2 Δ _0; lys2 Δ 0; ura3 Δ 0 pfk1Δ: KanMX6*
pfk2Δ	BY4742	*MAT_α; his3 Δ 1; leu2 Δ _0; lys2 Δ 0; ura3 Δ 0 pfk2Δ: KanMX6*
vm3Δ	BY4742	*MAT_α; his3 Δ 1; leu2 Δ _0; lys2 Δ 0; ura3 Δ 0 vm3Δ : KanMX6*

Table 2

Primers used to clone *PFK2* in pRS426

Primer	Sequence (5'-3')
PFK2-XmaI	GGGCCCGGGCTCATGTTTCTTATTAGG
PFK2-XhoI	GGGCTCGAGTTAATCAACTCTCTTTCTTCC

3.3 Results

We recently showed that both phosphofructokinase-1 subunits make contributions to V-ATPase activity, but the most critical subunit is Pfk2p (Chan and Parra 2014). Pfk2p expression is necessary for optimal V-ATPase function at steady state and under glucose-dependent V_1V_o reassembly conditions. The *PFK2* deletion (*pfk2Δ*) cells cannot sufficiently reassemble V_1V_o and do not acidify their vacuoles. The enzyme phosphpfructokinase-1 catalyzes a limiting step of glycolysis and *pfk2Δ* has reduced downstream glycolytic intermediates, glucose consumption, and ethanol production (Heinisch 1986; Heinisch 1986; Arvanitidis and Heinisch 1994). In this study, we examined the interplay between V-ATPase, Pfk2p, and glycolysis to determine whether Pfk2p itself or its glycolytic function control V-ATPase function.

Pfk2p overexpression interferes with glucose-dependent vacuolar acidification. We reasoned that we might alter the V-ATPase function by modulating *PFK2* production. Cells lacking *PFK2* had a reduced capacity to reassemble V-ATPase complexes (by 50%) and cannot acidify the vacuoles after re-addition of glucose following a brief glucose deprivation period. We overexpressed the *PFK2* gene from a 2μ plasmid to get insights into the functional interrelation between *PFK2* and V-ATPase. If Pfk2p itself is crucial for V-ATPase function and glucose-dependent reassembly, the overexpression of Pfk2p might enhance V-ATPase activity and/or affect V_1 reversible dissociation from V_o.

First, we confirmed overexpression of Pfk2p by Western blots. The presence of Pfk2p in

whole cell lysates was assessed using a polyclonal antibody to phosphofructokinase-1 that recognizes both Pfk1p and Pfk2p subunits (Fig. 1A). The Pfk2p expression was increased by about 2.5 fold in the cells transformed with the multi-copy plasmid carrying the exogenous *PFK2* gene, compared to wild type cells transformed with the empty 2m plasmid.

Next, we asked if the glucose-dependent V_1V_o reversible disassembly was affected by overexpressing Pfk2p. We performed co-immunoprecipitation experiments under nondenaturing conditions to measure the proportion of V_1V_o complexes that reversibly disassemble in response to glucose depletion and glucose re-addition. V-ATPase disassembled normally after 10 min of glucose depletion (Fig. 1B, -G condition). The amount of V_o subunit a co-immunoprecipitated with V_1 subunit A by the antibody 13D11 to the V_1 subunit B decreased by about 90 % in the wild-type. About 70 % of the V_1V_o complexes disassembled in the Pfk2p overexpressing cells. Re-addition of glucose to a final concentration of 2 %, which is the amount of glucose present in yeast growth media, triggered reassembly of the V_1V_o complexes in both strains (-/+G condition in Fig. 1B). Reassembly was evident by the reassociation of the V_o subunit a with V_1 subunits A and B.

We next determined whether the reassembled pump acidified the vacuolar lumen of the cells overexpressing Pfk2p. We monitored the vacuolar pH *in vivo* under disassembly and reassembly conditions using the pH sensitive fluorophore BCECF (Fig. 1C) (Martinez-Munoz and Kane 2008; Chan and Parra 2014). Glucose re-addition steadly increased the

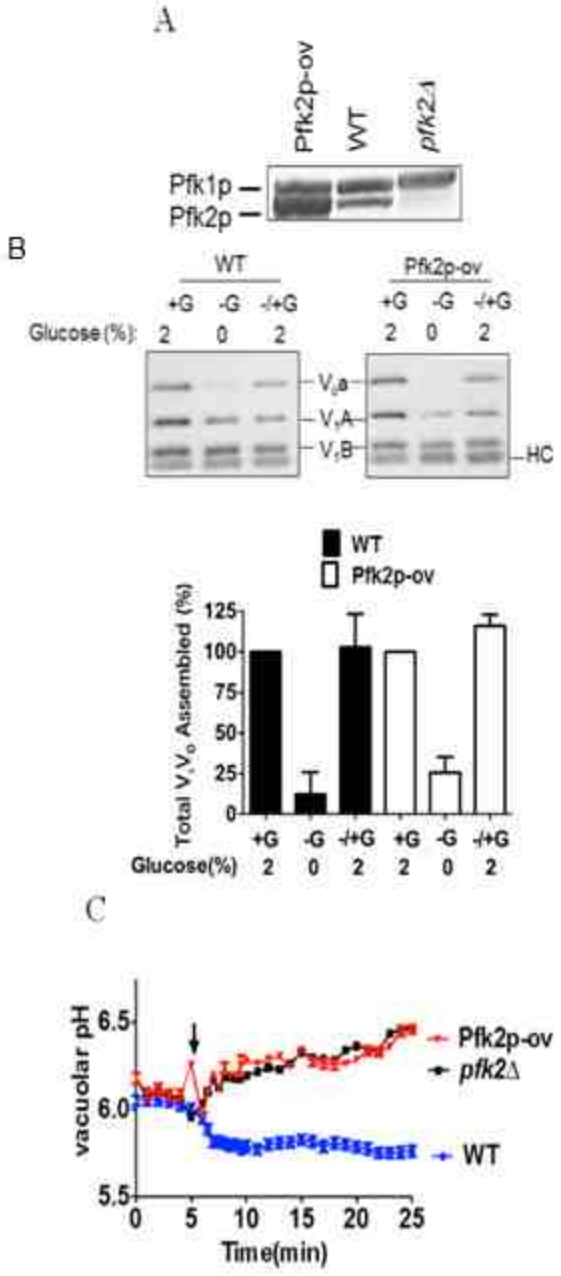

Figure 1. G**lucose-dependent V_1V_o reassembly and vacuolar acidification in Pfk2p overexpressing cells. A.** *overexpression of exogenous Pfk2p*. Cells were cultured to mid-log phase (A_{600}/ml= 0.8). Whole cell extracts were obtained from Pfk2p overexpressing (Pfk2p-ov), pfk2 deletion (*pfk2Δ),* and an isogenic wild type cells carrying the empty vector pRS426. The whole cell extracts were separated in 10% SDS-PAGE gels and immunoblotted with a polyclonal antibody that recognizes Pfk1p and Pfk2p subunits of yeast phosphofructokinase-1. **B.** *Glucose-dependent disassembly and reassembly of V_1V_o is normal in Pfk2p-ov*. Pfk2p-ov and isogenic wild type cells were grown to 1.0 OD A_{600}/ml. The cells were converted to sheroplasts by zymolase treatment, incubated in YEPD plus 1.2 M sorbitol for 20 minutes (+G), YEP plus 1.2 M sorbitol for 10 minutes (-G) and YEP plus 1.2 M sorbitol for 10 minutes after which 2% glucose was added for another 10 minutes (-/+G). V-ATPase was immunoprecipitated using a monoclonal antibody to V_1 subunit B (13D11) and protein A sepharose beads (Chan and Parra 2014). The imunoprecipitated proteins were separated in 10% SDS-PAGE gel and immunoblotted with monoclonal antibodies to V_1 subunit A (V_1A), V_1 subunit B (V_1B) and V_o subunit a (V_oa). HC: antibody heavy chain. Data is representative of two independent experiments; error bars are standard deviation compared to wild-type **C.** *Glucose-dependent vacuolar acidification is impaired in Pfk2p-ov cells.* Mid-log phase cultures from wild type, *pfk2Δ* and Pfk2p-ov cells were grown in YEPD and selective media (SC-Ura) containing 2% glucose, respectively. Cells were harvested and stained with 50 mM BCECF-AM for 30 minutes at 30°C, after which cells were depleted of glucose for 10 minutes, and glucose added to a final concentration of 2% (arrow). Fluorescence was monitored for an additional 20 minutes. The ratio of fluorescent emission (525 nm) excited at 490 and 450 nm was measured in a FluoroMax 4 spectrofluorometer (Horiba Jobin Yvon Inc., NJ) and the fluorescence compared to standard curves to generate absolute pH values.

vacuolar pH of Pfk2p-ov cells resembling lose of function the V-ATPase mutants lacking a structural gene (Chan and Parra 2014).. These results indicated that the reassembled pumps did not re-activate at the vacuolar membrane. For reference, glucose re-addition immediately acidified the vacuolar lumen of the wild-type cells as expected. Thus, that reassembled pumps resumed proton transport. The absence of Pfk2p (*pfk2Δ* cells) partially impaired reassembly (Chan and Parra 2014), but excess Pfk2p (Pfk2p-ov cells) did not affect disassembly or reassembly. Nonetheless, the reassembled V_1V_o complexes failed to resume proton transport in Pfk2p-ov cells.

Reactivation of glycolysis after glucose re-addition is defective in pfk2Δ cells. Despite that Pfk2-ov and *pfk2Δ* cells cannot acidify the vacuole in response to glucose readdition, an important difference between Pfk2p-ov and *pfk2Δ* cells is that *pfk2Δ* cannot sufficiently reassemble V_1V_o in response to glucose (Chan and Parra 2014). In contract, Pfk2p-ov cells reassembled V_1V_o normally (Fig. 1B). Since the phosphofructokinase-1 enzyme catalyzes a limiting step in glycolysis we asked whether a reduced glycolytic flow could account for defective reassembly in *pfk2Δ*. We anticipated that *pfk2Δ* cells will have lower glycolytic flow than Pfk2p-ov.

In *Sacharomyces cerevisiae* the final product of glycolysis, pyruvate, is fermented into ethanol (Leskovac, Trivic et al. 2002). We measured ethanol concentration at steady state, and under disassembly (10 minutes after glucose depletion) and reassembly (10 min after glucose re-addition) conditions (Figs. 2A and 2B). At steady state the wild type strain

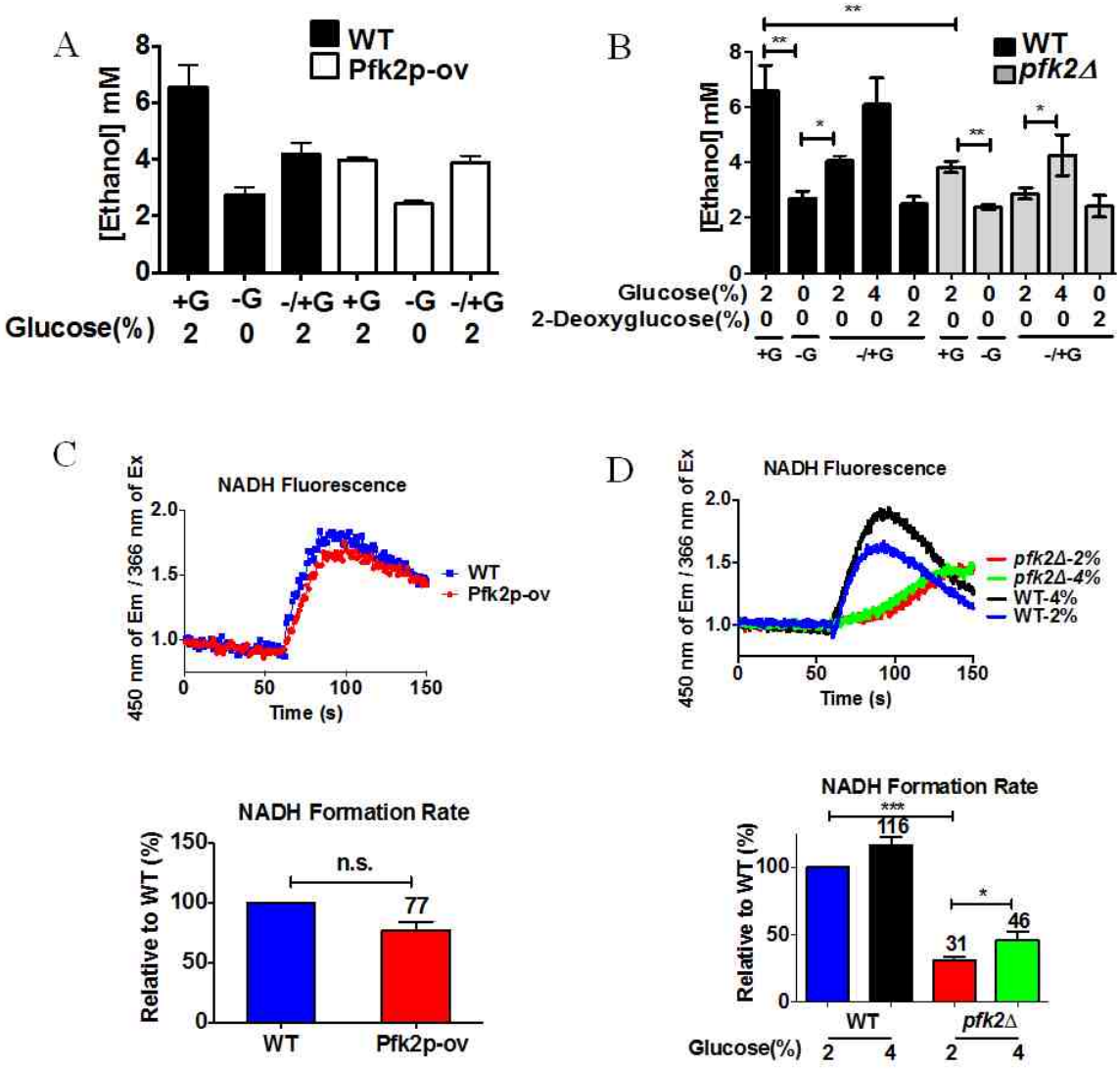

Figure 2. **Glucose-dependent metabolic reactivation after glucose depletion in Pfk2p-ov, *pfk2Δ*, and wild-type cells. A.** *2% glucose addition after brief glucose-depletion increases the ethanol concentration in wild type and Pfk2p-ov cells.* Cells were cultured to mid-log phase (0.6 - 0.8 OD Abs_{600}/ml) converted to spheroplasts and incubated in YEP pH 5.0 plus 1.2 M sorbitol media with 2% glucose for 20 minutes (+G), in YEP plus 1.2M sorbitol for 10 minutes (-G), and in YEP plus 1.2M sorbitol for 10 minutes followed by addition of 2% glucose for 10 minutes at 30°C (-/+G). Ethanol concentration was measured using a colorimetric assay from (Abcam Cambridge, MA). Data represent three independent experiments; error bars= +/- standard deviation. **B.** *The ethanol concentration is proportional to the amount of glucose added to wild-type and pfk2Δ cells.* Cells were cultured to mid-log phase (0.6 - 0.8 OD A_{600}/ml) in YEP containing 2% glucose (YEPD), converted to spheroplasts and incubated as described for Figure 1B in the presence and absence of glucose and after re-addition 2% glucose, 4% glucose, or 2% 2-deoxy-glucose (final concentrations). Ethanol concentrations were measured as described for Figure 2A. Data represent three independent measurements; error bars are standard deviation. Statistically significant differnces ($p<0.05$ *, $p<0.01$ **) as compared to the presence 2% glucose were determined by two-tailed unpaired *t*-test. **C.** *Pfk2p-ov NADH synthesis rate after re-addition of 2% glucose resembles wild type cells.* The wild type and *Pfk2p-ov* cells were grown overnight to 0.6 - 0.8 OD A_{600}/ml, washed twice in 50 mM potassium phosphate buffer pH 6.8 and resuspended in the same buffer to 10% wet weight. The cells were incubated with shaking at 30°C for three hours and kept on ice until use. The NADH fluorescence intensity (450 nm emission; 366 nm excitation) was monitored for 60 seconds in the absence of glucose and after 2% glucose (final concentration) was added (*arrow*) for another 120 seconds. Velocities were calculated for the initial 15 seconds following glucose addition and expressed relative to wild-type cells. Data represent two independent experiments; error bars are standard deviation. Statistically significant differences ($p<0.05$ *, $p<0.01$ **) as compared to the wild type cells in the presence of 2% glucose. **D.** *The NADH synthesis is significantly reduced in pfk2Δ cells.* The wild type and *pfk2Δ* cells were cultured overnight in YEPD pH 5.0 (2% glucose media) and the NADH fluorescence intensity monitored as described for Figure 2C but at 2% glucose and 4% glucose (final concentration). Data represent three independent experiments; error bars are standard deviation. Statistically significant differences ($p<0.05$ *, $p<0.01$ **) as compared to wild type cells in the presence 2% glucose and determined by two-tailed unpaired *t*-test.

produced 6.6 +/- 0.9 mM, Pfk2p-ov 4.0 +/- 0.1 mM, and *pfk2Δ* 3.8 +/- 0.2 mM ethanol. After glucose depletion the ethanol concentration dropped to about 2.5 +/- 0.2 mM in the three strains. As expected, the concentration of ethanol increased after re-addition of 2% glucose. The ethanol concentration was 4.1+/-0.2 mM in the wild-type (lower than the steady state concentration), 3.9 +/- 0.2 mM in Pfk2p-ov cells (same as steady state concentration), and 2.9 +/-0.2 mM in *pfk2Δ* (lower than steady state concentration). Thus, re-addition of 2% glucose resumed glycolysis in the three strains, but glycolysis may have been stimulated to a lesser extent in *pfk2Δ* cells.

Because ethanol production is an indirect metric of glycolysis, we examined real-time glucose-mediated metabolic activation by monitoring a glycolytic intermediate, NADH. NADH transiently peaks once metabolism resumes (Poulsen, Andersen et al. 2008) because addition of glucose after nutrient limitation triggers a rapid increase of $NADH/NAD^+$ that inhibits the glycolytic enzyme triose phosphate dehydrogenase (Williamson, Adiamah et al. 2012). This NADH spike was similar in the wild-type and Pfk2p-ov cells, although the relative rate of NADH formation the first 15 seconds after readdition of 2% glucose was slightly reduced (by 23 +/- 7.1 %) (Fig. 2C). These results indicate that glucose-mediated metabolic reactivation was comparable in Pfk2p-ov and wild-type cells. Notably, the NADH synthesis rate was significantly reduced (by 70 %) in *pfk2Δ* cells (Fig. 2D), suggesting that the glycolytic flow is considerably defective in *pfk2Δ*.

Addition of 4% glucose increases the glycolytic flow and rescues the reassembly defect in pfk2Δ. Our data indicate that glucose-dependent glycolytic reactivation is defective in *pfk2Δ* cells, which exhibit V_1V_o reassembly defects. In contrast, Pfk2p-ov cells have near wild type glycolytic flow, and reassemble V_1V_o normally (Fig. 2D). We asked whether stimulating the glycolytic flow in *pfk2 D* could rescue *pfk2Δ* glucose-dependent V_1V_o reassembly. We increased the concentration of glucose added to *pfk2Δ* cells, monitored ethanol and NADH as glycolytic metrics, and calculated the total level of V_1V_o that reassembled. As expected, the ethanol concentration and the rate of NADH formation rate increased. Ethanol levels and NADH formation increased about 1.5 - 2.0-fold after increasing the concentration of glucose added to the media from 2% to 4% (Figs. 2B and 2D). The concentration of ethanol was 2.4 +/- 0.1 mM at 2% glucose and to 4.3+/-0.7 mM at 4% glucose. The NADH synthesis rate was enhanced from 31% to 46% relative to wild-type cells. Thus the metabolic activation rate was increased by about 50% after doubling the concentration of glucose added to *pfk2Δ*. These results suggest that 4% glucose addition stimulated the glycolytic flow in relation to 2% glucose

To measure the proportion of reassembled V_1V_o complexes at 4% glucose we biosynthetically radiolabeled wild-type and *pfk2Δ* cells with ^{35}S (Fig. 3) (Ediger, Melman et al. 2009). The radiolabeled cells were chased with *i)* 2% glucose constitutively present (steady state condition) (+G, Fig. 3), *ii)* 10 min after glucose removal (glucose depletion condition) (-G, Fig. 3), and *iii)* 10 min after re-addition of glucose at varied concentrations up to 4% glucose (glucose re-addition condition) (-/+G, Fig. 3). The V-ATPase complexes were immunoprecipitated under nondenaturing conditions with the

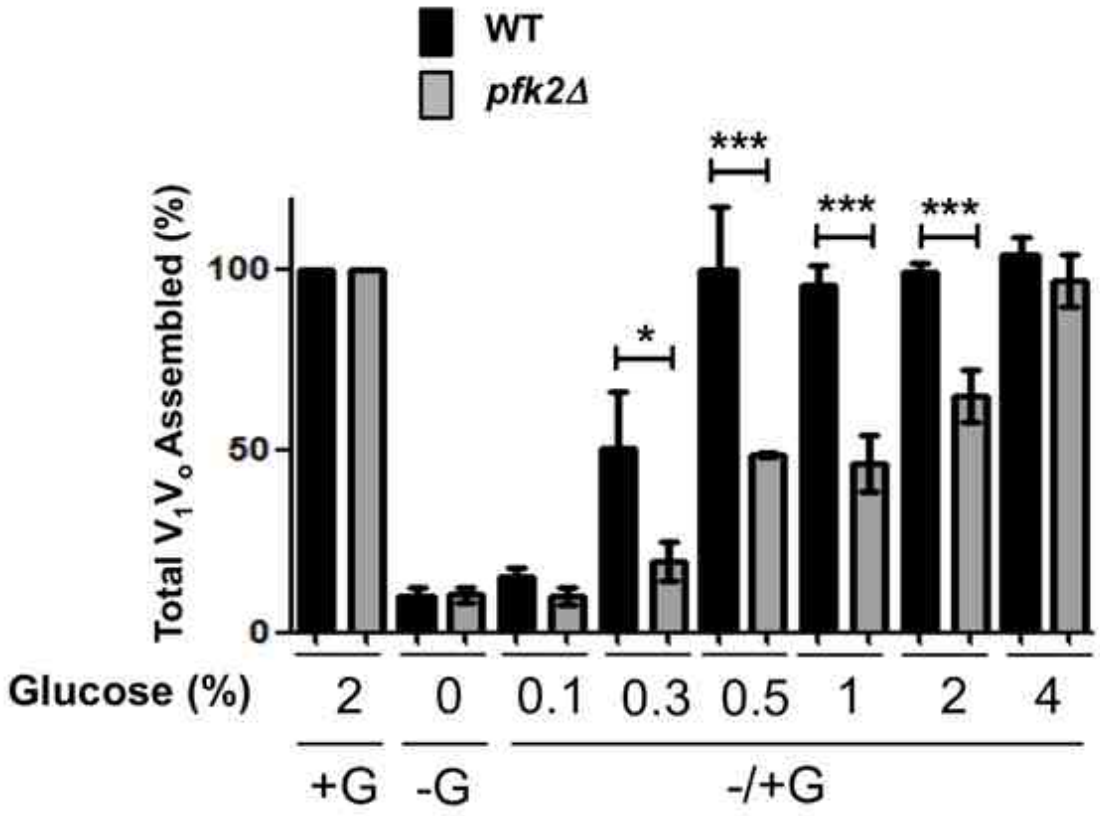

Figure 3. **Glucose-dose dependency of V-ATPase reassembly in *pfk2Δ* and wild-type cells.** Cells were cultured to mid-log phase (0.4 - 0.6 OD Abs_{600}/ml) in YEPD pH 5.0, converted to spheroplasts and radiolabeled with $Tran^{35}S$ for 60 minutes (Ediger, Melman et al. 2009). Biosynthetically radiolabeled wild-type and *pfk2Δ* cells were chased in the presence of glucose (+G) for 20 minutes (YEP media containing 2% glucose plus 1.2 M sorbitol), after glucose depletion (-G) for 10 minutes (YEP media plus 1.2 M sorbitol), and after glucose re-addition at varied concentrations (0.1, 0.3, 0.5 1, 2, and 4 %) to glucose-starved cells (-/+G) for an additional 10 minutes. The cells were lysed and V-ATPase complexes immunoprecipitated under non-denaturing conditions using anti-V_1 subunit B (recognizes V_1 an V_1V_o) and anti-V_o subunit a (recognizes V_o) monoclonal antibodies. The immunoprecipitates were separated by SDS-PAGE in 13% gels and the proportion of V_1V_o assembled calculated as the fraction of V_o (co-immunoprecipitated with anti-V_1 subunit B) relative to the total V_o (recognized by anti-V_1 subunit B and anti-V_o subunit a). Data was analyzed in a Fuji Scanner FLA-5100, Multi Gauge and GraphPad Prism 5 software. Results are presented as average from three independent experiments, and error bars are standard deviation. Statistically significant differences ($p<0.05$ *, $p<0.001$ ***) as compared to presence 2% glucose were determined by two-tailed unpaired *t*-test.

antibody 13D11 that recognizes the V_1 subunit B (immunoprecipitates V_1 and V_1V_o) and the antibody 10D7 (immunprecipitates V_o). 10D7 binds to a cryptic epitope in V_o subunit a when V_1 is not attached to V_o. The proportion of V_o assembled into V_1V_o was estimated by comparing the amount of V_o subunit a immunoprecipitated with 13D11 to the total immunoprecipitated with both antibodies (V_1 subunit B and V_o subunit a) (Kane 1995). About 80% of the assembled V_1V_o complexes at steady state disassembled after 10 minutes of glucose depletion (Fig. 3). Glucose re-addition triggered reassembly, which was proportional to the concentration of glucose added to both cell types (Fig. 3) (Parra and Kane 1998). However, a higher concentration of glucose was required for *pfk2Δ* to reach wild-type reassembly levels. In wild-type cells, addition of 0.3% glucose stimulated reassembly of 50% the complexes; 0.5% glucose stimulated 100% reassembly. In *pfk2Δ* cells, addition of 1% glucose was necessary to achieve 50% reassembly; steady state levels of assembly (100% reassembly) required 4% glucose. Thus, addition of 4% glucose rescued the *pfk2Δ* V_1V_o reassembly defect observed at 2% glucose.

4% glucose restores glucose-dependent vacuolar acidification in pfk2Δ cells. We next asked whether V_1V_o complexes that reassembled at 4% glucose were functional in *pfk2Δ*. We measured vacuolar pH after addition of 4% glucose to glucose depleted *pfk2Δ* cells, because vacuolar acidification is a direct consequence of V-ATPase reactivation (Chan and Parra 2014). We have previously shown that re-addition of 2% glucose to *pfk2Δ* cells did not acidify the vacuoles (Chan and Parra 2014). We loaded the wild-type and *pfk2Δ* cells with BCECF and deprived the cells of glucose for 10 minutes, after which 2% or 4% glucose was added and the vacuolar pH measured continuously as a function of time

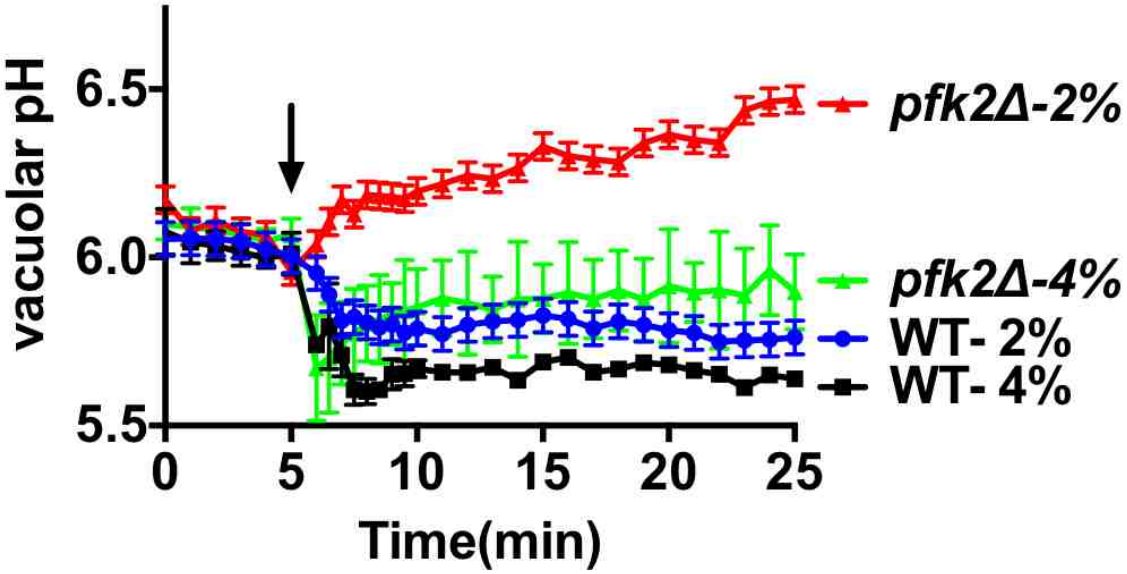

Figure 4. Vacuolar pH measurements after re-addition of 2% and 4% glucose to glucose-deprived *pfk2Δ* cells. *Addition of 4% glucose rescues vacuolar acidification in pfk2Δ cells.* The *pfk2Δ* cells were grown to 0.6 - 0.8 OD Ab_{600}/ml in YEPD pH 5.0 media. The cells were harvested and stained with 50 mM BCECF-AM for 30 minutes at 30°C. The stained cells were deprived of glucose (1 mM HEPE/MES pH 5.0 buffer) for 10 minutes after which glucose was re-added (2% or 4% glucose) (*arrow*) and the florescence measured for 20 minutes. The vacuolar pH was estimated as described in Figure 1C. (▲): *pfk2Δ*, 2% glucose, (▲): *pfk2Δ*, 4% glucose, (●): wild type, 2% glucose. (■): wild type, 4% glucose.

(Chan and Parra 2014). As expected, the wild-type cells acidified the vacuolar lumen immediately after 2% or 4% glucose addition (Fig. 4), indicating that the V-ATPase pumps were functional, consistent with previous studies (Martinez-Munoz and Kane 2008). The glycolytic mutant *pfk2Δ* did not acidify the vacuoles in response to 2% glucose (Chan and Parra 2014). Notably, addition of 4% glucose to *pfk2Δ* restored the vacuolar acidic pH, indicating that proton transport resumed. Together, our results showed that 4% glucose rescued glucose-dependent regulation, V_1V_o reassembly and reactivation of V-ATPase in *pfk2Δ* cells.

The presence of 4% glucose at steady state rescues V-ATPase functional defects in pfk2Δ.

In addition to glucose-dependent reassembly defects, the *pfk2Δ* mutant has alkalinized vacuoles and a growth phenotype suggestive of V-ATPase impairment at steady state in 2% glucose (Chan and Parra 2014). We asked whether 4% glucose can rescue V-ATPase-associated phenotypes in *pfk2Δ* cells at steady state. First, we measured the ethanol concentration at 2% and 4% glucose in *pfk2Δ*. As expected, we detected lower ethanol levels in *pfk2Δ* cells than the wild-type cells grown in 2% glucose. By increasing the concentration of glucose in the growth media from 2% to 4%, glycolysis was stimulated; the concentration of ethanol in Pfk2-ov approached wild type levels.

Defective V-ATPase function leads to growth defects known as the vacuolar membrane ATPase (*Vma*$^-$) phenotype. The *vma* mutant cells grow at pH 5.0 but exhibit severe growth defects at neutral pH (Nelson and Nelson 1990) and in the presence of calcium chloride (Ohya, Umemoto et al. 1991). Consistent with previous studies

A

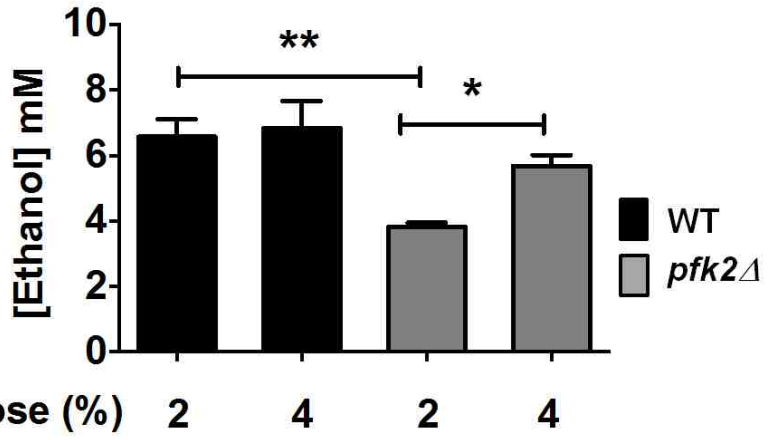

B

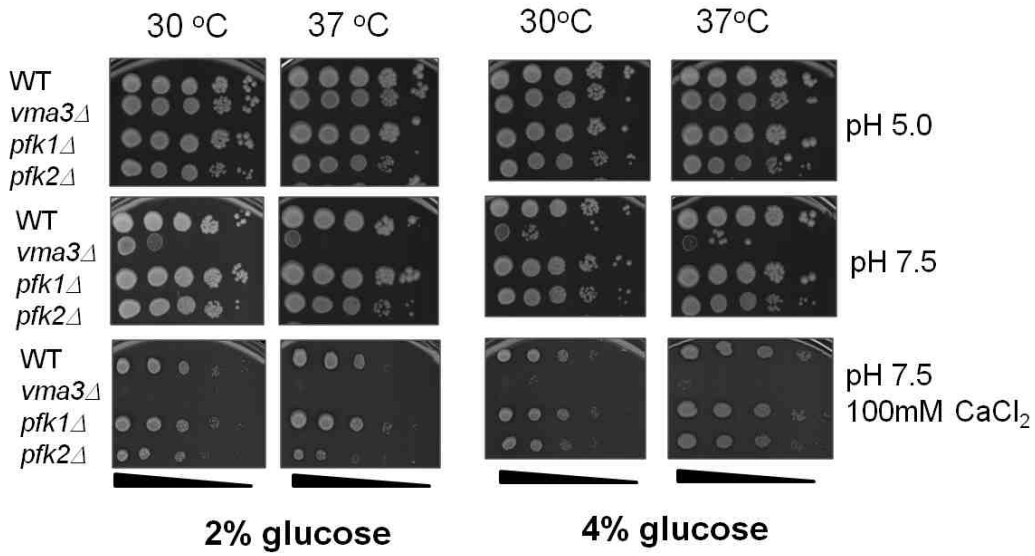

C

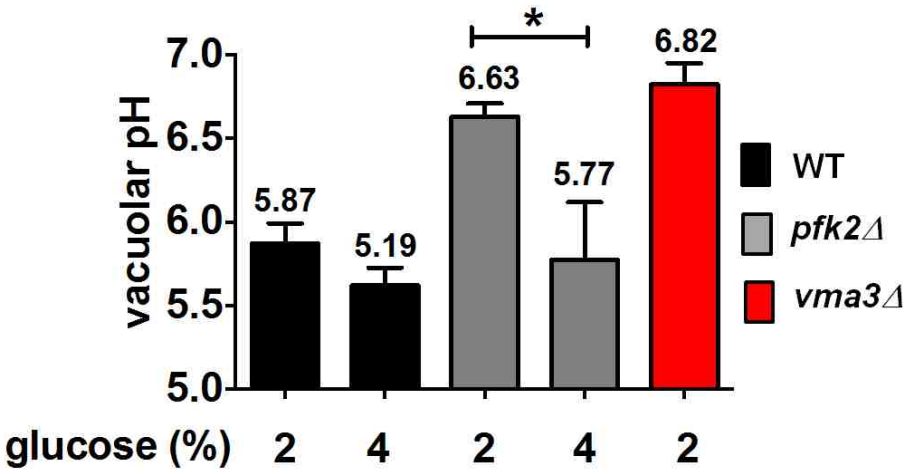

Figure 5. **Ethanol concentration, growth phenotype and vacuolar pH at steady state in presence of 4% glucose. A.** *4% glucose increased ethanol levels in pfk2Δ cells*. Cells were cultured to 0.6 - 0.8 OD A_{600}/ml in 2% or 4% glucose, converted to spheroplasts, resuspended in fresh YEP media containing 2% or 4% glucose plus 1.2 M sorbitol (2 OD A_{600}/ml), and incubated for 20 minutes at 30°C with shaking. The ethanol concentration was measured as described for Figure 2A. **B.** *4% glucose rescues pfk2Δ Vma⁻ growth defect***.** Cells were cultured to mid-log phase (0.6 - 0.8 OD A_{600}/ml) and ten-fold serial dilutions stamped onto YEP plates adjusted to pH 5.0, pH 7.5, and pH 7.5 plus 100 mM $CaCl_2$ containing 2% or 4% glucose. Cell growth was monitored for 3 days at 30°C and 37°C. Shown are representative plates of triplicates. **C.** *4% glucose rescues pfk2Δ vacuolar pH homeostasis.* Wild type and *pfk2Δ* cells were cultured to mid-log phase in YEP containing 2% and 4% glucose. Cells were stained with 50 mM BCECF-AM for 30 minutes as described for Figure 4. The ratio of fluorescent emission (535 nm) excited at 490 and 450 nm was measured to quantitatively assess vacuolar pH. The average fluorescence measured over 6 minutes was compared to standard curves to generate absolute pH values. Data are presented as average pH values from three independent experiments, and error bars are standard deviation. Statistically significant differnces ($p<0.05$ *) were determined by two-tailed unpaired *t*-test.

(Chan and Parra 2014), the *pfk2Δ* mutant displayed the *Vma*$^-$ phenotype at 37^{o}C on plates containing 100 mM calcium chloride buffered to pH 7.5 (Fig. 5B, left panel). Since those plates contained 2% glucose, we exposed the cells to the same conditions, except that 4% glucose was present. We monitored the cell growth on 4% glucose for 72 hours at 30 °C and 37 °C (Fig. 5B, right panel). The growth of *pfk2Δ* at neutral pH plus calcium chloride was rescued in the presence of 4% glucose. As expected, the wild-type strain grew on all the conditions while the negative control *vma3Δ,* which completely lacks V-ATPase function (Ohya, Umemoto et al. 1991) did not grow on pH 7.5 plates regardless of the presence of calcium. For reference, the mutant *pfk1Δ* that lacks the phosphofructokinase-1 subunit pfk1p was included. The *pfk1Δ* cells exhibited wild type growth and much mild phenotypes than *pfk2Δ* cells (Chan and Parra 2014).

We grew wild-type, *pfk2Δ* and *vma3Δ* cells in media containing 2% and 4% glucose and used BCECF to determine the vacuolar pH (Chan and Parra 2014). As expected, the vacuolar lumen of the wild-type cells was acidic at 2% and 4% glucose (pH 5.8 +/- 0.1), because V-ATPase pumps are fully functional (Fig. 5C). The *pfk2Δ* vacuoles were alkalinized (pH 6.6 +/- 0.1) at 2% glucose, resembling the *vma3Δ* mutant cells (pH 6.8 +/- 0.1) and indicating that V-ATPase proton transport was impaired. Notably, the vacuolar pH of *pfk2Δ* cells dropped to wild-type pH levels (pH 5.8 +/- 0.3) after growing the cells in 4% glucose. From these studies we concluded that V-ATPase proton transport is coupled to the glycolytic flow at steady state.

Phosphoglycerate kinase (Pgk1p) associates with vacuolar membranes in a glucose dose-dependent manner. Until know, our results have shown that 4% glucose restores vacuolar acidification in *pfk2Δ* cells. Glucose at 4% also stimulated the glycolytic flow Because glycolytic enzymes can bind V-ATPase and modulate its function (Kane 2012), we asked if phosphoglycerate kinase (Pgk1p) was present in vacuolar membranes and whether Pgk1p could be linked to vacuolar acidification. Pgk1p generates the first ATP downstream of phsphofructokinase-1

We purified vacuolar membrane fractions from wild-type and *pfk2Δ* cells grown in 2% and 4% glucose and conducted Western blot analyses using a monoclonal antibody to Pgk1p. Pgk1p was detected in the wild-type and *pfk2Δ* membranes (Fig. 6A), although it was at much lower levels in the *pfk2Δ* membranes fractions. The intensity of the band corresponding to Pgk1p increased at 4% glucose in both strains, so we determined the level of Pgk1p expression in whole cell lysates. Whole cell lysates from the wild type and *pfk2Δ* cells contained similar levels of Pgk1p at 2% and 4% (Fig. 6B). These results indicated that increased Pgk1p levels at the vacuolar membrane of cells exposed to 4% glucose were not due to increased expression levels of Pgk1p in the cells.

Unlike *pfk2Δ* cells, deletion of the other phosphofructokinase-1 subunit, *PFK1* gene, had a moderate effect on vacuolar pH (pH_{vac} = 6.2 +/- 0.04)(Chan and Parra 2014). The *pfk1Δ* cells also reassembled and reactivated V_1V_o normally after 2% glucose re-addition (Chan and Parra 2014). We compared Pgk1p levels in vacuolar membrane fractions from *pfk1Δ* and *pfk2Δ cells,* anticipating that *pfk1Δ* will have more Pgk1p because the vacuolar

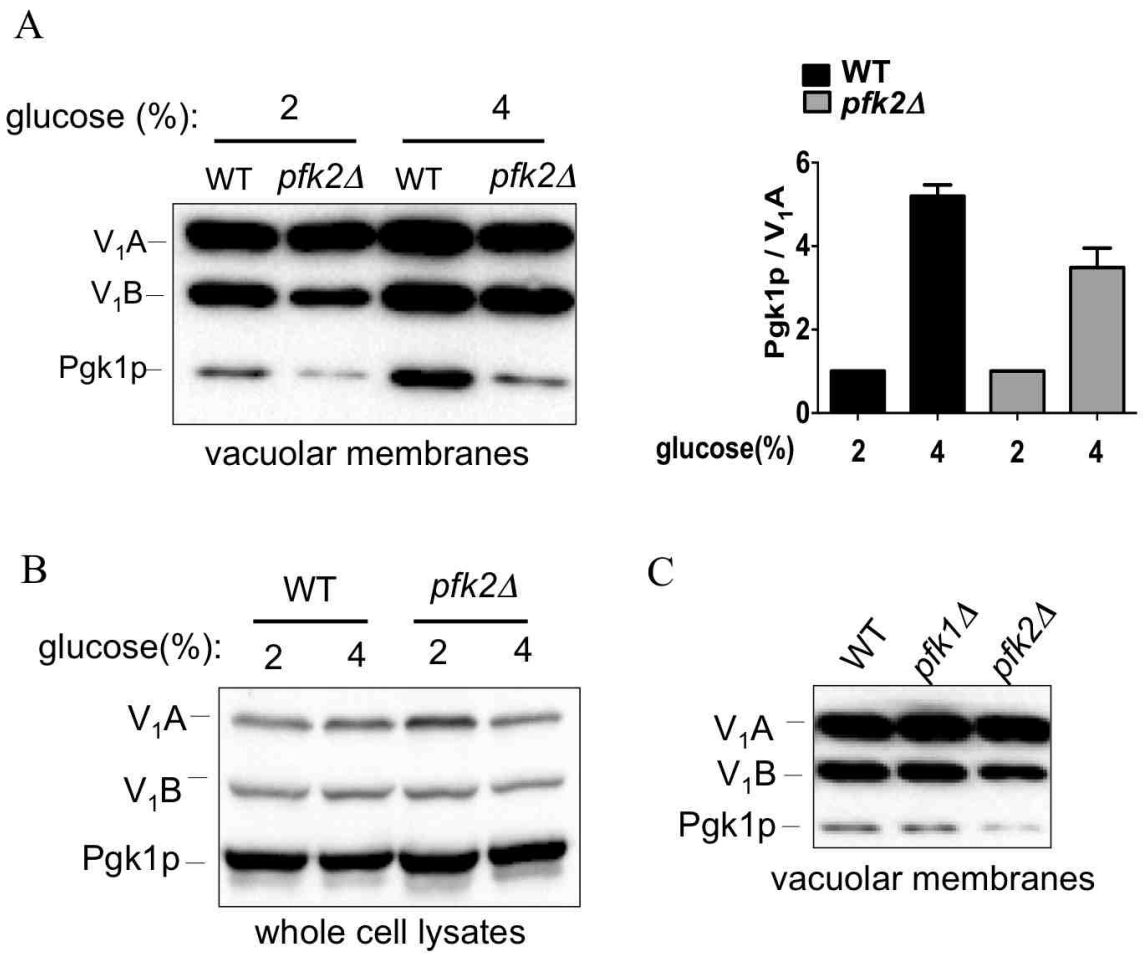

Figure 6. **The glycolytic enzyme Pgk1p co-purifies with vacuolar membrane fractions. A.** *Pgk1p in vacuolar membrane fractions from wild-type and pfk2Δ cells is proportional to the amount of glucose in the growth media.* Wild-type and *pfk2Δ* cells were cultured overnight to 1.0 OD Ab_{600}/ml in YEP pH 5.0 media containing 2 % or 4% glucose. Cells were converted to spheroplasts by zymolase treatment and vacuolar membrane fractions purified by ficoll density gradient centrifugation (Owegi, Pappas et al. 2006). The vacuolar membrane proteins (0.25 μg total protein) were separated in 10% SDS-PAGE gels and immunoblotted with anti-V_1 subunit A, anti-V_1 subunit B and anti-Pgk1p monoclonal antibodies. **B.** *Pgk1p expression is not enhanced at 4% glucose.* Whole cell lysates from wild type and *pfk2Δ* cells were prepared as described for Figure 1A, separated in 10% SDS-PAGE gels, and immnunoblotted to detect V-ATPase V_1 subunits A and B and Pgk1p. **C.** *Vacuolar membrane fractions from pfk1Δ cells have wild-type levels of Pgk1p.* Vacuolar membrane fractions from wild type, *pfk1Δ* and *pfk2Δ* cells were purified and immunoblotted to detect V-ATPase V_1 subunits A and B and Pgk1p as described above. . A-C: A representative gel from one of three independent experiments is shown.

lumen has lower pH. Western blots showed wild-type levels of Pgk1p in *pfk1Δ* membranes from cells grown in 2% glucose (Fig. 6C), in line with the hypothesis that Pgk1p could play a role in V-ATPase proton transport. These results also indicate that the inability of Pfk2p-ov and *pfk2Δ* cells to acidify vacuoles in the presence of 2% glucose correlates with a reduction in, but not absence of Pgk1p.

3.4 Discussion

We have studied the interplay between phosphofructokinase-1 subunit Pfk2p and V-ATPase in yeast. Both phosphofructokinase-1 subunits, Pfk1p and Pfk2p contribute to V-ATPase function *in vivo,* but we showed that the subunit Pfk2p has a major impact (Chan and Parra 2014). V-ATPase assembly at steady state and glucose-dependent reassembly are normal in *pfk1Δ* cells (Chan and Parra 2014). The *pfk1Δ* mutant has 2-fold lower concentration of the phosphofructokinase-1 reaction product, fructose 1,6 biphosphate, than wild-type cells (Arvanitidis and Heinisch 1994). By contrast, *pfk2Δ* cells have 10 – 15 fold lower levels of fructose 1,6 biphosphate (Arvanitidis and Heinisch 1994). Consistent with other studies (Heinisch 1986; Arvanitidis and Heinisch 1994), we showed that *pfk2Δ* has significantly reduced ethanol levels (30 - 40% lower concentration) than wild-type cells at steady state, indicative of a reduced glycolytic flow in *pfk2Δ* cells. The fact that *pfk2Δ* exhibited a partial *Vma*$^-$ growth phenotype, severely altered pH homeostasis, and defective glucose-dependent V-ATPase reassembly, prompted us to ask whether Pfk2p itself regulates V-ATPase. This study showed that Pfk2p is dispensable

for V-ATPase function. Instead, changes in the glycolytic flow are communicated to V-ATPase, which modify V-ATPase function *in vivo*.

The relationship between V_1V_o regulation by reversible disassembly and glycolysis has been described in yeast (Parra and Kane 1998). Glucose metabolism beyond glucose-6-phosphate formation is required for reassembly of V_1V_o (Parra and Kane 1998). Poorly fermentable carbon sources such as raffinose and galactose and non-fermentable carbon sources such as ethanol and glycerol cannot substitute for glucose in triggering reassembly (Kane 1995). Our results further support these studies by indicating that glycolysis controls V_1V_o reassembly. V_1V_o reassembly is proportional to the amount of glucose added to the medium (Fig. 3). By increasing the glucose concentration from 2% to 4% we restored the *Vma*$^-$ growth defects, glucose-dependent V_1V_o reassembly, and vacuolar acidification in the *pfk2Δ* cells. Glucose at 4% also stimulates glycolysis. The *pfk2Δ* cells in 4% glucose mimic the wild-type strain in 2% glucose with regards to V-ATPase function. We have extended previous findings by showing that glycolytic flow stimulation is sufficient to induce reassembly of V_1V_o complexes after glucose re-addition. Our data also showed that phosphofructokinase-1 binding to V-ATPase is not required for V_1V_o reassembly and reactivation, despite that the enzyme subunits co-precipitate with V-ATPase (Chan and Parra 2014).

Reactivation of glycolysis under reassembly conditions is significantly impaired in *pfk2Δ* cells, which cannot sufficiently reassemble V_1V_o. The rate of NADH formation after re-addition of 2% glucose to glucose-deprived *pfk2Δ* cells is reduced by about 70%,

compared to wild-type cells so its metabolic reactivation is significantly impaired. Addition of 4% glucose stimulated *pfk2Δ* metabolic reactivation up to ~50% of the wild-type rate (Fig. 2D). Addition of 4% glucose additionally restored glucose-triggered V_1V_o reassembly (Fig. 3) and vacuolar acidification (Fig. 4). These results suggest that 50% of the wild-type reactivation (NADH formation rate) can be the metabolic threshold to reassemble V_1V_o normally. Future studies will be necessary to validate this observation. For example, it will be required to measure NADH formation after addition of 0.5% glucose to wild type cells, because at 0.5% glucose wild-type cells showed complete V_1V_o reassembly (Fig. 3) (Parra and Kane 1998).

How does the glycolytic flow communicate to V-ATPase? Remains an open question. One possibility is that the glycolytic flow, perhaps changes of the ATP levels, directly communicate with RAVE to promote V-ATPase reassembly. RAVE interacts with cytosolic V_1-C complexes (Smardon, Tarsio et al. 2002), free V_1 subunit C (Smardon and Kane 2007) and the membrane-bound V_o subunit a (Smardon, Diab et al. 2014). We showed that binding of RAVE to cytosolic V_1-C is enhanced in *pfk2Δ* cells exposed to 2% glucose. It has to be determined whether this RAVE-(V1-C) binding is responsive to glycolytic flow changes. (Chan and Parra 2014).

Enhancing glycolysis prompts downstream signals proposed to stimulate V_1V_o reassembly. These signals include a transient cytosolic alkalinization (Martinez-Munoz and Kane 2008; Dechant, Binda et al. 2010), activation of the plasma membrane ATPase Pma1p (Rao, Drummond-Barbosa et al. 1993; Lecchi, Nelson et al. 2007), and

Ras/cAMP/PKA signaling (Bond and Forgac 2008). Cytosol pH changes resulting from stimulation of the glycolytic flow could be a signal for V-ATPase reassembly. The alkalinization of the cytosol by activation of glycolysis can be a sensitive readout of the glycolytic flow to control V_1V_o reassembly (Dechant, Binda et al. 2010). Pma1p, like V-ATPase, is activated by glucose (Rao, Drummond-Barbosa et al. 1993; Garcia-Arranz, Maldonado et al. 1994; Lecchi, Nelson et al. 2007) and glucose-dependent activation of both enzymes contribute to alkalinization of the cytosol pH (Ambesi, Miranda et al. 2000; Morsomme, Slayman et al. 2000).

Although additional studies will be necessary to further define the molecular mechanisms by which the glycolytic flow communicates to V-ATPase, our results are in good alignment with the hypothetic model summarized in the Figure 1 of Chapter 4. The *pfk2Δ* cells have significantly more acidic cytosolic pH than wild type cells (Chan and Parra 2014) and lower glycolytic re-activation capacity in response to 2% glucose (Fig. 2D). These two phenotypes combined could contribute to preventing normal V_1V_o reassembly at 2% glucose. Addition of 4% glucose stimulates the metabolic flow restoring ~ 50% of wild type glycolytic rate (Fig. 2D). This glycolytic stimulation alkalinizes the cytosol via Pma1p activation and supports reassembly of V_1V_o. V-ATPase reassembly which restores vacuolar pH also contributes to sustaining cytosol pH homeostasis (Martinez-Munoz and Kane 2008).

An important finding resulting study is that stimulation of glycolysis is not sufficient to resume proton transport. Thus, glucose-dependent reassembly and vacuolar acidification

are independently controlled processes. Our data indicate that both are linked to glycolysis. However, V_1V_o reassembly could be communicated through RAVE in the cytosol, and V_1V_o reactivation through Pgk1p at the vacuolar membranes. The Pfk2p-ov cells reassemble V_1V_o normally but cannot acidify the vacuolar lumen. Pfk2p-ov exhibits ~80% of the wild-type NADH synthesis rate but reduced Pgk1p levels at the vacuolar membranes (not shown). The fact that Pfk2-ov reassemble V_1V_o normally is in support of the concept that ~50% metabolic reactivation is the threshold for V_1V_o reassembly. Addition of 4% glucose to Pfk2p-ov restores the acidic vacuolar pH (not shown). Therefore, 4% glucose promotes different signal(s) downstream of stimulating the glycolysis flow; the signal for reassembly (e.g., RAVE-V1 binding) and the signal for reactivation (e.g., Pgk1p at the vacuolar membrane).

We detected Pgk1p at vacuolar membrane fractions from wild-type, *pfk1Δ*, and *pfk2Δ* cells. In every instance, Pgk1p levels increased when the cells were grown in 4% glucose, despite that Pgk1p cellular levels did not increase. We proposed that Pgk1p at the vacuole could facilitate activation of V-ATPase proton transport *in vivo*. In support of this hypothesis, we found that yeast Pgk1p co-immunoprecipitates with V-ATPase pumps from wild-type cells (not shown). Experiments addressing the glucose-dependency of this interaction are not yet conclusive. To our knowledge this is the first study to report the glycolytic enzyme Pgk1p at vacuolar membrane fractions and to co-immunoprecipitate with the V-ATPase complexes.

Our data strongly argue against direct regulation of V-ATPase through its physical interaction with phosphofructokinase-1, but we do not exclude the possibility that other glycolytic enzymes may perform this function (Lu, Holliday et al. 2001; Lu, Sautin et al. 2004; Lu, Ammar et al. 2007). *In vitro* reconstitution experiments will help demonstrate functional coupling between a super-complex of glycolytic enzymes and V-ATPase at the vacuolar membrane. Whether such supercomplex can supply V-ATPase with glycolytic ATP *in vivo* has to be determined (Lu, Holliday et al. 2001; Su, Zhou et al. 2003; Lu, Sautin et al. 2004; Lu, Ammar et al. 2007; Su, Blake-Palmer et al. 2008). As a precedent, Pgk1p associated with the synaptic vesicle membranes forms a functional complex with the glycolytic enzyme GAPDH that drives glutamine uptake by locally generating glycolytic ATP (Ikemoto, Bole et al. 2003).

We showed that Pgk1p co-purifies with yeast vacuolar membranes; Pgk1p also co-immunoprecipitates with V-ATPase (not shown). Whether Pgk1p could influence V-ATPase proton transport has not been shown. Pgk1p syntheses ATP in glycolysis and the levels of Pgk1p at vacuolar membranes could be important for stimulating V-ATPase proton transport *in vivo*. ATP locally made at the membranes could reach concentrations high enough to support both reassembly and V-ATPase proton transport. Re-binding of V_1 subunit C to V_1V_o at the membrane during reassembly is likely an energy consuming process (Oot and Wilkens 2010), which may justify why reassembly (not disassembly) requires its own V-ATPase specific chaperone, RAVE.

Is RAVE-V1-C binding responsive to glycolytic flow changes? Is glycolytic ATP made at the membrane? Is the Pgk1p reaction coupled to V-ATPase proton transport? These are questions that remain to be addressed to understand the mechanisms linking V-ATPase function and glycolysis? This study was brought new insights to our understanding of the mechanisms by which the presence of glucose is communicated to V-ATPases. We showed that glucose-dependent V-ATPase reassembly can be disengaged from V-ATPase reactivation. Reassembly is not sufficient to reactivate V-ATPase proton transport *in vivo* because V_1V_o reassembly and its reactivation are independently controlled. Reassembly, but not V-ATPase-mediated vacuolar acidification, requires sufficient glycolytic flow (measured as the NADH synthesis rate and ethanol levels). Our data indicate that reactivation of V-ATPase proton transport following reassembly (measured as vacuolar acidification) requires additional down stream signals also linked to glycolysis. A correlation between vacuolar acidification and Pgk1p at vacuolar membrane fractions is suggestive of a role for Pgk1p-mediated substrate-level phosphorylation for V_1V_o reactivation and proton transport. Clearly, our understanding of glucose-dependent V-ATPase regulation is not complete, despite of its significance implications in cancer (Michel, Licon-Munoz et al. 2013; Kubisch, Frohlich et al. 2014; Schempp, von Schwarzenberg et al. 2014; von Schwarzenberg, Lajtos et al. 2014), viral infections (Kohio and Adamson 2013), antigen maturation (Blander and Medzhitov 2006), and amino acid homeostasis (Zoncu, Bar-Peled et al. 2011; Efeyan, Zoncu et al. 2012; Jewell, Russell et al. 2013).

Chapter IV: Conclusions and future directions

4. Conclusions and future directions

The acidification of intracellular compartments distributed throughout the endomembrane system plays essential roles in a number of biological processes including membrane trafficking, protein processing, protein degradation, membrane fusion, and autophagy (Forgac 2007). Viral entry and uptake of therapeutic drugs also require a differential luminal pH among of endosomal and lysosomal compartments. V-ATPase pumps present in these organelles are crucial for maintenance of the pH gradients. V-ATPase at the plasma membrane of certain specialized cells acidifies extracellular environment and is necessary for sperm maturation, pH homeostasis in kidney, bone resorption and tumor metastasis (Forgac 2007).

The membrane localization and activity of V-ATPase pumps are accurately controlled, given the importance and diversity of physiological processes that require V-ATPase proton transport. Understanding the molecular mechanisms and cellular factors that modulate these proton pumps can have long-term implications for treatment of diseases involving V-ATPase pumps such as osteoporosis (Hinton, Bond et al. 2009; Thudium, Jensen et al. 2012), cancer (Sennoune, Bakunts et al. 2004; Perez-Sayans, Somoza-Martin et al. 2009; Fan, Niu et al. 2012; Garcia-Garcia, Perez-Sayans Garcia et al. 2012; Schempp, von Schwarzenberg et al. 2014), distal renal acidosis (Stehberger, Schulz et al. 2003; Ochotny, Van Vliet et al. 2006), and several infectious diseases (Huang, Tsai et al. 2006; Kohio and Adamson 2013; Rane, Bernardo et al. 2013; Hayek, Lee et al. 2014).

The reversible disassembly of V-ATPase is an important mechanism that controls V-ATPase activity in response to various extracellular stimuli. This study focused on the reassembly. Glucose-dependent regulation of V-ATPase is conserved in yeast, insects, and human renal epithelial cells (Kane 1995; Sumner, Dow et al. 1995; Nakamura 2004; Sautin, Lu et al. 2005). Our findings support the notion that dissociation of V_1 from V_o and its reassembly are independently controlled mechanisms. Prior studies have shown that: 1) The disruption of microtubules only blocks the dissociation of the V-ATPase but not its reassembly, suggesting that the complete microtubular system is only required for V-ATPase disassembly (Xu and Forgac 2001); 2) Deletion of Rav1p, a subunit of RAVE complex (V-ATPase assembly factor), suppresses glucose-dependent reassembly but not disassembly (Seol, Shevchenko et al. 2001), and 3) Up-regulation of the cAMP/Ras/PKA pathway prevents V_1 dissociation from the V_o complex (Bond and Forgac 2008). Our own findings (Chapter II) indicate that the yeast phosphofructokinase-1 subunit Pfk2p is necessary for reassembly, not for disassembly.

V_1V_o reversible disassembly does not require new protein synthesis (Kane 1995) and preserves energy (ATP consumption) under low energy state. So, it is important to understand how V_1V_o responds to low nutrient environments (low glucose and poorly fermentable carbon sources such raffinose and galactose). This and other studies have indicated that glycolysis is important for V_1V_o reassembly (Kane 1995; Parra and Kane 1998). Glucose metabolism is the main energy source for yeast, but the interplay between the energy state of a cell and reversible disassembly is still unclear. The cellular

mechanisms and signals involved are not understood and they may be different in different cell types.

The glycolytic enzymes, aldolase, GAPDH and phosphofructokinase-1, associate with V-ATPase and these interactions are important for V-ATPase function in yeast and mammalian cells (Lu, Holliday et al. 2001; Ikemoto, Bole et al. 2003; Su, Zhou et al. 2003; Lu, Sautin et al. 2004; Dhar-Chowdhury, Harrell et al. 2005; Lu, Ammar et al. 2007; Su, Blake-Palmer et al. 2008). Aldolase-V-ATPase binding is glucose-dependent and required for V_1V_o reassembly (Lu, Holliday et al. 2001; Lu, Sautin et al. 2004; Lu, Ammar et al. 2007). However, the factors that control interactions with aldolase are still unknown. Human phosphofructokinase-1 also binds to V_o subunit a4 of V-ATPase and mutants of V_o subunit a4 that interfere with this binding also cause distal renal acidosis (Su, Zhou et al. 2003; Su, Blake-Palmer et al. 2008). Until now, the role of phosphofructokinase-1 in V-ATPase function was unclear. Our studies demonstrated that phsphofructokinase-1 is dispensable for V-ATPase functions if the glycolytic flow is restored.

We addressed the role of each phosphofructokinase-1 subunit for V-ATPase activity separately. We studied single deletion strains of the yeast *PFK1* and *PFK2* genes to determine the interplay between phosphofructokinase-1, V-ATPase, and glycolysis. Each single deletion strain supports glucose metabolism and was suitable for studying the role of phosphfructokinase-1 in regulating V-ATPase.

The first part of this dissertation (Chapter II) focused on the role of individual yeast phosphofructokinase-1 enzymes in V-ATPase function at steady state and during glucose-dependent reversible V_1V_o disassembly. First, we demonstrated that both the Pfk1p subunit and Pfk2p subunits of phosphofructokinase-1 co-precipitate with V-ATPase in *pfk2Δ* and *pfk1Δ* cells, respectively. This suggests that individual Pfk1p and Pfk2p can bind to V-ATPase. Those studies did not exclude the possibility that Pfk1p and Pfk2p may interact with V-ATPase through other proteins (eq. other glycolytic enzymes). Notably, each phosphofructokinase-1 single deletion strain displayed *Vma*$^-$ phenotypic traits *in vivo*, including alkalinized vacuoles, partial loss of V-ATPase activity in purified vacuolar membranes, and acidified cytosol at steady state. These phenotypes suggest that the *pfk1Δ* and *pfk2Δ* mutants have defective V-ATPase pumps. Overall the *pfk2Δ* cells exhibited more dramatic phenotypes than *pfk1Δ* cells.

After glucose re-addition, *pfk2Δ* cells failed to reassemble 50% of the V_1V_o complexes and did not acidify the vacuolar lumen. In addition, *pfk2Δ* exhibited enhanced V_1-RAVE binding in the cytosol. Since the glucose-induced vacuolar acidification is the direct consequence of V_1V_o re-activation, we concluded that *pfk2Δ* cells couldn't reactivate V-ATPase and transport protons across the vacuolar membranes.

We reasoned that Pfk2p is the subunit mainly responsible for the interaction between phosphofructokinase-1 and V-ATPase. The crystal structure of the yeast phosphofructokianse-1 enzyme shows the four α (Pfk1p) subunits and four β (Pfk2p)

subunits arranged in a stable hero-octamer complex (α4β4), where α subunits localize in the center surrounded by the β subunit. This conformation makes the β subunits (Pfk2p) more accessible to other proteins, including V-ATPase. Nonetheless, we addressed other possibilities in Chapter III of my dissertation.

The Chapter III investigated the factors that cause V-ATPase functional defects in the *pfk2Δ* strain. Our results provide new evidence that V-ATPase function is closely linked to the glycolytic flow. Increasing the amount of glucose in the media from 2% to 4% reversed the growth defects, glucose-dependent V_1V_o reassembly defects, and vacuolar pH defects in the *pfk2Δ* cells. The *pfk2Δ* cells exposed to 4% glucose mimicked the wild-type strain grown in 2% glucose. As expected, glucose at 4% stimulated glycolysis in *pfk2Δ*, we detected an ~15 % increase in the rate of NADH formation after 4% glucose addition relative to 2% in both strains, wild-type and *pfk2Δ*. This modest increase allowed *pfk2Δ* to reach about 50% of the wild-type rate with 2% glucose. In addition, ethanol levels increased by 40% – 50% in *pfk2Δ* cells.

The glycolytic flow is reduced in *pfk2Δ* cells. The rate of NADH formation after glucose re-addition to glucose-deprived *pfk2Δ* cells is significantly reduced (by ~ 70%), compared to wild-type cells. Likewise, the concentration of ethanol is 30 - 40% lower. Theses finding are supported by independent studies in *pfk2Δ* showing reduced level of fructose 1,6 bisphosphate (the reaction product of phosphofructionase-1), accumulation

of fructose-6-phosphate (subtract of phosphofructokinase-1) (Heinisch 1986), and longer growth doubling times (120 minutes *vs* 90 minutes in wild type cells) (Arvanitidis and Heinisch 1994). Our data indicate that reaching ~50% of the wild-type glycolytic flow could be a metabolic threshold to reassemble V_1V_o normally. Thus, the level of V_1V_o reassembly correlates with the glycolytic rate.

The RAVE complex mediates V-ATPase re-assembly through its interactions with V_1-C in the cytosol (Smardon, Tarsio et al. 2002), free subunit C (Smardon and Kane 2007), and the V_o subunit a at the membrane (Smardon, Diab et al. 2014). We showed in Chapter II that the binding of RAVE to cytosolic V_1 is enhanced in *pfk2Δ* cells (Chan and Parra 2014), suggesting that lower V_1V_o reassembly is the consequence of the enchanced V_1-RAVE association in *pfk2Δ*. In Chapter III we demonstrated that Pfk2p itself is not required for normal reassembly, and that stimulation of the glycolytic flow is sufficient. Thus, together our results suggest that the glycolytic flow itself could communicate the presence of glucose to RAVE to drive V-ATPase reassembly. However, understanding the role of glycolysis in RAVE-dependent V_1V_o reassembly will require additiomal studies. For example, measuring V_1-Rav1p interaction at 4% glucose in *pfk2Δ,* wild type and Pfk2-ov cells. Those studies will establish whether glucose at 4% rescues normal V_1-RAVE association to help determine if involvement of the glycolytic flow is the signal that regulates glucose-dependent RAVE-mediated V_1V_o reassembly.

Interestingly, we found the glycolytic enzyme Pgk1p to co-purify with vacuolar membrane fractions. Elevated Pgk1p levels were isolated with membranes at 4% glucose, which correlated with vacuolar acidification *in vivo.* Pgk1p lies downstream of aldolase, and GAPDH in glycolysis. At the vacuolar membrane these enzymes could form a functional complex with Pgk1p that provides glycolytic ATP to V-ATPase pumps. The fact that the glycolytic function of aldolase is independent of its role for V-ATPase assembly (Lu, Ammar et al. 2007), does not exclude the possibility that Pgk1p activity (ATP synthesis) could stimulate reactivation of V-ATPase function *in vivo.* V_1V_o disassembly occurs if aldolase cannot bind to V-ATPase, even if glycolysis is fully functional. *In vitro* reconstitution experiments will help determine whether Pgk1p at the vacuolar membrane is sufficient to promote V-ATPase activity.

Neither Pfk2p excess (pfk2-ov cells) or absence (*pfk2Δ* cells) is sufficient to prevent V_1V_o dissociation or reassociation, suggesting that the glycolytic enzyme phosphfructokinase-1 itself is not required for V-ATPase reversible disassembly. This study brings new insight into our understanding of how glucose signals are communicated to V-ATPases. We separated glucose-dependent V-ATPase reassembly from V-ATPase reactivation; reassembly is not sufficient to reactivate V-ATPase proton transport *in vivo*. Thus, we conclude that V_1V_o reassembly and its reactivation are independently controlled events. V_1V_o Reassembly is controlled by glycolytic flow possibly through its effect on V_1-RAVE binding. On the other hand, V-ATPase proton transport may require locally made glycolytic ATP by Pgk1p at membrane. The Fig. 1 below summarized a model compatible with our results.

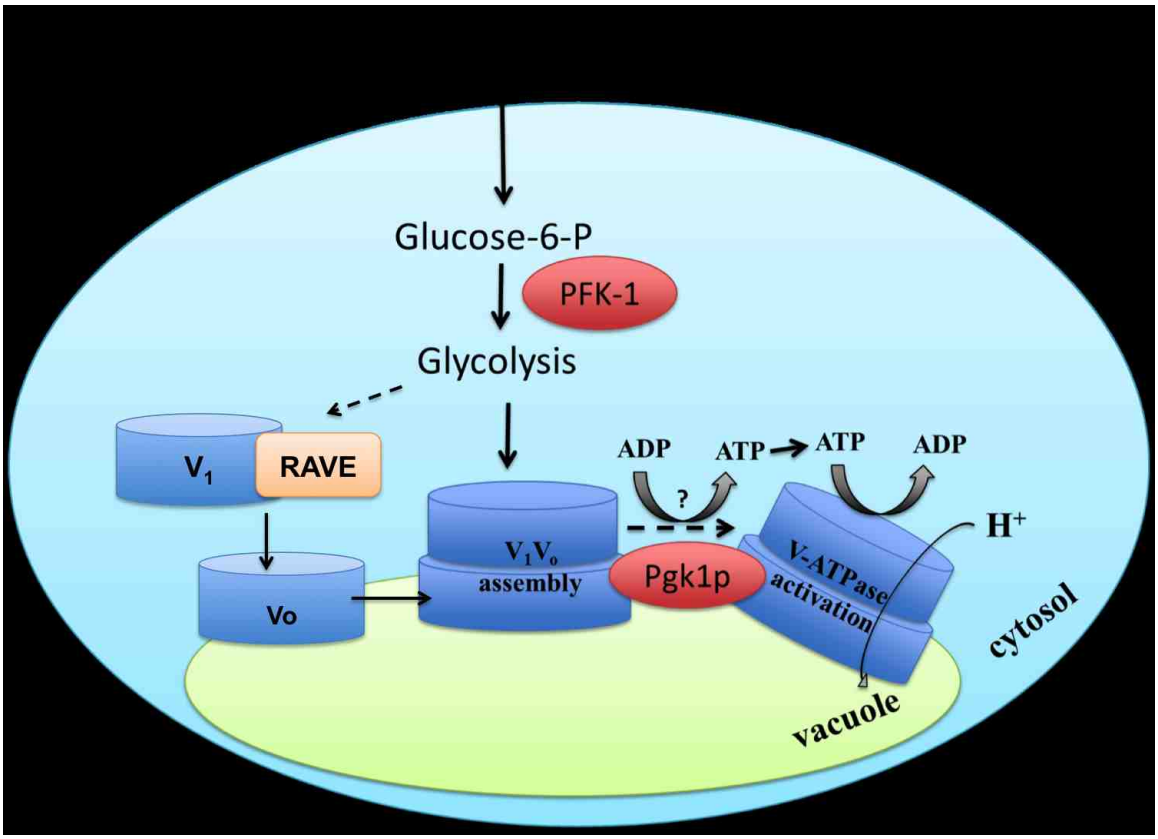

Figure 1. A model for the regulation of V-ATPase reassembly and function by glycolysis. In this model, glucose-dependent yeast V_1V_o reassembly is controlled by glycolysis via the RAVE complex. Glycolysis drives V_1V_o reassembly but not V-ATPase activation (proton transport). The V-ATPase activation involves Pgk1p, which generates glycolytic ATP. Arrows represents positive interactions. Dashed arrows: proposed interactions supported by these studies. PFK-1: phosphofructokinase-1. Pgk1p: phosphoglycerate kinase. RAVE: Regulator of ATPase of Vacuoles and Endosomes.

Chapter V

Appendices

Appendix A

Inhibitors of V-ATPase Proton Transport Reveal Uncoupling Functions of Tether Linking Cytosolic and Membrane Domains of V_o Subunit a (Vph1p)

Published in *Journal of Biological Chemistry*

January, 2012

Membrane Biology:

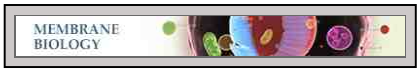

Inhibitors of V-ATPase Proton Transport Reveal Uncoupling Functions of Tether Linking Cytosolic and Membrane Domains of V_0 Subunit a (Vph1p)

Chun-Yuan Chan, Catherine Prudom, Summer M. Raines, Sahba Charkhzarrin, Sandra D. Melman, Leyma P. De Haro, Chris Allen, Samuel A. Lee, Larry A. Sklar and Karlett J. Parra

J. Biol. Chem. 2012, 287:10236-10250.
doi: 10.1074/jbc.M111.321133 originally published online January 3, 2012

THE JOURNAL OF BIOLOGICAL CHEMISTRY VOL. 287, NO. 13, pp. 10236–10250, March 23, 2012

Inhibitors of V-ATPase Proton Transport Reveal Uncoupling Functions of Tether Linking Cytosolic and Membrane Domains of V_0 Subunit a (Vph1p)*[S]

Received for publication, November 12, 2011, and in revised form, December 16, 2011 Published, JBC Papers in Press, January 3, 2012, DOI 10.1074/jbc.M111.321133

Chun-Yuan Chan[‡1], Catherine Prudom[§1,2], Summer M. Raines[‡3], Sahba Charkhzarrin[‡], Sandra D. Melman[‡], Leyma P. De Haro[‡], Chris Allen[§4], Samuel A. Lee[¶], Larry A. Sklar[§‖], and Karlett J. Parra[‡5]

From the [‡]Department of Biochemistry and Molecular Biology, the [¶]Department of Internal Medicine, the [‖]Department of Pathology and Cancer Center, and the [§]Center for Molecular Discovery, School of Medicine, University of New Mexico Health Sciences Center, Albuquerque, New Mexico 87131

Background: Vacuolar ATPase (V-ATPase) proton pumps maintain pH homeostasis.
Results: We discovered new V-ATPase inhibitors that uncouple the proton transport and ATPase activity of the pump.
Conclusion: Residues at the tether connecting V_0 subunit a to the membrane give uncoupling potential to V-ATPases.
Significance: The tether may offer new mechanisms to regulate V-ATPase and cellular pH *in vivo* by uncoupling the pump.

Vacuolar ATPases (V-ATPases) are important for many cellular processes, as they regulate pH by pumping cytosolic protons into intracellular organelles. The cytoplasm is acidified when V-ATPase is inhibited; thus we conducted a high-throughput screen of a chemical library to search for compounds that acidify the yeast cytosol *in vivo* using pHluorin-based flow cytometry. Two inhibitors, alexidine dihydrochloride (EC_{50} = 39 μM) and thonzonium bromide (EC_{50} = 69 μM), prevented ATP-dependent proton transport in purified vacuolar membranes. They acidified the yeast cytosol and caused pH-sensitive growth defects typical of V-ATPase mutants (*vma* phenotype). At concentrations greater than 10 μM the inhibitors were cytotoxic, even at the permissive pH (pH 5.0). Membrane fractions treated with alexidine dihydrochloride and thonzonium bromide fully retained concanamycin A-sensitive ATPase activity despite the fact that proton translocation was inhibited by 80–90%, indicating that V-ATPases were uncoupled. Mutant V-ATPase membranes lacking residues 362–407 of the tether of Vph1p subunit a of V_0 were resistant to thonzonium bromide but not to alexidine dihydrochloride, suggesting that this conserved sequence confers uncoupling potential to V_1V_0 complexes and that alexidine dihydrochloride uncouples the enzyme by a different mechanism. The inhibitors also uncoupled the *Candida albicans* enzyme and prevented cell growth, showing further specificity for V-ATPases. Thus, a new class of V-ATPase inhibitors (uncouplers), which are not simply ionophores, provided new insights into the enzyme mechanism and original evidence supporting the hypothesis that V-ATPases may not be optimally coupled *in vivo*. The consequences of uncoupling V-ATPases *in vivo* as potential drug targets are discussed.

Endogenous V-ATPase proton pumps are present throughout the endomembrane system where they energize the membranes, acidify organelles, and contribute to regulating the cytosolic pH (1–3). V-ATPases carefully control the acidic pH essential for endocytic and exocytic vesicular transport, zymogen activation, and protein sorting and degradation. Cells specialized for active proton secretion also express V-ATPases at the plasma membrane, where the efflux of cytosolic protons sustains the acidic luminal pH necessary for sperm maturation (4), urinary acidification (5), and bone resorption (6).

Maintaining pH homeostasis by V-ATPases[6] entails the active transport of protons at the expense of ATP. The two domains forming the V-ATPase complex, V_1 and V_0, functionally and structurally couple ATP hydrolysis and proton transport via a rotational mechanism of catalysis. V_1 is bound peripherally to the cytosolic side of the membrane and catalyzes the hydrolysis of ATP inside a hexameric structure consisting of subunits A and B (A_3B_3) (1–3). V_0 is membrane-bound and forms the path for proton transport, which involves subunit a and a proteolipid ring structure (3, 7). During catalysis, hydrolysis of ATP in A_3B_3 of V_1 drives rotation of a central rotor connected to the proteolipid ring of V_0. Protons are transferred from the cytosol to a hemichannel in the V_0 subunit a and from subunit a to the proteolipid ring. Hydrolysis of three molecules of ATP in V_1 drives a 360° rotation of the ring, allowing the exit of protons. Exiting protons are transferred to a second hemichannel, located in the luminal side

* This work was supported, in whole or in part, by National Institutes of Health Grants 5R01GM086495 (to K. J. P.), 1U54MH084690 (to L. A. S., C. P., and C. A.), and CA118100 (to the University of New Mexico Cancer Center).
[S] This article contains supplemental Table 1.
[1] Both authors contributed equally to this work.
[2] Current address: SRI International, 140 Research Dr., Harrisonburg, VA 22802.
[3] Supported by National Institutes of Health Grant K12GM088021.
[4] Present address: Dept. of Environmental and Radiological Health Sciences, College of Veterinary Medicine and Biomedical Sciences, Colorado State University, Fort Collins, CO 80523.
[5] To whom correspondence should be addressed: Dept. of Biochemistry and Molecular Biology, University of New Mexico, MSC08 4670, Albuquerque, NM 87131. Tel.: 505-272-1633; Fax: 505-272-6587; E-mail: kjparra@salud.unm.edu.

[6] The abbreviations used are: V-ATPase, vacuolar proton-translocating ATPase; DMSO, dimethyl sulfoxide; SC, synthetic complete; ACMA, 9-amino-6-chloro-2-methoxyacridine.

of subunit a, and expelled to the other side of the membrane against a concentration gradient.

V-ATPase activity is essential, and blocking of rotational catalysis is lethal. When V-ATPase activity is impaired at physiological (neutral) pH, yeast and most eukaryotic cells are not viable (2). However, yeast have developed a conditionally lethal pH-sensitive growth phenotype in which cells grow under acidic conditions. This phenotypic trait has made yeast an ideal system for the study of the downstream consequences of genetically impairing V-ATPase function *in vivo* (8). Yeast V-ATPase mutant strains have provided valuable information regarding the molecular mechanism of catalysis and the broad spectrum of physiological processes in which V-ATPases are involved.

It is precisely because V-ATPases are critical for many cellular events that yeast V-ATPase mutants often develop compensatory mechanisms that can mask important V-ATPase functions (9–11). In this context, V-ATPase inhibitors are important research tools for studies requiring sudden inhibition of V-ATPases. The most commonly used V-ATPase inhibitors, bafilomycin A and concanamycin A, have been fundamental to the understanding of V-ATPase catalysis, regulation, and cellular functions (12–15). Bafilomycin A and concanamycin A are now indispensable research tools for the study of important processes in which V-ATPases are involved, including autophagy (16, 17) and membrane fusion (18) under normal physiology and pathophysiology.

It has been proposed that bafilomycin A and concanamycin A act as a stone in a gear, blocking rotation when they bind to the proteolipid ring of V_0 (19, 20). A new kind of V-ATPase inhibitors, archazolids (12), also bind to the proteolipid ring to block rotation (21). By ending rotation, bafilomycin A, concanamycin A, and archazolids inhibit ATPase activity in V_1 and proton transport in V_0 simultaneously. Unfortunately, they cannot offer information regarding the mechanisms by which proton transport and ATP hydrolysis are coupled. Mutagenesis studies of individual V_1 and V_0 subunits in yeast indicate that coupling is accomplished by the contribution of multiple subunits (22–26). However, exactly how proton transport and ATP hydrolysis are coupled in the V-ATPase complex is not known.

Changing the coupling efficiency of V-ATPase may regulate the pump by offering a mechanism for control of organelle acidification *in vivo* (27, 28). The hypothesis that V-ATPase may not couple proton transport and ATP hydrolysis optimally is supported by the fact that increased coupling efficiency is observed at lower ATP concentrations (27) and in some genetic mutants (25). An intrinsic uncoupling potential argues against the energetic efficiency of the V-ATPase machine, and intrinsic uncoupling is poorly understood. As such, to gain new insights into this important regulatory mechanism of V-ATPase proton transport, it would be beneficial to find specific V-ATPase inhibitors that modulate coupling of the enzyme.

We took advantage of the fact that V-ATPase inhibition prevents the redistribution of protons and lowers the cytosolic pH (29) to screen the Prestwick Chemical Library of small compounds. We searched for drugs that acidified the yeast cytosol *in vivo* as a means of identifying new V-ATPase inhibitors. By using *Saccharomyces cerevisiae* cells expressing a cytosolic pHluorin (29–31) and the HyperCyt® high-throughput flow cytometry platform (32), we identified two V-ATPase inhibitors, alexidine dihydrochloride and thonzonium bromide. They acidified the yeast cytosol, inhibited ATP-dependent proton transport in vacuolar membrane fractions, and caused pH-sensitive growth defects characteristic of yeast cells with impaired V-ATPase function.

We showed that these inhibitors functionally uncoupled V-ATPase pumps and that a mutant V-ATPase lacking the tether (residues 362–407) of V_0 subunit a Vph1p was resistant to thonzonium bromide. This finding revealed novel roles for the tether connecting the N- and C-terminal domains of subunit a. The tether confers uncoupling potential to V_1V_0 complexes and a mechanism for regulating V-ATPase coupling efficiency *in vivo*. We showed further that alexidine dihydrochloride and thonzonium bromide uncouple V-ATPase pumps of the pathogenic fungi *Candida albicans* and inhibit cell growth providing evidence for the universal nature of this regulatory mechanism.

EXPERIMENTAL PROCEDURES

Materials and Strains

Zymolase 100T was purchased from Seikagaku (Tokyo), concanamycin A from Wako Biochemicals (Richmond, VA), and Ficoll from United Stated Biologicals (Swampscott, MA). All other reagents were from Sigma. The yeast *S. cerevisiae* strains referred to throughout the *in vivo* studies are BY4742 (*MATα his3*Δ1 *leu2*Δ0 *lys2*Δ0 *ura3*Δ0), *vma2*Δ (*MATα his3*Δ1 *leu2*Δ0 *lys2*Δ0 *ura3*Δ0 *VMA2*::KanMX), and *vma3*Δ (*MATα his3*Δ1 *leu2*Δ0 *lys2*Δ0 *ura3*Δ0 *VMA3*::KanMX). For flow cytometry and pH measurements, the cells were transformed by the lithium acetate method (33) with the 2 μ plasmid pHluorin under control of the phosphoglycerate kinase promoter (31); this plasmid was created by Dr. Rajini Rao (Department of Physiology, Johns Hopkins University). After transformation, the strains expressing pHluorin were maintained in fully supplemented synthetic complete (SC) medium lacking uracil (SC-Ura) buffered to pH 5.0 with 50 mM sodium phosphate and 50 mM sodium succinate (SC-Ura pH 5.0). The pHluorin plasmid was a generous gift from Patricia Kane (Upstate Medical University, State University of New York, Syracuse).

The yeast *S. cerevisiae* strains referred to throughout the *in vitro* studies involving vacuolar membranes and phenotype analyses are SF838-1Dα (*MATα ade6 leu2–3,112 ura3–52 pep4–3 his4–519 gal2*), the *vph1*Δ*stv1*Δ strain, MM112 (*MATα his3-*Δ*200 leu2 lys2* Δ*stvl*::*LYS2 ura3–52* Δ*vphl*::*LEU2*) (34), and the *vph1*Δ*stv1*Δ strain transformed with the CEN plasmid pRS316 carrying either the wild-type *VPH1* gene or the tether-less *VPH1* gene (*vph1–362-407*Δ) (35). MM112 was a gift from Dr. Morris Manolson (University of Toronto, Toronto, Ontario, Canada), and pRS316-HA-VPH1 was a gift from Michael Forgac (Tufts University, Boston). The *C. albicans* strain referred to throughout the study is DAY185 (*ura3::*λ*imm434/ura3::*λ*imm434his1::his6/his1::his6::HIS1arg-4::his6/arg4::his6::ARG4::URA3*), a generous gift from Aaron Mitchell, Carnegie Mellon University, Pittsburgh. DAY185 cells were maintained in YEPD, pH 5.0 (yeast extract-peptone-2% dextrose medium buffered to pH 5.0 with 50 mM

sodium phosphate and 50 mM sodium succinate), supplemented with uridine (80 μg/ml).

Assay Validation

Overnight mid-log phase cultures of yeast *S. cerevisiae* (BY4742) expressing pHluorin were resuspended in 2-fold diluted fresh SC medium to an optical density of 0.4 A_{600}/ml (1–2 × 10^7 cells/ml). Cells (0.004 A_{600}) were transferred to polypropylene 384-well plates (Greiner, Frickenhausen, Germany) containing an equal volume of disulfiram (134 and 26 mM) in 2% DMSO or 2% DMSO alone prepared in the same medium. Wash wells (columns 23 and 24) contained the same volume (10 μl) of 2-fold diluted SC medium plus 0.1% BSA. After incubation (0–120 min) at 30 °C with rotation, the plates were read using a CyAn flow cytometer (Beckman Coulter) and HyperCyt automation (IntelliCyt) (32) on filter sets 1 (ex 488/em 530) and 7 (ex 405/em 530), referred to as FL1 and FL7 hereafter. The ratio of these two measurements (FL1/FL7) was calculated. Cytosolic acidification was monitored as an increase of the FL1/FL7 ratio resulting from a simultaneous increase of the mean intensity at FL1 and a decrease of the mean intensity at FL7.

High-throughput Screening

Polypropylene 384-well plates were configured with 32 control wells and 32 wash wells. Column 1 contained the negative control (1% DMSO), column 2 contained the positive control (67 μM disulfiram), and columns 23 and 24 were the wash wells containing 2-fold diluted SC medium plus 0.1% BSA. This left 320 wells (columns 3–22) to which test compounds were added. The SC medium (2-fold diluted) was distributed into columns 1 and 3–22 (10 μl/well). An equal volume of 134 μM disulfiram or 2% DMSO was distributed into columns 2 and 1, respectively. Compounds of the Prestwick Library were added using the Biomek NX robotic liquid handler with a 200-nl pin tool attachment (V&P Scientific) to a final concentration of 0.1 mg/ml in 1% DMSO. Overnight cultures of the yeast *S. cerevisiae* expressing pHluorin were pelleted and resuspended in 2-fold diluted fresh SC medium to a cell density of 0.4 A_{600}/ml (1–2 × 10^7 cells/ml). Cells (0.004 A_{600}) were transferred to columns 1–22 and incubated for 60 min at 30 °C in a rotator, and the FL1/FL7 ratio was calculated as described above. Compounds that lowered the cytosolic pH (increased the FL1/FL7 ratio) were retested in single-point confirmation assays and dose-response assays (between 1 and 100 μM).

Cytosolic pH Measurement

Yeast cells expressing pHluorin were grown overnight to mid-log phase (0.4–0.6 A_{600}) in SC-Ura or SC-Ura, pH 5.0 (*vma2*Δ and *vma3*Δ). Cultures were collected, washed three times in SC-Ura, pH 5.0, and resuspended in the same medium to 0.5 A_{600}/μl. Aliquots of cells (10 A_{600}) were treated with 0.2% DMSO or the indicated compounds (100 μM in 0.2% DMSO) for 30 min at 30 °C with shaking. The cells were harvested, washed, resuspended in SC-Ura, pH 5.0 (0.5 A_{600}/ml), and transferred to cuvettes containing 1 mM HEPES/MES, pH 5.0, and 2% glucose (5 A_{600}/ml). The fluorescence intensity was monitored (ex 405, ex 485; em 508) for 10 min at 30 °C with constant stirring, and fluorescence units were converted into pH units by using calibration curves as described previously (29, 30). For calibration curves, the cells were resuspended (5 A_{600}/ml) in calibration buffers (50 mM MES, 50 mM HEPES, 50 mM KCl, 50 mM NaCl, 0.2 M ammonium acetate, 10 mM sodium azide, 10 mM 2-deoxyglucose, 75 μM monensin, 10 μM nigericin) at pH 5.0, 5.5, 6.0, 6.5, 7.0, 7.5, and 8.0 for 30 min at 30 °C after which the fluorescence measured. The background signals (cells without pHluorin) were subtracted, and cytosolic pH values were calculated. A calibration curve was constructed for each strain used.

Proton Transport

Vacuolar membranes were purified by Ficoll density gradient centrifugation (23), and proton transport was measured by monitoring 9-amino-6-chloro-2-methoxyacridine (ACMA) quenching after the addition of MgATP as described previously (36). Briefly, membrane vesicles (10 μg of vacuolar protein) were preincubated with 1% DMSO, 0.1 μM concanamycin A, or the indicated concentrations of the compounds on ice for 10 min. The membranes were transferred to 1.8 ml of reaction buffer (20 mM HEPES, pH 7.0, 50 mM NaCl, 30 mM KCl, 1 μM ACMA), and fluorescence was monitored (ex 410 nm, em 490 nm) for 60 s. MgATP (0.5 mM ATP, 1 mM $MgSO_4$) was added, and fluorescence quenching was monitored for an additional 40 s in a FluoroMax 4 spectrofluorometer (Horiba Jobin Yvon Inc.). The proton transport rates were estimated for the initial 15 s following the addition of MgATP. Proton transport measurements involving *C. albicans* were conducted as described above, except that 30 μg of vacuolar protein was used. To calculate EC_{50} values, the vacuolar membranes were preincubated with 0.4, 1.2, 3.6, 11.1, 22.2, 33.3, 50, 100, 200, and 300 μM alexidine dihydrochloride and thonzonium bromide on ice for 10 min, and then proton transport was measured.

ATP Hydrolysis

Vacuolar membranes (4 μg of vacuolar protein) were preincubated with 0.1 μM concanamycin A, 1 μM nigericin, or test compounds (100 μM) on ice for 10 min in the presence of 1% DMSO. ATP hydrolysis was followed spectrophotometrically by using an enzymatic assay coupled to the oxidation of NADH (37). ATPase assays involving *C. albicans* were conducted as described for yeast, except that each reaction contained 20 μg of vacuolar membrane protein. The protein concentration was measured as described by Bradford (38).

Growth Phenotype

Cell cultures of the yeast *S. cerevisiae* were grown overnight to 0.5–1.0 A_{600}/ml in YEPD, pH 5.0, at 30 °C. Cells were pelleted, resuspended to 0.5 A_{600}/ml, and incubated in YEPD, pH 5.0 (no treatment), 1% DMSO, or 100, 50, 10, or 1 μM alexidine dihydrochloride, thonzonium bromide, or disulfiram at 30 °C with shaking for 1 h. The cells were harvested, resuspended in 200 μl of sterile ddH_2O, and transferred to a 96-well plate. Serial dilutions (1:3) were stamped on YEPD, pH 5.0 and 7.5, plates and incubated at 30 and 37 °C for 48 h. A growth phenotype analysis of *C. albicans* was conducted as described above,

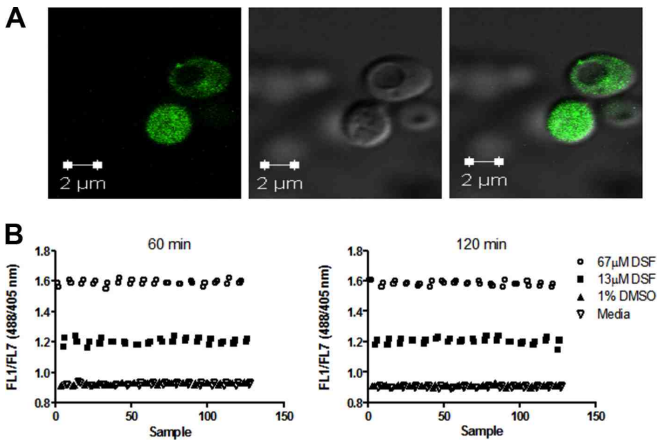

FIGUR 1. **Yeast cytosolic acidification monitored with pHluorin by high throughput.** *A*, stable expression of pHluorin in the cytosol. Wild-type yeast *S. cerevisiae* cells expressing pHluorin were grown overnight to mid-log phase (0.6 A_{600}/ml) and observed with a Zeiss LSM 520 confocal system. Cells were excited at 488 nm and emission detected with a 505-nm long pass filter (*left*); the same field was viewed at ×63 differential interference contrast (*middle*), and with images merged (*right*). *B*, pHluorin is responsive to V-ATPase inhibition *in vivo*. Cells expressing pHluorin were grown overnight to mid-log phase (0.6 A_{600}/ml), harvested, resuspended at 0.4 A_{600}/ml in 2-fold diluted SD medium containing 0.1% BSA, and distributed into 384-well plates to which SD medium alone, 1% DMSO, or disulfiram (*DSF*) at 13 and 67 μM was added for 60–120 min before sampling started. Plates were rotated at 30 °C and sampled with a HyperCyt® autosampler for flow cytometry pHluorin fluorescence measurements. After excitation with both the 488 and 405 nm lasers, fluorescence emission was collected using a 530/40-nm filter set and data files processed using IDLQuery software programs. The mean fluorescence intensity for each sample was calculated and used for subsequent analysis. Each point represents the ratio of FL1/FL7 from a single well.

except that the cells were resuspended in 1 ml of sterile H_2O before stamping.

Other Methods

Western Blot—Vacuolar membrane protein was separated by SDS-PAGE in 8% polyacrylamide gels and transferred to a nitrocellulose membrane, and V-ATPase subunits a, A, and B were visualized with the monoclonal antibodies 10D7, 8B1, and 13D11 as described previously (35).

Microscopy—*S. cerevisiae* cells transformed with the pHluorin plasmid were grown to mid-log phase (0.5 A_{600}/ml), harvested, and washed in SC medium three times by centrifugation. Cells (0.5 A_{600}/ml) were transferred to microscope slides and observed with a Zeiss LSM 510 confocal microscope (Zeiss) at ×63 magnification by differential interference contrast microscopy and FITC lens. All images were taken using the same settings on the microscope.

RESULTS

Cytosolic pH Changes Monitored by pHluorin-based High Throughput—V-ATPase inhibition prevents redistribution of cytosolic protons into the vacuolar lumen (29), resulting in acidification of the cytosol. Thus, to search for new V-ATPase inhibitors we used yeast cells expressing a pH-sensitive GFP (pHluorin) in the cytosol (30, 31). We transformed yeast cells with pHluorin, confirming its cytosolic localization by fluorescence microscopy (Fig. 1*A*). We sorted the cells with the brightest fluorescence signal by flow cytometry (data not shown) and used those cells to develop a pHluorin-based high-throughput flow cytometry assay, which would allow us to identify molecules that acidify the yeast cytosol.

We took advantage of the pH-sensitive emission spectrum of pHluorin in which the dual excitation wavelength (405 and 488 nm) of pHluorin exhibits opposite pH-dependent fluorescence responses despite both emitting at 535 nm (39). As the pH drops, the intensity of the fluorescent signal from 405 nm excitation decreases, whereas the intensity of the signal from excitation at 488 nm increases. Therefore, cytosolic acidification corresponds to a raise in the excitation 488/405 nm ratio (referred to as FL1/FL7). The benefit of a response that changes the signal on two filter sets is an automatic control for false positives in which fluorescent compounds that increase FL1 independent of cytosolic pH changes were excluded.

Concanamycin A and bafilomycin A are not suitable for studies involving high-throughput screenings *in vivo* (40). Inhibition of yeast V-ATPase pumps with concanamycin A requires 3 orders of magnitude larger concentrations of concanamycin A *in vivo* (EC_{50} = 2.10–2.27 μM) (40) than *in vitro* (EC_{50} = 1 nM) (20, 21). Likewise, bafilomycin A exhibits poor permeability. We tested the responsiveness of pHluorin to cytosolic acidification by treating yeast cells with disulfiram (tetraethylthiuram disulfide). Disulfiram (EC_{50} = 26 μM) exhibits both lower specificity and lower potency than concanamycin A and bafilomycin A *in vitro* (20, 40), but disulfiram is suitable for studies involving high-throughput screening. Disulfiram is stable and readily incorporated into yeast cells (40).

We treated the cells with an inhibitory concentration of disulfiram (67 μM) (40) and monitored the FL1/FL7 ratio. An increased FL1/FL7 ratio relative to control cells treated with 1% DMSO was measured (Fig. 1*B*). The cells had a FL1/FL7 ratio of 1.2 to 1.6 after 1 h of incubation with disulfiram at 30 °C com-

pared with a FL1/FL7 ratio of 0.9 with 1% DMSO. The FL1/FL7 ratio was dose-dependent, stable for at least 2 h, and exhibited an average Z′ of 0.76 (±0.036) for the 60–120-min time period (supplemental Table 1). The Z′ is a statistical parameter used in high-throughput screening to evaluate the quality of an assay; Z′ establishes whether significant differences exist between the controls. An assay with a Z′ value greater than 0.5 is considered appropriate for screening, that is, where consistent significant differences between the controls, in this case DMSO and disulfiram, are observed. We concluded that cells expressing pHluorin could be used to assay for pharmacological inhibition of V-ATPase pumps *in vivo* and that disulfiram-treated cells would be an appropriate positive control for identification of molecules (or compounds) that lower the cytosolic pH of yeast cells.

High-throughput Screening of the Prestwick Chemical Library—The yeast cells expressing pHluorin were used to screen a collection of 1120 off-patent drugs (Prestwick Chemical Library). For controls, we treated the cells with either 1% DMSO alone or 67 μM disulfiram. The hit cutoffs were set at a FL1/FL7 ratio of 0.86, which corresponded to the average plus 3-fold the standard deviation of the test compounds. All compounds that resulted in an increased ratio and satisfied the hit cutoff were scrutinized further to confirm that they enhanced fluorescence at 488 nm (FL1) and lowered fluorescence at 405 nm (FL7) concurrently, indicating an actual pH change.

One representative plate is shown in Fig. 2*A*. We identified nine compounds that met the cutoff criteria. Seven of these hits were validated (hit rate of 0.63%) These drugs differentially altered the magnitudes of the FL1/FL7 ratio, suggesting that some hits acidified the cytosol more significantly than others. Disulfiram, the positive control used, is also a test compound in the Prestwick Chemical Library. The fact that disulfiram itself was identified as a hit (Fig. 2*A*) validated the cutoff criteria applied and demonstrated the effectiveness of the pHluorin-based assay in high-throughput screening for inhibitors of V-ATPase proton pumps.

Benzbromarone, Alexidine Dihydrochloride, and Thonzonium Bromide Acidify the Yeast Cytosol—To verify that lack of V-ATPase function acidifies the cytosol, we measured fluorometrically the cytosolic pH of yeast V-ATPase mutant strains that do not assemble functional V_1V_0 complexes and lack all V-ATPase function (2). Yeast *vma2*Δ (pH_{cyt} 6.68 ± 0.081) and *vma3*Δ (pH_{cyt} 6.81 ± 0.044) exhibited lower cytosolic pH than wild-type cells (pH_{cyt} 7.5 ± 0.04) (Fig. 2*B*). These results are consistent with other studies (29) and with the notion that V-ATPases are key players in maintaining yeast cytosolic pH homeostasis.

We treated wild-type cells expressing pHluorin with the hit compounds and measured the cytosolic pH to confirm that the increased FL1/FL7 ratio was the direct outcome of cytosolic acidification. The cells treated with disulfiram (pH_{cyt} 6.78 ± 0.13) resembled *vma2*Δ and *vma3*Δ cells (Fig. 2*B*), whereas DMSO treatment had no effect (pH_{cyt} 7.4 ± 0.01), thus confirming that the positive and negative controls responded properly during the high-throughput screening. Treatment of yeast cells with the hit compounds revealed two groups of drugs. One group, consisting of benzbromarone (pH_{cyt} 6.03 ± 0.07), alexidine dihydrochloride (pH_{cyt} 6.10 ± 0.04), and thonzonium bromide (pH_{cyt} 6.22 ± 0.02), significantly lowered the pH. A second group, consisting of bisoprolol fumarate (pH_{cyt} 7.18 ± 0.08) and dyclonine hydrochloride (pH_{cyt} 7.33 ± 0.05), induced only subtle pH changes (Fig. 2*B*).

Alexidine Dihydrochloride and Thonzonium Bromide Functionally Uncouple V-ATPase Proton Pumps—Benzbromarone, alexidine dihydrochloride, and thonzonium bromide acidified the cytosol to different extents, suggesting that they may lower the pH by inhibiting the V-ATPase pump with different efficacy or, alternatively, by affecting different targets. To address these two possibilities, we measured proton transport in vacuolar membrane fractions fluorometrically by monitoring ACMA quenching after the addition of MgATP in the presence of each compound. As anticipated, V-ATPase proton transport was very sensitive to concanamycin A treatment *in vitro*. At 100 nM concanamycin A, ACMA quenching was blocked, indicating that a pH gradient could not be formed across the vacuolar membrane because the V-ATPase pump was inhibited (Fig. 3*A*). Alexidine dihydrochloride and thonzonium bromide inhibited proton transport in a dose-dependent manner. We estimated an EC_{50} at 39 and 69 μM for alexidine dihydrochloride and thonzonium bromide, respectively (Fig. 3*B*). Benzbromarone, however, did not inhibit proton transport (Fig. 3*A*), suggesting that it acidified the cytosol by V-ATPase-independent mechanisms. None of the remaining drugs blocked proton transport at the highest concentration tested (100 μM), consistent with their negligible effects on cytosolic pH (Fig. 2*B*).

Because V-ATPases couple active transport of protons and ATP hydrolysis, we measured ATP hydrolysis as well. We could discriminate between V-ATPase inhibitors, which block both proton transport and ATP hydrolysis, and uncouplers, which block proton transport preferentially. As expected (40), disulfiram inhibited ATP hydrolysis in vacuolar membranes, albeit with less potency than concanamycin A (Fig. 3*C*). None of the hit compounds inhibited ATP hydrolysis (Fig. 3*C*), including alexidine dihydrochloride and thonzonium bromide, even at concentrations that completely blocked proton transport (100 μM). Alexidine dihydrochloride and thonzonium bromide therefore uncoupled V-ATPase proton pumps.

The ATPase activity was not stimulated by alexidine dihydrochloride and thonzonium bromide, suggesting that they do not simply act as ionophores that uncouple V-ATPase pumps by dissipating the proton gradient across the membrane (41). To distinguish between V-ATPase-specific uncoupling and unspecific ionophore effects, we treated vacuolar membranes with 1 μM nigericin. Nigericin also uncoupled the enzyme; it abolished proton transport (Fig. 4*B*) but stimulated concanamycin A-sensitive ATP hydrolysis (by 1.4-fold) (Fig. 4*A*). We additionally showed that lower concentrations of alexidine dihydrochloride and thonzonium bromide (1–75 μM) did not stimulate ATPase activity (Fig. 4*C*). This disproves the possibility that the inhibitors act as proton ionophores at low concentrations while inhibiting activity at high concentrations, such that at 100 μM the two effects (stimulation and inhibition of ATP hydrolysis) cancel each other out. These results indicate that alexidine dihydrochloride and thonzonium bromide did

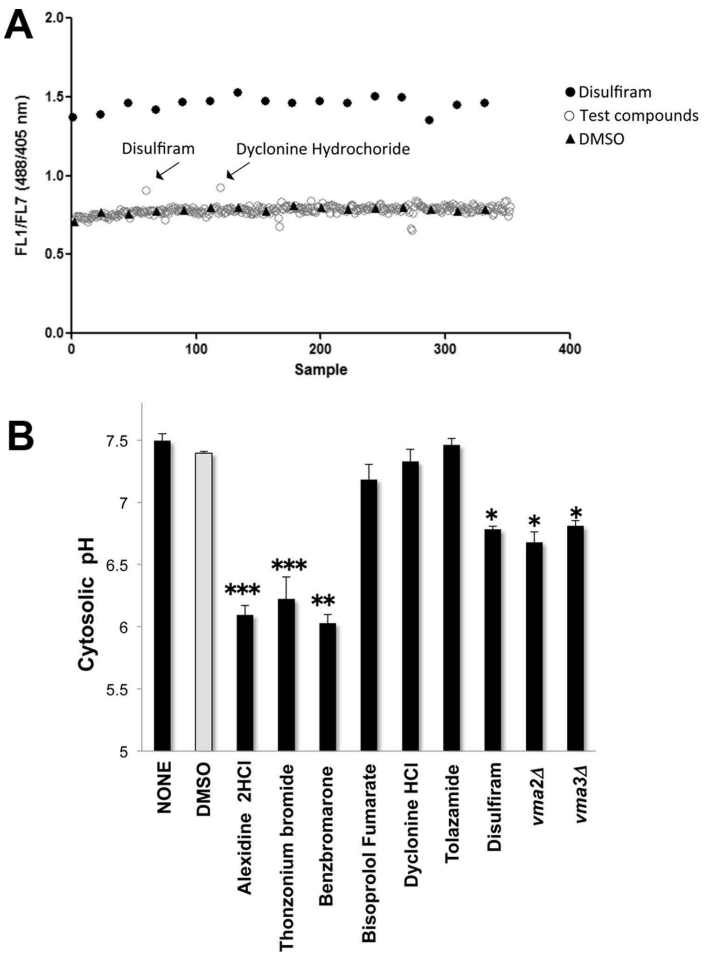

FIGURE 2. **High-throughput screening using a pHluorin-based assay identified drugs that acidify the cytosol.** *A*, high-throughput screening of the Prestwick Chemical Library revealed drugs that increase the FL1/FL7 (488/405 nm) ratio of pHluorin. Mid-log phase cultures of cells expressing pHluorin were distributed in 384-well plates (0.2 A_{600}/ml) to which test compounds, 1% DMSO (negative control), or 67 μM disulfiram (positive control) was added. Test compounds were added by robotic pintool and incubated in a rotator at 30 °C for 60 min, and sampling was started. Sampling, data collection, and processing were as described in the legend for Fig. 1*B*. One representative plate of compounds that enhanced the FL1/FL7 ratio is shown. The *x* axis displays each well; time bins were drawn automatically around the clusters by using the IDLQuery software program. *B*, cytosolic pH measurement. Yeast cells expressing pHluorin were grown overnight to mid-log phase (0.4–0.6 A_{600}/ml) and preincubated with 0.2% DMSO or with 100 μM drug in 0.2% DMSO. Following 30-min incubations at 30 °C, cells were transferred to 1 mM HEPES/MES buffer, pH 5.0, containing 2% glucose at a cell density of 5.0 A_{600}/ml; fluorescence was measured for 6 min at 1-min intervals, and pH values were averaged. The cytosolic pH was estimated using calibration curves made in parallel (pH values ranging from 5.0 to 8.0). Data are presented as average pH values. *Error bars* = ± S.D., $n = 2$; *, $p < 0.05$; **, $p < 0.01$; and ***, $p < 0.001$ compared with DMSO as measured by two-tailed paired Student's *t* test.

not uncouple V-ATPase pumps by simply dissipating the membrane proton gradient.

Yeast Cells Exposed to V-ATPase Uncouplers Develop Growth Defects—To further assess the specificity of alexidine dihydrochloride and thonzonium bromide for V-ATPases *in vivo*, we asked whether yeast cells treated with the drugs would develop growth defects that could be attributed to impairment of V-ATPase function. Lack of yeast V-ATPase activity leads to pH-sensitive growth (42, 43); cells grow at pH 5.0 but cannot grow at pH 7.5 (Fig. 5*A*). This growth defect is known as the *vma* (vacuolar membrane ATPase) mutant growth phenotype (2). We addressed whether exposure to alexidine dihydrochloride and thonzonium bromide leads to a *vma* growth phenotype by treating the cells with varied concentrations of the drugs for 1 h

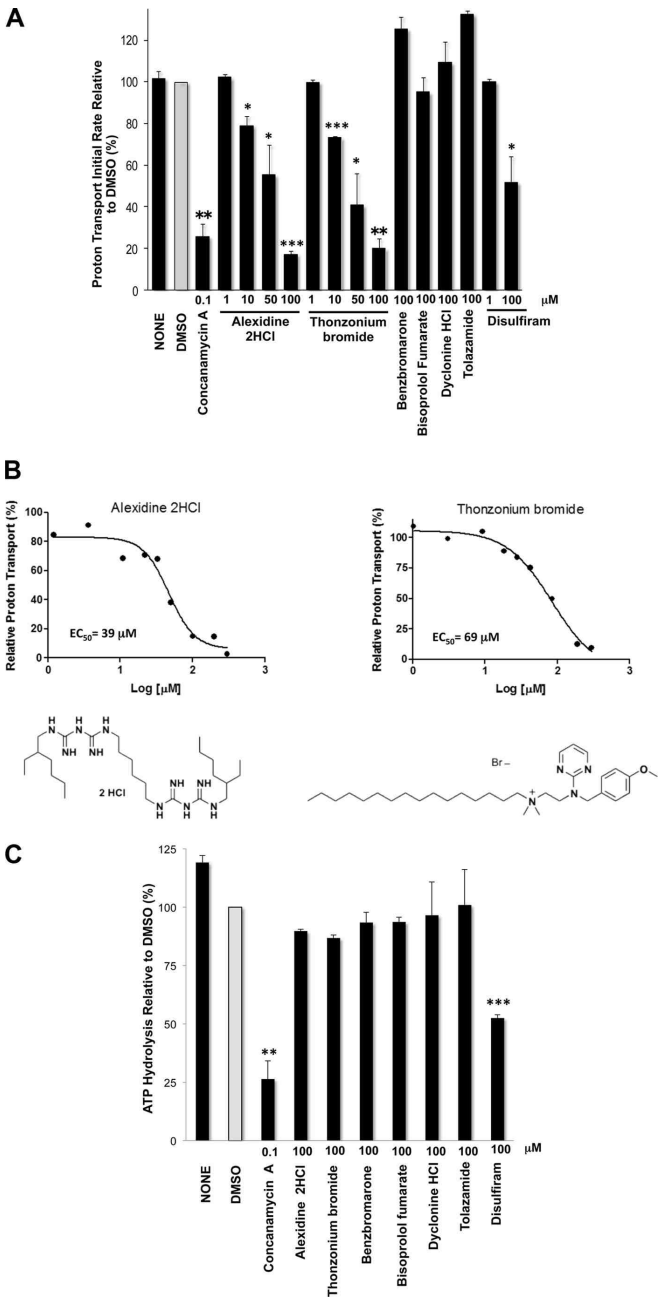

at 30 °C and plating the cells on medium buffered to pH 5.0 and 7.5. Yeast cell growth was then monitored at 30 and 37 °C for 48 h.

Predictably, cells treated with DMSO and disulfiram did not show a *vma* phenotype (Fig. 5*B*), as DMSO did not inhibit the enzyme and disulfiram only partially inhibited V-ATPase activity (by about 50%) at the highest concentration used (Fig. 3, *A* and *C*). Cells treated with the lowest concentration (1 μM) of alexidine dihydrochloride and thonzonium bromide exhibited normal cell growth (Fig. 5*B*). However, exposure to 10 μM alexidine dihydrochloride resulted in a markedly slow growth at pH 5.0 and 7.5, with cells developing the typical *vma* mutant growth phenotype at 37 °C. Likewise, 10 μM thonzonium bromide reduced cell growth, with the cells developing a mild *vma* phenotype at 37 °C. Alexidine dihydrochloride and thonzonium bromide completely prevented yeast growth at 50 and 100 μM concentrations. Previous work has shown that yeast cells must lose at least 75% of their wild-type V-ATPase function to develop a *vma* growth phenotype (23, 37). Thus, we concluded that V-ATPase function was significantly impaired *in vivo* by treatment with 10 μM uncouplers and that larger concentrations were cytotoxic.

Tether Connecting the Cytosolic Domain of Subunit a (Vph1p) to the Membrane Has Uncoupling Functions—V_0 subunit a consists of two domains: a cytosolic N-terminal domain (~45 kDa) that interacts with several V_1 subunits to allow rotation of rotor-forming subunits during catalysis and a membrane-bound C-terminal domain (~50 kDa) that contributes to the path of proton transport (3). Cleavage of Vph1p at the tether connecting the two domains uncouples yeast V-ATPase complexes (26), suggesting that Vph1-mediated assembly of the two domains is necessary for coupling. We asked whether residues forming the tether were necessary for the observed pharmacological uncoupling.

To gain insight into the mechanisms by which alexidine dyhydrochloride and thonzonium bromide uncouple V-ATPase pumps, we expressed a truncated allele of Vph1p lacking residues 362–407 of the tether (*vph1–362-407*Δ) in *vph1*Δ*stv1*Δ cells. Yeast *vph1*Δ*stv1*Δ does not express endogenous subunit a, because the gene *VPH1* and its functional homolog, *STV1*, are deleted (34). Previously, we showed that biosynthetic assembly of tether-less V_1V_0 (*vph1–362-407*Δ) complexes is complete when cells modestly overexpress V_0 subunit d (Vma6p) and that the assembled *vph1–362-407*Δ V_1V_0 fully retains ATP hydrolytic activity (35). Thus, we simultaneously co-transformed the *vph1*Δ*stv1*Δ cells with *VPH1–362-407*Δ and subunit d (*VMA6*), each of them expressed from a CEN plasmid (pRS316) under control of their natural promoters as described previously (35). We compared the mutant *vph1–362-407*Δ vacuolar membranes with isogenic wild-type membranes obtained in parallel from *vph1*Δ*stv1*Δ cells expressing the wild-type allele of *VPH1* from pRS316. As expected, the tether-less mutant assembled wild-type levels of V_1 (A and B) and V_0 (a) subunits at the vacuolar membrane and retained about 90% of the wild-type concanamycin A-sensitive ATP hydrolytic activity (Fig. 6*A*). The tether-less V_1V_0 also retained wild-type levels of proton transport (Fig. 6, *A* and *B*), suggesting that the length of the tether does not affect coupling efficiency when the physical connection between the N- and C-terminal domains of subunit a is maintained.

Tether-less V_1V_0 complexes were resistant to uncoupling by thonzonium bromide (Fig. 6*B*). Whereas 80% of the wild-type proton transport was inhibited by 100 μM thonzonium bromide, tether-less V_1V_0 was inhibited by only 40%, suggesting that the tether is involved in uncoupling by thonzonium bromide. Partial-to-no resistance against alexidine dihydrochloride suggests that uncoupling by alexidine dihydrochloride may entail other uncoupling mechanisms.

Next, we asked whether cells expressing tether-less V_1V_0 would be resistant to the uncouplers *in vivo*. We assessed cell growth at pH 7.5, the nonpermissive growth condition for *vma* mutants, after preincubation with varied concentrations of alexidine dihydrochloride and thonzonium bromide (at 1–100 μM). The *vph1–362-407*Δ cells required 2–2.5-fold larger concentrations of drugs to decrease growth than the isogenic wild-type cells (Fig. 6*C*), further suggesting that the tether plays an uncoupling function.

Alexidine Dihydrochloride and Thonzonium Bromide Uncouple C. albicans V-ATPase Proton Pumps and Impair Cell Growth—The tether constitutes the most conserved sequence at the N-terminal end of subunit a. It has 47–51% identity (63–72% conserved) between yeast and human isoforms. Based on the previous results, which indicate that this conserved sequence of Vph1p confers uncoupling potential to V-ATPase pumps, we extended our studies to *C. albicans*. This pathogenic fungi contains Vph1p with 67% sequence identity (83% conserved) with yeast at the tether region of the protein. We isolated vacuolar membrane fractions from *C. albicans* and measured proton transport and ATP hydrolysis in the presence of the uncouplers. The results in *C. albicans* (Fig. 7) mirrored the

FIGURE 3. **Alexidine dihydrocloride and thonzonium bromide uncouple V-ATPase pumps *in vitro*.** *A*, ATP-dependent proton transport is inhibited by alexidine dihydrocloride and thonzonium bromide. Purified vacuolar membrane vesicles (10 μg of protein) were preincubated for 10 min on ice with 1% DMSO alone or concanamycin A (100 nM) or with drugs at the indicated concentrations in the presence of 1% DMSO. Fluorescence quenching of ACMA was monitored (ex 410 nm, em 490 nm) upon the addition of 0.5 mM ATP and 1 mM $MgSO_4$. Initial velocities were calculated for 15 s following addition of MgATP ($n = 2$). The apparently enhanced rate measured with benzbromarone and tolazamide was not dose-dependent and was sustained in the controls, when the drugs were added to the reaction mixture prior to the membrane vesicles. *, $p < 0.05$; **, $p < 0.01$; and ***, $p < 0.001$ for decreased transport compared with DMSO as measured by two-tailed paired Student's *t* test. *B*, V-ATPase inhibition by alexidine dihydrochloride and thonzonium bromide is dose-dependent. Purified vacuolar membrane vesicles (10 μg of protein) were incubated with alexidine dihydrochloride or thonzonium bromide at the indicated concentrations for 10 min on ice. ATP-dependent proton transport was measured as described in *A*. EC_{50} values were estimated using GraphPad Prism 5.0. The structures of alexidine dihydrochloride (*left*) and thonzonium bromide (*right*) are shown. *C*, ATP hydrolysis is resistant to alexidine dihydrochloride and thonzonium bromide treatments. Purified vacuolar membranes (4 μg of total protein) were preincubated for 10 min on ice with the indicated drug concentrations in 0.2% DMSO or with 0.2% DMSO alone. Following each treatment, ATP hydrolysis was measured spectrophotometrically using an enzymatic assay coupled to oxidation of NADH (340 nm) (59). Data are expressed as the average ± S.D.; $n = 3$ separate vacuolar purifications. Relative averaged values were used to express percentage activity. The specific activity of the concanamycin A-sensitive ATPase activity of the vacuoles was 1.3–1.5 μmol of ATP/min/mg of protein. **, $p < 0.01$; and ***, $p < 0.001$ for decreased ATPase activity (2-fold or more) compared with DMSO as measured by two-tailed paired Student's *t* test.

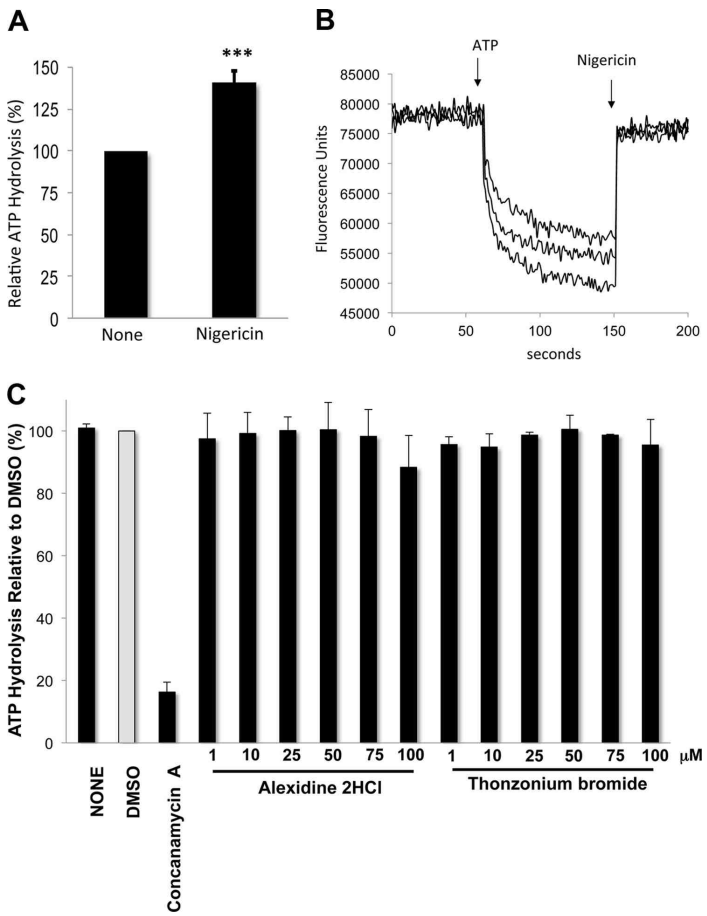

FIGURE 4. **Uncoupling by alexidine dihydrocloride and thonzonium bromide differs from ionophore-mediated uncoupling.** *A*, nigericin stimulates ATPase activity. Concanamycin A-sensitive ATPase specific activity was measured as described in the legend for Fig. 3*C*, except that 1 μM nigericin in 0.1% ethanol was added to the reaction. An equal concentration of ethanol in the reaction had no effect on the activity. Shown is the average activity relative to untreated controls (*None*) of three independent vacuolar purifications. *Error bars* = ± S.D. ***, $p < 0.001$ compared with no treatment as measured by two-tailed paired Student's *t* test. *B*, nigericin inhibits proton transport. Proton transport was monitored in three independent vacuolar membrane preparations (10 μg of protein) by measuring ACMA quenching as described in the legend for Fig. 3*A*, except that nigericin (1 μM) was added 90 s after the addition of MgATP, and florescence was measured for an additional 50 s. *C*, ATP hydrolysis is not stimulated by lower concentrations of alexidine dihydrochloride and thonzonium bromide. Concanamycin A-sensitive ATPase specific activity was measured as described in the legend to Fig. 3*C*. Data are expressed as the average ± S.D.; $n = 3$ separate vacuolar purifications. Relative averaged values were used to express percentage activity.

studies in *S. cerevisiae*. Alexidine dihydrochloride and thonzonium bromide inhibited proton transport in a dose-dependent manner (Fig. 7*A*) but had no effect on ATP hydrolysis (Fig. 7*B*), showing that alexidine dihydrochloride and thonzonium bromide also uncoupled *C. albicans* V-ATPase pumps.

For *in vivo* analyses, *C. albicans* was exposed to various concentrations of the inhibitors for 1 h at 30 °C, and growth was assessed at pH 5.0 and 7.5 at both 30 and 37 °C (Fig. 7*C*). Like the yeast *S. cerevisiae*, *C. albicans* cells exposed to 1 μM alexidine dihydrochloride, 1 μM thonzonium bromide, and up to 100 μM disulfiram mimicked the untreated and DMSO control cells. Although the cells did not develop a *vma* growth phenotype, they exhibited significant general growth defects after treatment with 10 μM alexidine dihydrochloride or thonzonium bromide at both pH 5.0 and 7.5. Alexidine dihydrochloride was more toxic than thonzonium bromide, but both drugs completely blocked growth at the higher concentrations tested (50 and 100 μM).

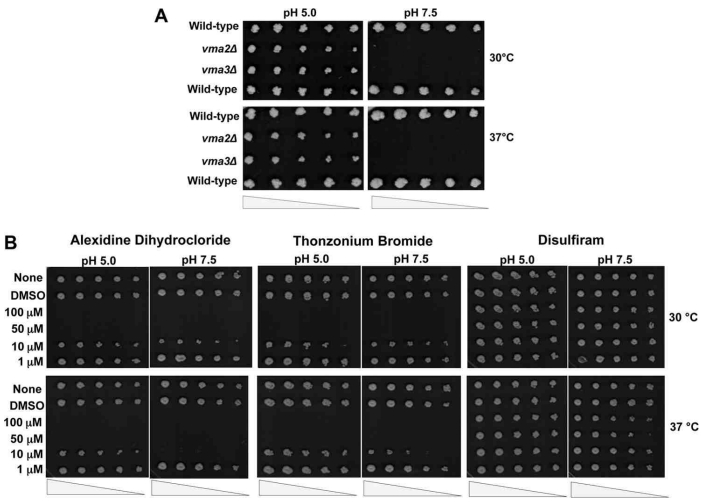

FIGURE 5. **Alexidine dihydrochloride and thonzonium bromide treatments lead to growth defects in *S. cerevisiae*.** *A*, yeast *vma* mutants cannot grow at neutral pH. Overnight mid-log phase cultures of *vma2*Δ and *vma3*Δ cells (lacking all V-ATPase function) and an isogenic wild type were diluted to 0.5 A_{600}/ml in YEPD medium, pH 5.0, and serial dilutions (1:3) were stamped on YEPD plates adjusted to pH 5.0 and 7.5 and incubated at 30 and 37 °C. *B*, alexidine dihydrochloride and thonzonium bromide prevent growth. Overnight yeast cell cultures were diluted to 0.5 A_{600}/ml in YEPD medium, pH 5.0. Cells were rotated at 30 °C for 1 h with the drugs at the indicated concentrations containing 1% DMSO. Controls included cells resuspended in 1% DMSO alone or an equal volume of YEPD, pH 5.0 (*None*). Serial dilutions (1:3) were stamped on YEPD, pH 5.0 and pH 7.5, plates and incubated at 30 and 37 °C. Cell growth was monitored for 48 h.

DISCUSSION

We screened a chemical library using a pHluorin-based high-throughput flow cytometry assay to identify compounds that acidify the yeast cytosol as a means of identifying new *in vivo* inhibitors of *S. cerevisiae* V-ATPase proton pumps. We identified two drugs, alexidine dihydrochloride and thonzonium bromide, which selectively target the V-ATPase complex *in vitro* and *in vivo* by blocking proton transport. Our studies indicate that they are *bona fide* uncouplers of V-ATPase pumps.

New Inhibitors of V-ATPase Pumps Acidify the Cytosol and Uncouple the Enzyme—This unbiased screen identified six drugs that lower the yeast cytosolic pH, albeit to different extents (Fig. 2*B*). Benzbromarone, alexidine dihydrochloride, thonzonium bromide, and disulfiram showed the strongest effects, whereas dyclonine hydrochloride and bisoprolol fumarate induced smaller pH changes. Only disulfiram, alexidine dihydrochloride, and thonzonium bromide acidified the cytosol through inhibition of V-ATPase pumps. The remaining drugs did not inhibit ATP hydrolysis and/or proton transport in purified yeast vacuolar membranes, indicating that they act on different targets and acidify the cytosol through V-ATPase-independent mechanisms.

Yeast cytosolic pH is maintained through a concerted movement of protons out of the cytosol by the V-ATPase and Pma1p pumps, the major electrogenic pumps at the vacuolar and plasma membranes, respectively (13, 29). Whereas V-ATPase transfers protons into the vacuolar lumen, Pma1p moves cytosolic protons out of the cell, helping yeast to sustain a favorable acidic growth environment. Therefore, by using the pHluorin system to monitor cytosolic acidification, we anticipated the identification of inhibitors of Pma1p in addition to V-ATPase inhibitors. We also most likely identified general inhibitors of protonophore activity, because they would be expected to dissipate cellular proton gradients, accelerate the leakage of protons from organelles, and result in net cytosolic acidification.

Disulfiram was identified previously as a V-ATPase inhibitor in a high-throughput screen of the Prestwick Chemical Library, and we showed that disulfiram treatment alkalinizes the yeast vacuoles (40). In that study, we characterized the inhibitory effect of disulfiram on ATP hydrolysis (40). Here, we have further shown that disulfiram treatment acidified the yeast cytosol *in vivo* (Fig. 2*B*) and inhibited V-ATPase proton transport (Figs. 3*A* and 7*A*) in addition to ATP hydrolysis (Figs. 3*C* and 7*B*) *in vitro*.

Alexidine dihydrochloride and thonzonium bromide inhibited proton transport in vacuolar membrane fractions without inhibiting ATP hydrolysis. At high concentrations (100 μM), proton transport was significantly impaired (by 80–90%), whereas ATP hydrolysis remained intact. Our results indicate that alexidine dihydrochloride and thonzonium bromide are not simply ionophores, because they do not stimulate ATP hydrolysis, in contrast with nigericin, which both inhibits proton transport and stimulates hydrolysis of ATP (Fig. 4). Alexidine dihydrochloride and thonzonium bromide selectively uncouple V-ATPase pumps.

Although less potent than concanamycin A (EC_{50} = 1 nM), uncouplers such as alexidine dihydrochloride (EC_{50} = 39 μM) and thonzonium bromide (EC_{50} = 69 μM) are anticipated to be highly toxic. In addition to disturbing cytosolic and vacuolar pH

homeostasis, alexidine dihydrochloride and thonzonium bromide should deplete the energy reserves of the cell, because uncoupled V-ATPase pumps will hydrolyze cytosolic ATP continuously. In a global sense, V-ATPase uncouplers hinder multiple cellular processes and constitute a quick acting way to block vital functions.

As anticipated, yeast was more sensitive to treatment with the uncouplers *in vivo* than *in vitro*. Treatment with alexidine

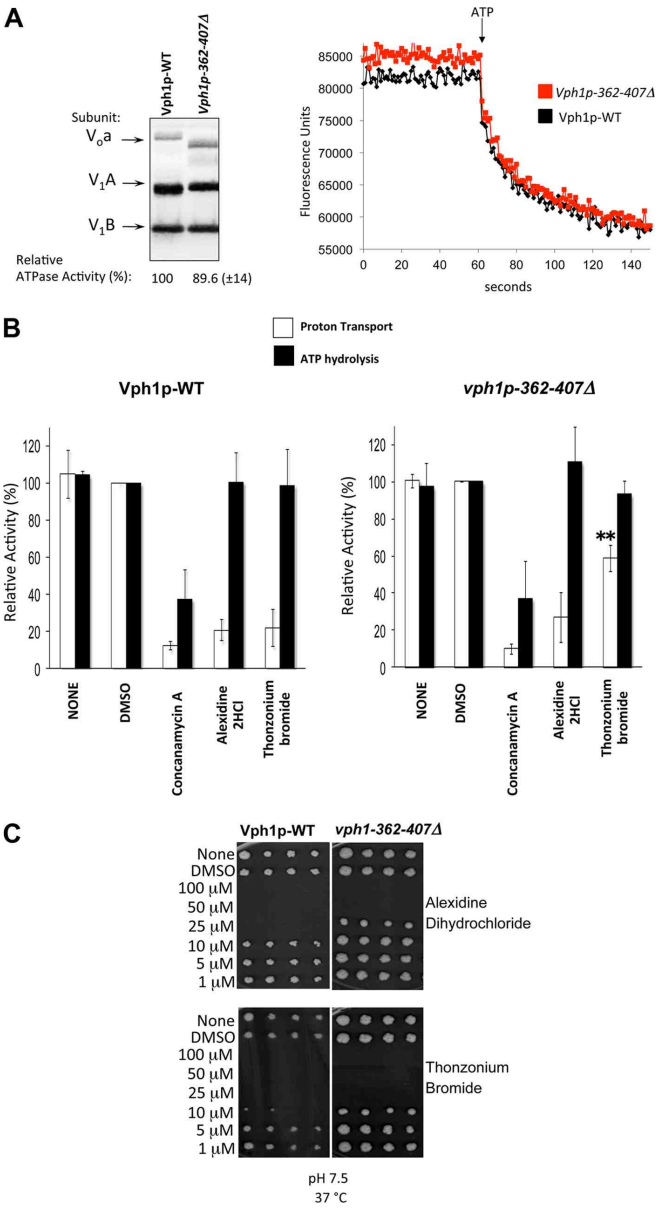

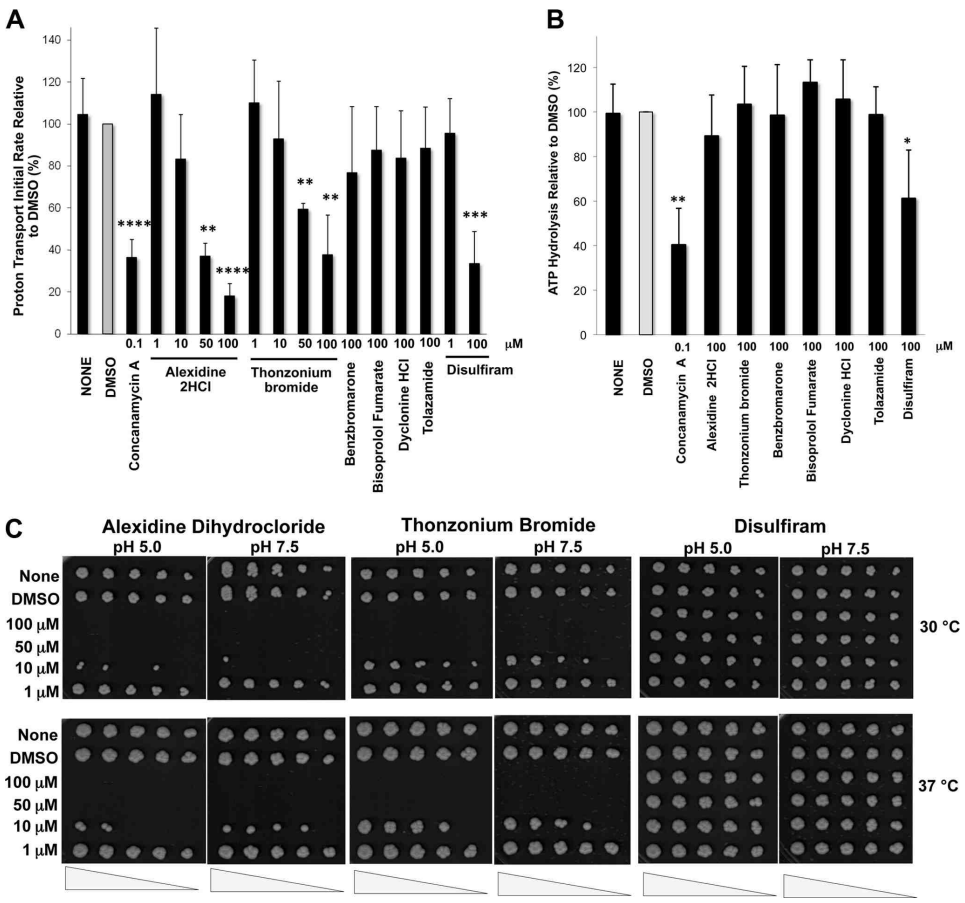

FIGURE 7. **Alexidine dihydrocloride and thonzonium bromide uncouple *C. albicans* V-ATPase pumps and prevent growth.** *A*, *C. albicans* ATP-dependent proton transport is inhibited by the uncouplers. Fluorescence quenching of ACMA was measured as described in Fig. 3*A*, except that 30 μg of vacuolar membrane protein was used for each treatment. *B*, ATPase activity is resistant to the uncouplers. ATP hydrolysis was measured as described in the legend for Fig. 3*C*, except that 20 μg of purified vacuolar membrane protein was used for each treatment. In both *A* and *B*, the indicated concentrations of drugs were present in 1% DMSO. Data are expressed as the average ± S.D. for $n = 3$–5 independent vacuolar purifications. The specific activity of the concanamycin A-sensitive ATPase activity of the vacuoles was 0.2–0.4 μmol of ATP/min/mg of protein. *, $p < 0.05$; **, $p < 0.01$; ***, $p < 0.001$; and ****, $p < 0.0001$ by two-tailed paired Student's *t* test. *C*, uncouplers reduced the growth of *C. albicans*. Cultures of *C. albicans* were grown overnight and treated as described in the legend for Fig. 5*B*.

dihydrochloride and thonzonium bromide was cytotoxic at concentrations (50 μM) that inhibited proton transport by only 40% *in vitro* (Figs. 3*A* and 5*B*). Yeast cells treated with a lower concentration of the drugs (10 μM) developed a *vma* growth phenotype, despite the fact that proton transport was barely inhibited (by 20–25%) *in vitro*. Therefore, a fine threshold (20–

FIGURE 6. **The tether of subunit a (Vph1p) is crucial for functional uncoupling by thonzonium bromide.** *A*, tether-less V_1V_o complexes are coupled functionally. *Left*, vacuolar membrane vesicles were purified from *vph1*Δ*stv1*Δ cells transformed with either wild-type *VPH1* or *VMA6* plus mutant (*Vph1p-362–407*Δ). Protein separated by SDS-PAGE (5 μg of total vacuolar protein) was analyzed by Western blot using antibodies against V_o subunit a and V_1 subunits A and B. Concanamycin A-sensitive ATPase activity (10 μg of total protein) was measured as described in the legend for Fig. 3*C*. *Right*, proton transport was measured as described in the legend for Fig. 3*A*. *B*, tether-less V_1V_o complexes are resistant to thonzonium bromide-induced uncoupling. Wild-type (*Vph1p-WT*) and tether-less mutant (*vph1p-362–407*Δ) vacuolar membranes were treated with 100 μM thonzonium bromide or alexidine dihydrochloride, and ATP hydrolysis and proton transport were measured as described in the legend for Fig. 3, *A* and *C*. **, $p < 0.01$ compared with Vph1p-WT treated with thonzonium bromide, as measured by two-tailed paired Student's *t* test. *C*, tether-less V_1V_o yeast mutants show growth resistance to thonzonium bromide and alexidine dihydrochloride. Wild-type and tether-less mutant cells were grown overnight to 0.5 A_{600}/ml in SC-Ura medium, pH 5.0, treated with the indicated concentrations of drugs as described in the legend for Fig. 5, and plated on YEPD, pH 7.5 (1:3-fold serial dilutions). Plates were incubated at 37 °C for 72 h.

40% uncoupling) delineates conditional growth (*vma* phenotype) and cell death following uncoupling of the proton transport and ATPase activity by alexidine dihydrochloride and thonzonium bromide.

Yeast V-ATPase mutants develop the *vma* phenotype when V-ATPase function (proton transport and ATP hydrolysis) is impaired by about 75% (23, 37). Yet, a more modest loss of proton transport (by about 60%) leads to *vma* growth phenotype if the pump is uncoupled (44). The fact that yeast died after 40% proton transport inhibition by the uncouplers (Figs. 3 and 5) indicates that the cells are more susceptible to pharmacological (acute) than genetic (chronic) V-ATPase uncoupling. Perhaps, V-ATPase mutants can develop compensatory ATP conservation mechanisms that will allow yeast to survive in the face of uncoupling. In addition, alexidine dihydrochloride and thonzonium bromide at concentrations greater than 50 μM could have additional targets and effects unrelated to V-ATPase that could also contribute to cytotoxicity.

Nonetheless, the *vma* growth phenotype as defined by significantly slow growth (thonzonium bromide) or no growth (alexidine dihydrochloride) at pH 7.5 showed selectivity of the drugs for V-ATPase (Fig. 5*B*). The *vma* phenotype is the hallmark trait of yeast cells with impaired V-ATPase function (8, 43) and is a legitimate indicator of V-ATPase defects in yeast. In line with this notion, we found that 1 μM alexidine dihydrochloride or thonzonium bromide does not inhibit the pumps or affect cell growth at pH 7.5. Additionally, benzbromarone (100 μM), which does not inhibit V-ATPase pumps (Fig. 3, *A* and Fig. *C*), does not inhibit cell growth at pH 7.5 (data not shown), despite acidifying the cytosol (Fig. 2*B*). Thus, cytosolic acidification alone is not enough to develop *vma* mutant growth phenotype; V-ATPase function also must be impaired.

Uncoupling Roles of the Cytosolic Tether Connecting Vph1p to the Membrane—V_0 subunit a structurally bridges the V_0 and V_1 domains of the V-ATPase complex. Subunit a interacts with V_1 subunits E, G, C, H, and A at its N terminus (cytosolic domain) and the proteolipid ring at its C terminus (integral membrane domain) (45–48). Its unique topography makes subunit a an attractive candidate for the coupling of proton transport in V_0 and ATP hydrolysis in V_1. Subunit a is the only stator subunit anchored in the membrane. By holding the three peripheral stators (EG dimers) at its cytosolic domain, subunit a secures the steady catalytic sites in the A_3B_3 hexamer while transferring protons through its membrane domain. Providing evidence that the V_1V_0 association facilitated by subunit a is necessary for coupling of the enzyme, separation of the N terminus from the C terminus of Vph1 by cleavage at residue 376 of the tether partially uncouples V-ATPases (26). Cleavage reduces proton transport by 2-fold without affecting ATPase activity. We showed in an earlier study that the tether of the subunit a Vph1p is a flexible element and that Vph1p tether-less mutant V_1V_0 complexes are functional, as they retain concanamycin A-sensitive ATP hydrolytic activity and disassemble and reassemble normally (35).

Here we show that tether-less V_1V_0 completely retained wild-type levels of proton transport activity. Wild-type levels of both proton transport and ATPase activity in tether-less V_1V_0 indicate that the length of the tether is not essential for functional coupling of the enzyme. Our results indicate instead that the intact tether facilitates uncoupling. Amino acid residues 362–407 of the tether conferred uncoupling potential to V-ATPases, as their truncation made the enzyme resistant to treatment with thonzonium bromide. In the presence of thonzonium bromide, the coupling efficiency (the ratio of relative proton transport to relative ATPase activity) of tether-less V_1V_0 was greater than that of the wild-type enzyme (Fig. 6*B*).

In line with the idea that the tether of Vph1p confers sensitivity to thonzonium bromide, wild-type strains SF838-1Dα (Fig. 5*B*) and Vph1p-WT (Fig. 6*C*), which express Vph1p, showed similar sensitivity to thonzonium bromide. Both strains had reduced growth at pH 7.5 and 37 °C (*vma* phenotype) after exposure to 10 μM thonzonium bromide. The additional finding that only SF838-1Dα developed the *vma* growth phenotype when the cells were challenged with alexidine dihydrochloride further supports this notion. The major difference between these two strains is that SF838-1Dα expresses both isoforms of subunit a (the vacuolar isoform, Vph1p, and the Golgi isoform, Stv1p), whereas Vph1p-WT expresses only Vph1p. Thus, if alexidine dihydrochloride additively uncoupled Stv1p- and Vph1p-containing V-ATPases, the absence of Stv1p could explain Vph1p-WT growth resistance.

The presence of a structural element that gives uncoupling potential to V-ATPase complexes is consistent with the hypothesis that wild-type V-ATPase pumps may not be coupled optimally (27, 28) and that the tightness of coupling may be adjusted *in vivo* to modulate organelle acidification (2, 28). The tightness of coupling of proton transport and ATPase activity has been shown to be modulated by ATP concentrations (27) and by the nonhomologous region of V_1 subunit A (25). The mutation P217V in the nonhomologous region of subunit A generates more tightly coupled complexes because it stimulates proton transport and reduces ATPase activity. As the nonhomologous region of the V_1 subunit A interacts with V_0 subunit a (25), such tightness of coupling could be explained if structural changes are transmitted from subunit A to the tether of subunit a.

Other uncoupling elements may exist in addition to the tether of the V_0 subunit a. Our results indicate that alexidine dihydrochloride uncouples the enzyme by a mechanism unique from thonzonium bromide, despite their similar EC_{50}. Alexidine dihydrochloride is an amphipathic bisbiguanide that binds to lipopolysaccharides (49) and is used as an antibacterial agent (50), whereas thonzonium bromide is a monocationic detergent surface-active agent. Although both may have adverse effects on lipid domains (51), and we cannot eliminate the possibility that they could affect V-ATPase function by altering V_0 interactions with membrane lipids, our results indicate that thonzonium bromide and alexidine dihydrochloride selectively inhibited V-ATPase proton transport *in vitro*. Arguing against unspecific effects are the fact that ATP hydrolysis was kept intact even at high concentrations of the drugs (100 μM); that uncoupling by thonzonium bromide and alexidine dihydrochloride was demonstrated in two different sources of vacuolar membranes (*S. cerevisiae* and *C. albicans*); that uncoupling by thonzonium bromide and alexidine dihydrochloride differed from uncoupling by ionophores such as nigericin; and that

*vph1–362-407*Δ mutants showed selective resistance to uncoupling by thonzonium bromide only.

V-ATPase Uncouplers as Potential Anti-V-ATPase Drugs—Alexidine dihydrochloride and thonzonium bromide effectively inhibit V-ATPase proton transport in vacuolar membranes from *C. albicans* (Fig. 7). Although uncoupling *in vitro* is very similar between *C. albicans* and *S. cerevisiae, C. albicans* does not develop the *vma* growth phenotype. *In vivo*, the uncouplers significantly reduce cell growth at 10 μM and are cytotoxic at greater concentrations. This may be because complete inactivation of V-ATPase activity appears to be necessary for development of the *vma* phenotype in *C. albicans* (52), as cells expressing genetic mutations that partially inactivate V-ATPase function do not develop pH-sensitive growth.[7] Our results indicate that V-ATPase uncoupling must be lethal, because deletions of V-ATPase subunits that prevent enzyme function leading to the *vma* growth phenotype do not cause general cytotoxicity in *C. albicans* (52).

Fungi need vacuolar and trafficking functions to infect their hosts, and genetic inactivation of V-ATPase prevents virulence of *C. albicans* and other pathogenic fungi (52–54). We have provided evidence that V-ATPase uncoupling would be a highly effective mechanism to control virulence, because in addition to preventing proton transport, uncouplers are expected to deplete the energy reserve of the cell. Although V-ATPase inhibitors that have therapeutic applications have yet to be identified, the Prestwick Chemical Library is a useful resource for drug repurposing, as most of the compounds have known safety and toxicity profiles. In fact, cytotoxicity by alexidine dihydrochloride has been shown previously in *Cryptococcus neoformans*, *C. albicans, and Paracoccidioides brasiliensis* (55, 56). Together, those studies and our current findings make alexidine dihydrochloride and thonzonium bromide attractive candidates to evaluate for repurposing as potential antifungal therapeutic drugs. Further studies will specifically assess the anti-virulence mechanisms behind these drugs and the efficacy of combining these uncouplers with other antifungal therapeutics such as azoles, which also alter V-ATPase activity (57).

In conclusion, alexidine dihydrochloride and thonzonium bromide disengaged proton transport and ATPase activity, and to our knowledge, they are the only uncouplers of V-ATPase proton pumps described. This study revealed new information regarding the mechanisms of V-ATPase coupling, a region within V_o subunit a (the tether) that confers "uncoupling potential" to V-ATPase pumps, supporting the hypothesis that wild-type V-ATPase complexes may not be optimally coupled *in vivo* (27, 28). Uncouplers of V-ATPase pumps may offer new knowledge to the understanding of the mechanisms governing rotational catalysis and V-ATPase regulation, and they may be useful as potential therapeutic drugs. Because alexidine dihydrochloride and thonzonium bromide uncouple *C. albicans* V-ATPase, additionally they can help to elucidate the cellular processes pertaining to fungal infection and virulence in pathogens like *C. albicans*, the single most important cause of opportunistic mycoses worldwide for which available treatment methods remain suboptimal (58).

[7] S. M. Raines, S. A. Lee, and K. J. Parra, unpublished results.

Acknowledgments—We thank Juan Strouse, Anna Waller, Mark Carter, and other researchers and staff at the University of New Mexico Center for Molecular Discovery for helpful discussions. Images in this article were generated at the University of New Mexico Cancer Center Fluorescence Microscopy Shared Resource.

REFERENCES

1. Nishi, T., and Forgac, M. (2002) The vacuolar (H+)-ATPases: nature's most versatile proton pumps. *Nat. Rev. Mol. Cell Biol.* **3,** 94–103
2. Kane, P. M. (2006) The where, when, and how of organelle acidification by the yeast vacuolar H+-ATPase. *Microbiol. Mol. Biol. Rev.* **70,** 177–191
3. Forgac, M. (2007) Vacuolar ATPases: rotary proton pumps in physiology and pathophysiology. *Nat. Rev. Mol. Cell Biol.* **8,** 917–929
4. Shum, W. W., Ruan, Y. C., Da Silva, N., and Breton, S. (2011) Establishment of cell-cell cross-talk in the epididymis: control of luminal acidification. *J. Androl.* **32,** 576–586
5. Brown, D., Breton, S., Ausiello, D. A., and Marshansky, V. (2009) Sensing, signaling and sorting events in kidney epithelial cell physiology. *Traffic* **10,** 275–284
6. Ochotny, N., Flenniken, A. M., Owen, C., Voronov, I., Zirngibl, R. A., Osborne, L. R., Henderson, J. E., Adamson, S. L., Rossant, J., Manolson, M. F., and Aubin, J. E. (2011) The V-ATPase a3 subunit mutation R740S is dominant negative and results in osteopetrosis in mice. *J. Bone Miner. Res.* **26,** 1484–1493
7. Nakanishi-Matsui, M., Sekiya, M., Nakamoto, R. K., and Futai, M. (2010) The mechanism of rotating proton pumping ATPases. *Biochim. Biophys. Acta* **1797,** 1343–1352
8. Kane, P. M. (2007) The long physiological reach of the yeast vacuolar H+-ATPase. *J. Bioenerg. Biomembr.* **39,** 415–421
9. Forster, C., and Kane, P. M. (2000) Cytosolic $Ca2^+$ homeostasis is a constitutive function of the V-ATPase in *Saccharomyces cerevisiae*. *J. Biol. Chem.* **275,** 38245–38253
10. Zhang, J. W., Parra, K. J., Liu, J., and Kane, P. M. (1998) Characterization of a temperature-sensitive yeast vacuolar ATPase mutant with defects in actin distribution and bud morphology. *J. Biol. Chem.* **273,** 18470–18480
11. Bishop, A. L., Rab, F. A., Sumner, E. R., and Avery, S. V. (2007) Phenotypic heterogeneity can enhance rare cell survival in "stress-sensitive" yeast populations. *Mol. Microbiol.* **63,** 507–520
12. Huss, M., and Wieczorek, H. (2009) Inhibitors of V-ATPases: old and new players. *J. Exp. Biol.* **212,** 341–346
13. Bowman, E. J., O'Neill, F. J., and Bowman, B. J. (1997) Mutations of *pma-1*, the gene encoding the plasma membrane H+-ATPase of *Neurospora crassa*, suppress inhibition of growth by concanamycin A, a specific inhibitor of vacuolar ATPases. *J. Biol. Chem.* **272,** 14776–14786
14. Bowman, E. J., and Bowman, B. J. (2000) Cellular role of the V-ATPase in *Neurospora crassa*: analysis of mutants resistant to concanamycin or lacking the catalytic subunit A. *J. Exp. Biol.* **203,** 97–106
15. Huss, M., Vitavska, O., Albertmelcher, A., Bockelmann, S., Nardmann, C., Tabke, K., Tiburcy, F., and Wieczorek, H. (2011) Vacuolar H(+)-ATPases: intra- and intermolecular interactions. *Eur. J. Cell Biol.* **90,** 688–695
16. Mijaljica, D., Prescott, M., and Devenish, R. J. (2011) V-ATPase engagement in autophagic processes. *Autophagy* **7,** 666–668
17. Klionsky, D. J., Elazar, Z., Seglen, P. O., and Rubinsztein, D. C. (2008) Does bafilomycin A1 block the fusion of autophagosomes with lysosomes? *Autophagy* **4,** 849–950
18. El Far, O., and Seagar, M. (2011) A role for V-ATPase subunits in synaptic vesicle fusion? *J. Neurochem.* **117,** 603–612
19. Bowman, B. J., McCall, M. E., Baertsch, R., and Bowman, E. J. (2006) A model for the proteolipid ring and bafilomycin/concanamycin-binding site in the vacuolar ATPase of *Neurospora crassa*. *J. Biol. Chem.* **281,** 31885–31893
20. Bowman, E. J., and Bowman, B. J. (2005) V-ATPases as drug targets. *J. Bioenerg. Biomembr.* **37,** 431–435
21. Bockelmann, S., Menche, D., Rudolph, S., Bender, T., Grond, S., von Zezschwitz, P., Muench, S. P., Wieczorek, H., and Huss, M. (2010) Archazolid A binds to the equatorial region of the c-ring of the vacuolar H+-ATPase.

J. Biol. Chem. **285,** 38304–38314
22. Xu, T., and Forgac, M. (2000) Subunit D (Vma8p) of the yeast vacuolar H+-ATPase plays a role in coupling of proton transport and ATP hydrolysis. *J. Biol. Chem.* **275,** 22075–22081
23. Owegi, M. A., Pappas, D. L., Finch, M. W., Jr., Bilbo, S. A., Resendiz, C. A., Jacquemin, L. J., Warrier, A., Trombley, J. D., McCulloch, K. M., Margalef, K. L., Mertz, M. J., Storms, J. M., Damin, C. A., and Parra, K. J. (2006) Identification of a domain in the V_0 subunit d that is critical for coupling of the yeast vacuolar proton-translocating ATPase. *J. Biol. Chem.* **281,** 30001–30014
24. Liu, M., Tarsio, M., Charsky, C. M., and Kane, P. M. (2005) Structural and functional separation of the N- and C-terminal domains of the yeast V-ATPase subunit H. *J. Biol. Chem.* **280,** 36978–36985
25. Shao, E., and Forgac, M. (2004) Involvement of the nonhomologous region of subunit A of the yeast V-ATPase in coupling and *in vivo* dissociation. *J. Biol. Chem.* **279,** 48663–48670
26. Qi, J., and Forgac, M. (2008) Function and subunit interactions of the N-terminal domain of subunit a (Vph1p) of the yeast V-ATPase. *J. Biol. Chem.* **283,** 19274–19282
27. Arai, H., Pink, S., and Forgac, M. (1989) Interaction of anions and ATP with the coated vesicle proton pump. *Biochemistry* **28,** 3075–3082
28. Moriyama, Y., and Nelson, N. (1988) The vacuolar H+-ATPase, a proton pump controlled by a slip. *Prog. Clin. Biol. Res.* **273,** 387–394
29. Martínez-Muñoz, G. A., and Kane, P. (2008) Vacuolar and plasma membrane proton pumps collaborate to achieve cytosolic pH homeostasis in yeast. *J. Biol. Chem.* **283,** 20309–20319
30. Brett, C. L., Tukaye, D. N., Mukherjee, S., and Rao, R. (2005) The yeast endosomal Na+K+/H+ exchanger Nhx1 regulates cellular pH to control vesicle trafficking. *Mol. Biol. Cell* **16,** 1396–1405
31. Tarsio, M., Zheng, H., Smardon, A. M., Martínez-Muñoz, G. A., and Kane, P. M. (2011) Consequences of loss of Vph1 protein-containing vacuolar ATPases (V-ATPases) for overall cellular pH homeostasis. *J. Biol. Chem.* **286,** 28089–28096
32. Edwards, B. S., Oprea, T., Prossnitz, E. R., and Sklar, L. A. (2004) Flow cytometry for high-throughput, high-content screening. *Curr. Opin. Chem. Biol.* **8,** 392–398
33. Elble, R. (1992) A simple and efficient procedure for transformation of yeasts. *BioTechniques* **13,** 18–20
34. Manolson, M. F., Wu, B., Proteau, D., Taillon, B. E., Roberts, B. T., Hoyt, M. A., and Jones, E. W. (1994) *STV1* gene encodes functional homologue of 95-kDa yeast vacuolar H(+)-ATPase subunit Vph1p. *J. Biol. Chem.* **269,** 14064–14074
35. Ediger, B., Melman, S. D., Pappas, D. L., Jr., Finch, M., Applen, J., and Parra, K. J. (2009) The tether connecting cytosolic (N terminus) and membrane (C terminus) domains of yeast V-ATPase subunit a (Vph1) is required for assembly of V_0 subunit d. *J. Biol. Chem.* **284,** 19522–19532
36. Forgac, M., Cantley, L., Wiedenmann, B., Altstiel, L., and Branton, D. (1983) Clathrin-coated vesicles contain an ATP-dependent proton pump. *Proc. Natl. Acad. Sci. U.S.A.* **80,** 1300–1303
37. Owegi, M. A., Carenbauer, A. L., Wick, N. M., Brown, J. F., Terhune, K. L., Bilbo, S. A., Weaver, R. S., Shircliff, R., Newcomb, N., and Parra-Belky, K. J. (2005) Mutational analysis of the stator subunit E of the yeast V-ATPase. *J. Biol. Chem.* **280,** 18393–18402
38. Bradford, M. M. (1976) A rapid and sensitive method for the quantitation of microgram quantities of protein utilizing the principle of protein-dye binding. *Anal. Biochim.* **72,** 248–254
39. Mahon, M. J. (2011) chlorine: an enhanced, radiometric, pH-sensitive green florescent protein. *Adv. Biosci. Biotechnol.* **2,** 132–137
40. Johnson, R. M., Allen, C., Melman, S. D., Waller, A., Young, S. M., Sklar, L. A., and Parra, K. J. (2010) Identification of inhibitors of vacuolar proton-translocating ATPase pumps in yeast by high-throughput screening flow cytometry. *Anal. Biochem.* **398,** 203–211
41. Vasilyeva, E., and Forgac, M. (1998) Interaction of the clathrin-coated vesicle V-ATPase with ADP and sodium azide. *J. Biol. Chem.* **273,** 23823–23829
42. Ohya, Y., Umemoto, N., Tanida, I., Ohta, A., Iida, H., and Anraku, Y. (1991) Calcium-sensitive *cls* mutants of *Saccharomyces cerevisiae* showing a Pet− phenotype are ascribable to defects of vacuolar membrane H(+)-ATPase activity. *J. Biol. Chem.* **266,** 13971–13977
43. Nelson, H., and Nelson, N. (1990) Disruption of genes encoding subunits of yeast vacuolar H(+)-ATPase causes conditional lethality. *Proc. Natl. Acad. Sci. U.S.A.* **87,** 3503–3507
44. Shao, E., Nishi, T., Kawasaki-Nishi, S., and Forgac, M. (2003) Mutational analysis of the non-homologous region of subunit A of the yeast V-ATPase. *J. Biol. Chem.* **278,** 12985–12991
45. Zhang, Z., Zheng, Y., Mazon, H., Milgrom, E., Kitagawa, N., Kish-Trier, E., Heck, A. J., Kane, P. M., and Wilkens, S. (2008) Structure of the yeast vacuolar ATPase. *J. Biol. Chem.* **283,** 35983–35995
46. Landolt-Marticorena, C., Williams, K. M., Correa, J., Chen, W., and Manolson, M. F. (2000) Evidence that the NH_2 terminus of vph1p, an integral subunit of the V_0 sector of the yeast V-ATPase, interacts directly with the Vma1p and Vma13p subunits of the V1 sector. *J. Biol. Chem.* **275,** 15449–15457
47. Inoue, T., and Forgac, M. (2005) Cysteine-mediated cross-linking indicates that subunit C of the V-ATPase is in close proximity to subunits E and G of the V_1 domain and subunit a of the V_0 domain. *J. Biol. Chem.* **280,** 27896–27903
48. Kawasaki-Nishi, S., Nishi, T., and Forgac, M. (2003) Interacting helical surfaces of the transmembrane segments of subunits a and c′ of the yeast V-ATPase defined by disulfide-mediated cross-linking. *J. Biol. Chem.* **278,** 41908–41913
49. Zorko, M., and Jerala, R. (2008) Alexidine and chlorhexidine bind to lipopolysaccharide and lipoteichoic acid and prevent cell activation by antibiotics. *J. Antimicrob. Chemother.* **62,** 730–737
50. Roberts, W. R., and Addy, M. (1981) Comparison of the bisbiguanide antiseptics alexidine and chlorhexidine. I. Effect on plaque accumulation and salivary bacteria. *J. Clin. Periodontol.* **8,** 213–219
51. Chawner, J. A., and Gilbert, P. (1989) Interaction of the bisbiguanides chlorhexidine and alexidine with phospholipid vesicles: evidence for separate modes of action. *J. Appl. Bacteriol.* **66,** 253–258
52. Poltermann, S., Nguyen, M., Günther, J., Wendland, J., Härtl, A., Künkel, W., Zipfel, P. F., and Eck, R. (2005) The putative vacuolar ATPase subunit Vma7p of *Candida albicans* is involved in vacuole acidification, hyphal development, and virulence. *Microbiology* **151,** 1645–1655
53. Hilty, J., Smulian, A. G., and Newman, S. L. (2008) The *Histoplasma capsulatum* vacuolar ATPase is required for iron homeostasis, intracellular replication in macrophages, and virulence in a murine model of histoplasmosis. *Mol. Microbiol.* **70,** 127–139
54. Erickson, T., Liu, L., Gueyikian, A., Zhu, X., Gibbons, J., and Williamson, P. R. (2001) Multiple virulence factors of *Cryptococcus neoformans* are dependent on VPH1. *Mol. Microbiol.* **42,** 1121–1131
55. Ganendren, R., Widmer, F., Singhal, V., Wilson, C., Sorrell, T., and Wright, L. (2004) *In vitro* antifungal activities of inhibitors of phospholipases from the fungal pathogen *Cryptococcus neoformans*. *Antimicrob. Agents Chemother.* **48,** 1561–1569
56. Soares, D. A., de Andrade, R. V., Silva, S. S., Bocca, A. L., Soares Felipe, S. M., and Petrofeza, S. (2010) Extracellular *Paracoccidioides brasiliensis* phospholipase B involvement in alveolar macrophage interaction. *BMC Microbiol.* **10,** 241
57. Zhang, Y. Q., Gamarra, S., Garcia-Effron, G., Park, S., Perlin, D. S., and Rao, R. (2010) Requirement for ergosterol in V-ATPase function underlies antifungal activity of azole drugs. *PLoS Pathog.* **6,** e1000939
58. Ostrosky-Zeichner, L., Casadevall, A., Galgiani, J. N., Odds, F. C., and Rex, J. H. (2010) An insight into the antifungal pipeline: selected new molecules and beyond. *Nat. Rev. Drug Discov.* **9,** 719–727
59. Lötscher, H. R., deJong, C., and Capaldi, R. A. (1984) Interconversion of high and low adenosinetriphosphatase activity forms of *Escherichia coli* F1 by the detergent lauryldimethylamine oxide. *Biochemistry* **23,** 4140–4143

Appendix B

Saccharomyces cerevisiae Vacuolar H^+-ATPase Regulation by Disassembly and Reassembly: One Structure and Multiple Signals

Published in *Eukaryotic Cell*

April, 2014

EC Journals.ASM.org

MINIREVIEW

Saccharomyces cerevisiae Vacuolar H^+-ATPase Regulation by Disassembly and Reassembly: One Structure and Multiple Signals

Karlett J. Parra, Chun-Yuan Chan, Jun Chen

Department of Biochemistry and Molecular Biology of the School of Medicine, University of New Mexico Health Sciences Center, Albuquerque, New Mexico, USA

Vacuolar H^+-ATPases (V-ATPases) are highly conserved ATP-driven proton pumps responsible for acidification of intracellular compartments. V-ATPase proton transport energizes secondary transport systems and is essential for lysosomal/vacuolar and endosomal functions. These dynamic molecular motors are composed of multiple subunits regulated in part by reversible disassembly, which reversibly inactivates them. Reversible disassembly is intertwined with glycolysis, the RAS/cyclic AMP (cAMP)/protein kinase A (PKA) pathway, and phosphoinositides, but the mechanisms involved are elusive. The atomic- and pseudo-atomic-resolution structures of the V-ATPases are shedding light on the molecular dynamics that regulate V-ATPase assembly. Although all eukaryotic V-ATPases may be built with an inherent capacity to reversibly disassemble, not all do so. V-ATPase subunit isoforms and their interactions with membrane lipids and a V-ATPase-exclusive chaperone influence V-ATPase assembly. This minireview reports on the mechanisms governing reversible disassembly in the yeast *Saccharomyces cerevisiae*, keeping in perspective our present understanding of the V-ATPase architecture and its alignment with the cellular processes and signals involved.

Vacuolar H^+-ATPases (V-ATPases) are ATP-driven proton pumps distributed throughout the endomembrane system of all eukaryotic cells (1, 2). V-ATPase proton transport acidifies organelles and energizes secondary transport systems. Zymogen activation, protein processing and trafficking, and receptor-mediated endocytosis are fundamental cellular processes that require V-ATPase activity. Cells specialized for active proton secretion express also V-ATPases at the plasma membrane. Proton transport by plasma membrane V-ATPases in osteoclasts, epididymal clear cells, and renal intercalated cells is necessary for bone resorption, sperm maturation, and maintenance of the systemic acid-base balance, respectively (3, 4). V-ATPase has been implicated in several pathological states, including osteopetrosis, distal renal tubular acidosis, male infertility, and cancers (2). Not surprisingly, studies of V-ATPase function and regulation are increasing, as is our knowledge of these dynamic proteins.

V-ATPase structure and function are highly conserved and well characterized in *Saccharomyces cerevisiae* (referred to here as yeast). Lack of V-ATPase function leads to a conditionally lethal phenotype that is characterized by pH sensitivity in yeast; complete lack of V-ATPase function is lethal in higher eukaryotes (5). Recent atomic- and pseudo-atomic-resolution structures of V-ATPase and its subunits have helped shed light on the molecular dynamics that regulate V-ATPase function (6, 7). V-ATPases are large multisubunit complexes structurally organized into two major domains, V_1 and V_o (Fig. 1). Eight peripheral subunits (A to H) form the V_1 domain, where ATP hydrolysis takes place. Six subunits (a, c, c′, c″, d, and e) comprise V_o, the membrane intrinsic domain that forms the path for proton transport. An important mechanism by which cells control organelle acidification is by disassembling and reassembling the V-ATPase complex (1, 2, 8, 9). Disassembly rapidly inactivates the pumps, resulting in three constituents: V_1 subunit C, V_1 (without subunit C), and V_o (Fig. 2). Disassembly is reversible, and reassociation of the three components rapidly restores ATP hydrolysis and proton transport across membranes. Catalytic inactivation and reactivation entail conformational changes in V_1 subunit H (Fig. 2) (12, 13). This subunit is necessary to silence cytosolic V_1 and activate V_1V_o complexes (11, 15).

Yeast V-ATPase inactivation by disassembly is a response to glucose deficit (10). V_1V_o disassembly prevents energy depletion (e.g., loss of ATP). Reassembly is a response to glucose readdition following a brief period of glucose deprivation; it rapidly restores vacuolar acidification. Because V_o is not an open proton pore and cytosolic V_1 cannot hydrolyze MgATP (7, 11–14), protons do not leak across membranes and cellular ATP is not depleted. Thus, disassembly can be sustained for a long time. Long-term disassembly is also rapidly reversed by addition of glucose (8), indicating that the structural and functional integrity of the V_1 and V_o domains is preserved in the midst of scarcity.

All eukaryotic V-ATPases may be built with the potential to reversibly disassemble. However, not all V-ATPases appear to disassemble and reassemble. V-ATPase subunit isoforms and V-ATPase interactions with an assembly factor (RAVE; discussed below) in the cytosol and phosphoinositides at the membrane can dictate which pumps reversibly disassemble in response to environmental cues (16, 17). Recent studies have begun to elucidate the mechanisms that allow cells to communicate extracellular signals to intracellular V-ATPases located at the vacuolar membrane. In yeast, V-ATPase assembly is regulated by glucose, pH, and osmotic stress, and it is intertwined with glycolysis, RAS/cyclic AMP (cAMP)/protein kinase A (PKA), and phosphatidylinositol-(3,5)-bisphosphate [PI(3,5)P_2] (16, 18–21). In insects, starvation and hormone stimulation influence V_1V_o assembly by mechanisms involving cAMP/PKA signaling (9, 22, 23). In higher eukaryotes, glucose (renal epithelial cells) and mechanical stimulation (dendritic cells)

Published ahead of print 4 April 2014

Address correspondence to Karlett J. Parra, kjparra@salud.unm.edu.

doi:10.1128/EC.00050-14

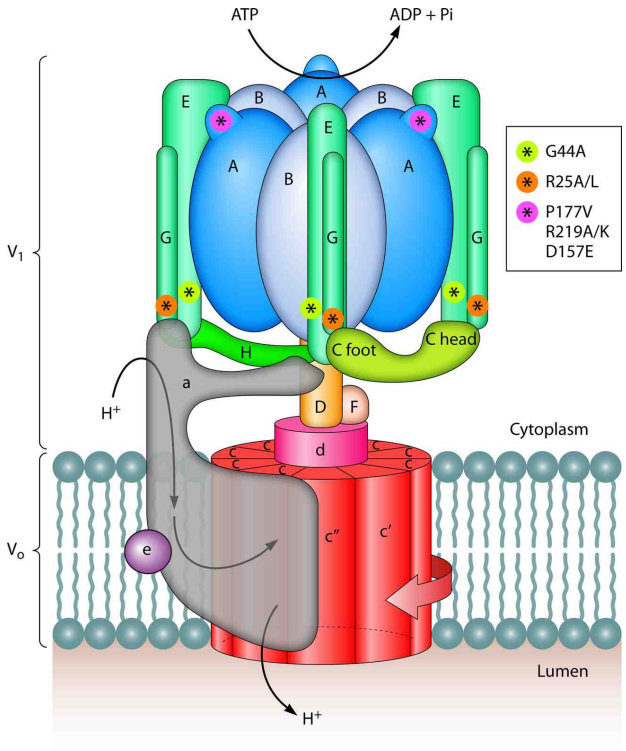

FIG 1 The V-ATPase complex: subunit composition and organization. V-ATPase is composed of 14 different subunits, organized into two major domains: V_1 is the catalytic ATPase domain and V_o is the proton translocation domain. Active transport of protons across the membrane entails rotation of a rotor (subunits F, D, d, c, c′, and c″) that is driven by ATP hydrolysis in V_1 (subunits A). Three elongated peripheral stalks (subunits EG) connect the V_1 and V_o domains and allow relative rotation of subunits during catalysis, by working as stators. Three stators are necessary for regulation of V-ATPase by disassembly and reassembly. Shown are mutations in the peripheral stalk subunits E (G44A) and G (R25A/L) and the catalytic subunit A at its nonhomologous domain (P177V and R219A/K). These mutations simultaneously alter V_1V_o disassembly and catalysis, suggesting that disassembly requires wild-type catalytic activity (rotation). The mutation D157E in subunit A, which also prevents V_1V_o disassembly, does not affect catalysis; it is proposed that D157E acts by stabilizing subunit-subunit interactions.

have been shown to modulate V-ATPase assembly by a process that requires PIP 3-kinase and mTOR activation (24–27).

This review reports on the mechanisms of reversible disassembly in yeast, particularly in regard to our present understanding of the V-ATPase architecture. Next, we summarize recent structural discoveries on the yeast V-ATPase, their interrelation with V-ATPase regulation by reversible disassembly, and our current understanding of the mechanisms and signals involved.

ARCHITECTURE OF EUKARYOTIC V-ATPase

ATPase rotary motors include F-ATP synthase, archaeal A-type ATP synthase, bacterial A/V-like ATPase, and eukaryotic V-ATPase (28). V-ATPase and other members in this family share common structural features essential for the mechanical rotation of protein subunits during ATP catalysis. They all have (i) a protuberant globular domain peripherally attached to the membrane that houses three catalytic sites, (ii) a membrane domain that forms the path for ion transport, (iii) a centrally located rotor that couples ATP hydrolysis and ion transport across membranes, and (iv) one or more peripheral stalks that connect the peripheral and membrane domains.

Rotation of rotor-forming subunits relative to the steady catalytic sites is driven by hydrolysis of ATP inside the globular structure of V_1 (A_3B_3) (Fig. 1). ATP hydrolysis promotes rotation of the rotor's shaft (subunits D, F, and d) at the center of the A_3B_3 hexamer. The shaft is connected to a hydrophobic proteolipid ring inside the membrane (c-ring), which consists of subunits c, c′, and c″ and transfers the protons. Active transport requires entrance of cytosolic protons to the V_o subunit a in order to reach the c-ring. The protons bind to an acidic residue in the c-ring, and after a 360° rotation, protons exit the other side of the membrane, traveling through V_o subunit a. This general mechanism of rotational catalysis is shared with all rotary ATPases (28).

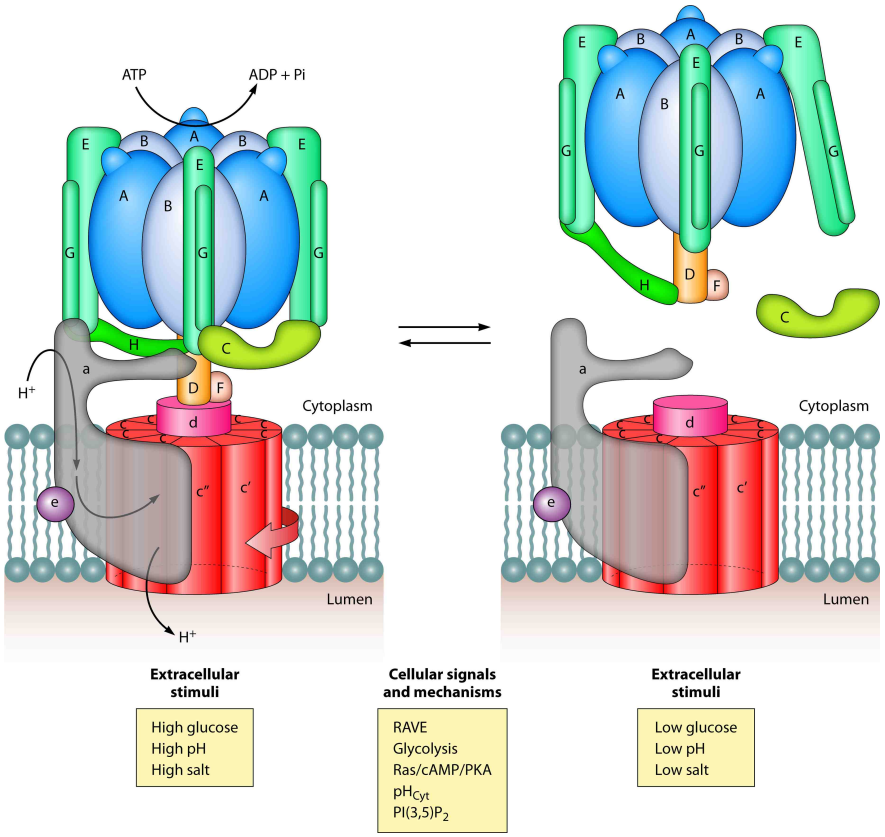

FIG 2 Reversible disassembly of V-ATPase: extracellular stimuli and intracellular signals. V-ATPase disassembly breaks the complex apart, as V_1, V_o, and the V_1 subunit C separate. Disassembly is reversible, and reassembly of the three components restores ATP hydrolysis and proton transport. Yeast cells adjust the number of assembled V-ATPases in response to environmental stressors, including changes in glucose, pH, and salts. These extracellular cues are communicated to V-ATPases by several signals and unknown mechanisms that require an assembly factor (RAVE) and are intertwined with glycolysis and glycolytic enzymes, RAS/cAMP/PKA components, cytosolic pH (pH_{Cyt}) homeostasis, and $PI(3,5)P_2$.

Eukaryotic V-ATPases distinguish themselves from other rotary ATPases in three ways. First, V-ATPases are dedicated proton pumps. Second, V-ATPases are regulated by reversible disassembly. Third, V-ATPases contain three peripheral stalks. In contrast, the A and bacterial A/V-ATPases have two peripheral stalks and F-ATPases have one (28). The V-ATPase peripheral stalks are made of a heterodimer of E and G subunits; reversible disassembly requires the third peripheral stalk (EG_3) (Fig. 3) (6, 29). It also requires a soluble subunit that is absent in other rotary ATPases (subunit C). The yeast subunit C contains two globular domains, the head (C_{head}) and foot (C_{foot}) (30). The C_{head} domain interacts with EG_3 with high affinity (6, 31). Through its C_{foot} domain, subunit C interacts with the second peripheral stalk (EG_2) and the N terminus of the V_o subunit a (a-NT). These subunit interactions are broken and reformed when V-ATPases disassemble and reassemble.

Subunit C is released to the cytosol during disassembly (8). Reassembly requires the subunit C to be rapidly reincorporated into the complex and its interactions with EG_3, EG_2, and a-NT to be restored. Reintroduction of subunit C into V_1V_o requires significant bending of the third peripheral stalk (6, 29). This compression imposes physical stress in its coiled-coil structure, like "spring-loading." The EG_3 tension, which persists within assembled V_1V_o complexes, is released when V_1V_o disassembles. Thus, it is proposed that spring-loading requires energy for reassembly and primes V-ATPases to easily disassemble after glucose depletion, when ATP must be preserved.

These new structural discoveries hopefully will lead to a better

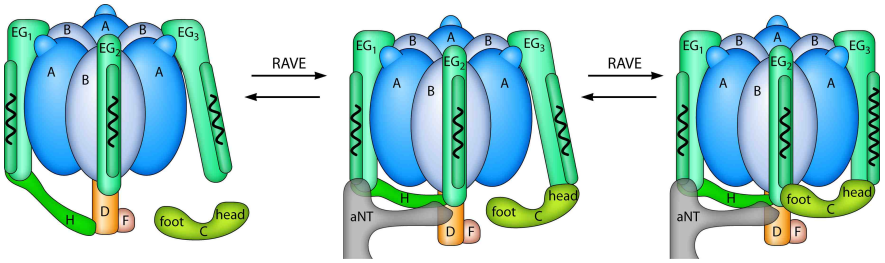

FIG 3 Spring-loading: a model for disassembly and reassembly. The V_1 domain and subunit C detach from V_o at the membrane and are released into the cytosol during disassembly. Reassembly requires reassociation of subunit C with the peripheral stalks EG_3 and EG_2 and the N terminus domain of the V_o subunit a (a-NT). Restoration of the native complex probably requires bending of EG_3, like spring-loading, which is accomplished with the assistance of the chaperone complex RAVE. The tension contained in EG_3 within the assembled V_1V_o complex, is then released when V_1V_o disassembles.

understanding of how glucose and other cellular signals regulate V-ATPase function and assembly. The spring-loading mechanism of reversible disassembly is compatible with our current understanding of the structural architecture of the eukaryotic V-ATPase complex. It is also consistent with our knowledge of the major cellular processes associated with V_1V_o disassembly and reassembly. Below, we discuss our view of the alignment of the V-ATPase architecture with these cellular processes and signals.

CONNECTING GLUCOSE METABOLISM TO V-ATPase ASSEMBLY

The concept of spring-loading requires energy to bend EG_3 and reestablish proper binding of subunit C in V_1V_o (6). Glucose, the primary energy source for most organisms, is an important driver of reassembly, suggesting that glucose oxidation could provide the necessary chemical energy (e.g., ATP). In addition to glucose, reassembly of V_1V_o can be triggered by fructose and mannose, other rapidly fermentable sugars, suggesting that glycolysis itself may be necessary for V_1V_o reassembly and spring-loading of EG_3 (19). Further evidence that glucose metabolism is involved includes the facts that (i) conversion of glucose-6-phosphate to fructose-6 phosphate is necessary for reassembly and (ii) the intracellular pool of assembled V_1V_o complexes is proportional to the concentration of glucose in the growth medium, demonstrating that V_1V_o reassembly is not an all-or-none response (19).

The glycolytic enzymes aldolase (21), phosphofructokinase-1 (32), and glyceraldehyde-3-phosphate dehydrogenase (33) interact with V-ATPase. These enzymes coimmunoprecipitate with V-ATPases and can be detected in yeast vacuolar membrane fractions. Aldolase binding to V-ATPase is glucose dependent and necessary for stable V_1V_o complex formation (21, 34). Lu et al. (21) were able to differentiate the function of aldolase in glycolysis from its function for V-ATPase assembly. The authors showed reduced V_1V_o complex formation in an aldolase mutant that retained catalytic activity *in vitro*. These studies suggest that aldolase may play a direct role in V_1V_o reassembly. Whether the same holds true for other glycolytic enzymes is not known. Glycolytic mutants cannot efficiently utilize glucose, which suppresses glycolysis and glucose-dependent signals, altering V_1V_o assembly. This makes it challenging to study the interplay of V-ATPase with other glycolytic enzymes. Nonetheless, these studies merit additional examination because phosphofructokinase-1 can directly bind yeast and human V-ATPase subunits (24), suggesting that several aspects of this mechanism are conserved.

The interrelation between V-ATPase and glycolysis cannot be overlooked; it is conserved in yeast (1, 19, 35, 36), plants (37), and mammals (38, 39). Moreover, V-ATPase mutations that impair binding to phosphofructokinase-1 are associated with distal renal tubular acidosis (24), and V-ATPase regulation by glycolysis plays a role in viral infections (40) and the metabolic switch in cancers (41, 42). It has been proposed that glycolytic enzymes form a supercomplex with V-ATPase that funnels ATP directly to V-ATPase and propels proton transport (21, 24, 32, 34, 37, 43). A similar molecular machinery has been described at synaptic vesicle membranes where ATP synthesized by phosphoglycerate kinase supports glutamate uptake (44); this process is energized by V-ATPase proton pumps. A model of this kind will require glycolytic ATP production at the yeast vacuolar membrane, but functional interactions of phosphoglycerate kinase or pyruvate kinase (glycolytic enzymes that produce ATP) with V-ATPase have yet to be demonstrated. However, it is clear that ATP levels modulate V-ATPase coupling efficiency *in vitro* (45). ATP-dependent modifications of V-ATPase proton transport *in vivo* will probably need to work tightly coupled with glycolysis, the main source of ATP; glycolytic enzymes at the membrane could produce the ATP that fine-tunes the number of protons transported per ATP hydrolyzed. Collectively, these data suggest that V-ATPase reassembly and/or V-ATPase activity can be controlled by interactions with glycolytic enzymes and the ATP that they produce.

ONE "RAVE" PATH TOWARD V_1V_o REASSEMBLY

The regulator of ATPase of vacuoles and endosomes (RAVE) complex is a V-ATPase-exclusive assembly factor. It is required for V_1V_o assembly at steady state (biosynthetic assembly) and reassembly in response to glucose readdition to glucose-deprived cells (46–48). The RAVE complex chaperones loading of subunit C into V_1V_o, a job that requires aligning C_{head} with the EG_3 and EG_2 peripheral stalks in addition to introducing structural stress in EG_3 (Fig. 3) (6). In the absence of RAVE, V-ATPases at the vacuolar membrane are unstable and inactive, with V_1 and subunit C loosely associated (48). Importantly, although several assembly factors are required for V-ATPase assembly (49–54), only RAVE appears to be involved in V-ATPase reversible disassembly.

The RAVE complex has three components, the adaptor protein

Skp1p and its two subunits, Rav1p and Rav2p (46). Skp1p associates with other cellular complexes. Rav1p and Rav2p are solely found in the RAVE complex. Of the two subunits, Rav1p constitutes the central component; it binds Rav2p and Skp1p (47). Rav1p also forms the interface between RAVE and V-ATPase subunits. In the cytosol, Rav1p binds V-ATPase subunit C and the V_1 peripheral stalk-forming subunits EG (48). At the membrane, Rav1p interacts with the N-terminal domain of V_o subunit a (17). Genetic and biochemical data have shown that binding of Rav1p to subunit C can occur independently of its binding to V_1. Preloading RAVE with subunit C and V_1 simultaneously in the cytosol may expedite reassembly, which is known to be a fast response completed within 3 to 5 min of glucose readdition (19, 55). Importantly, formation of RAVE-C and RAVE-V_1 subcomplexes in the cytosol is not glucose dependent, indicating that RAVE binding is not the signal for V_1V_o reassembly.

Deletion of the genes *RAV1* and *RAV2* leads to growth defects characteristic of V-ATPase mutants (46, 47); the vacuolar membrane ATPase (*vma*) growth phenotype displays growth sensitivity at pH 7.5 and in the presence of calcium (1). The *rav1*Δ and *rav2*Δ mutant cells also exhibit temperature sensitivity, but the *vma* traits are detected at 37°C. This phenotype is more substantial in *rav1*Δ than *rav2*Δ cells (46, 47), likely because Rav1p constitutes the functional subunit of the RAVE complex. The *rav1*Δ mutant has major V-ATPase assembly and functional defects *in vivo*, although its *vma* growth phenotype is fairly mild and considered "partial."

The *rav1*Δ mutant resembles the yeast mutant strain *vph1*Δ, which lacks the isoform Vph1p of the V_o subunit a (56). The V_o subunit a is the only yeast V-ATPase subunit encoded by two functional homologs, *VPH1* and *STV1* (56, 57); *VPH1* encodes the vacuolar isoform and *STV1* has sorting information for the Golgi/endosomal compartments (58). Genome-level synthetic genetic analyses (17) showed that a synthetic *vma* growth phenotype can be generated after combining the *rav1*Δ mutation with class E mutants of endosomal and vacuolar transport (59), suggesting that the physiological basis for the *rav1*Δ partial *vma* phenotype is that RAVE is a Vph1p-specific chaperone. The discovery that RAVE assists in the assembly of Vph1p-containing V-ATPases but that Stv1p-containing complexes do not need RAVE to properly assemble is in agreement with prior studies showing that Vph1p-containing V-ATPases are more responsive to glucose than are Stv1p-containing pumps (60). Since Vph1p targets V-ATPase to the vacuole and Stv1p to the Golgi and endosomal compartments, these results also suggest that only vacuole-associated pumps reversibly disassemble.

The functions of the RAVE complex are likely conserved in other eukaryotes. The Rav1p sequence homologs, rabconnectins, are necessary for acidification of endosomes and synaptic vesicles (61–63). The human V_o subunit a exists in four different isoforms; mutations in particular isoforms cause osteopetrosis and renal tubular acidosis (64). Identifying the V_o subunit a isoform(s) recognized by rabconnectins could help in understanding these and other pathologies associated with V-ATPases. The RAVE subunit Rav2p is found only in fungi and does not have human homologs. Therefore, Rav2p offers unique opportunities to selectively disrupt RAVE complex functions in fungal human pathogens for which V-ATPase pumps are desirable targets (65–72).

IS ATP HYDROLYSIS NECESSARY FOR V-ATPase DISASSEMBLY AND REASSEMBLY?

How energy can be used to reassemble V_1V_o is virtually unknown. ATP facilitates *in vitro* reconstitution of V_1 and V_o (73–75), suggesting that ATP could promote reassembly *in vivo*. Genetic screens aimed at identifying V-ATPase mutants defective in V_1V_o reassembly are challenging because V_1V_o disassembly is not absolute. There is a cellular fraction of V-ATPase complexes that does not disassemble in response to glucose depletion; it probably yields basal V-ATPase activity necessary to support critical cellular functions (1, 10). These pumps constitute about 30% of the total V_1V_o and likely include V-ATPases at nonvacuolar membranes (Stv1p-containing V-ATPase pumps) (19, 60). Coincidentally, 25 to 30% of V-ATPase activity is sufficient to support wild-type growth, which makes the growth phenotype of these types of mutants very subtle. A few mutants, primarily disassembly mutants, have been identified by site-directed mutagenesis experiments. Intriguingly, many of those mutations also alter V-ATPase catalysis. Those studies suggest that peripheral stalks may regulate rotational catalysis by influencing ATP binding, chemical reaction, or release of ADP/P_i (76–78).

As expected, site-directed mutations at conserved amino acids of the peripheral stalk subunits E and G can suppress glucose-dependent disassembly (Fig. 1) (76, 79). The mutations *vma4*-D44A and *vma10*-R25A/L in subunits E and G, respectively, suppress disassembly; they also stimulate the enzyme activity (76, 79). The *vma4*-T202A mutation near the C terminus enhances V_{max} by about 2-fold without significantly affecting the K_m of the enzyme (77), resembling the mutant *vma4*-D44A (76). Although the ability of *vma4*-T202A to reversibly disassemble has not been determined, these studies indicate that the peripheral stalks can communicate with the catalytic sites inside the A_3B_3 hexamer and they can affect disassembly and catalysis.

Paradoxically, the rate of ATP hydrolysis by V-ATPase can alter V_1V_o disassembly (Fig. 1). Pharmacologic inhibition of V-ATPase pumps with the V-ATPase inhibitor concanamycin A reduces V_1V_o disassembly, without affecting reassembly (19). Inactive V-ATPases carrying mutations at a V_o proton-binding subunit (*vma11*-E145L) of the c-ring (19) or the V_1 catalytic subunit A (*vma1*-R219K) (78) are defective for disassembly. Likewise, *vma1*-P177V and *vma1*-R219A, which are partially inactive (by 30% to 50%), also are defective in disassembly. Thus, it appears that wild-type levels of activity are necessary to disassemble V_1V_o; hyperactive, hypoactive, and inactive pumps cannot sufficiently disassemble (19, 45, 76). Obviously, not all disassembly mutants are catalytically impaired. The mutations *vma1*-G150 and *vma1*-D157E inhibit disassembly without affecting V-ATPase activity (78), perhaps by stabilizing subunit interactions.

From these studies, it becomes clear how little we still know about the intramolecular mechanisms that drive disassembly and reassembly. Although additional studies will be necessary to determine how intrinsic subunit interactions and differential conformations impact disassembly and reassembly, it appears that V-ATPases adopt conformations prone for disassembly during a catalytic cycle of rotation driven by ATP hydrolysis (19). Still, we cannot exclude the possibility that catalysis may also drive reassembly. In this context, ATP-driven subunit rotation in V_1 may stimulate its own reassembly in the presence of RAVE. This process will require the inhibitory subunit of V_1 (subunit H) to be

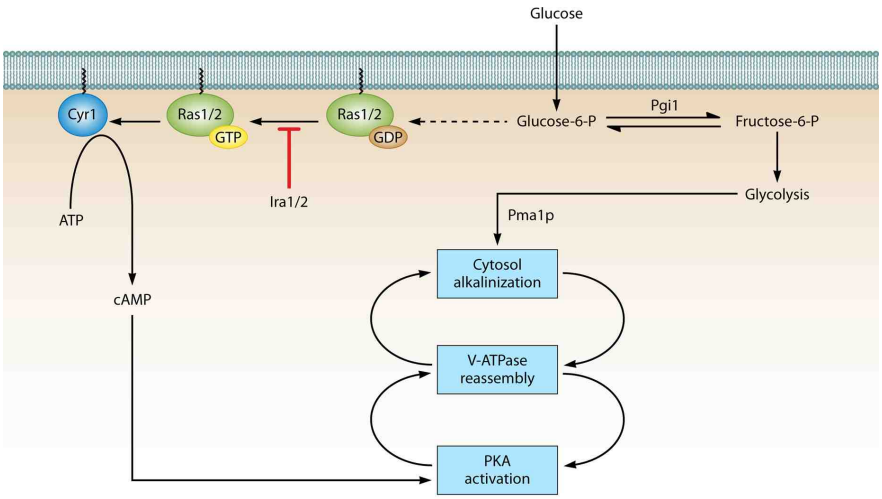

FIG 4 Hypothetical positive feedback for the regulation of V-ATPase assembly by cytosolic pH and Ras/cAMP/PKA signaling. In this model, two positive feedback loops control glucose-dependent yeast V-ATPase assembly by promoting cytosol pH alkalinization and protein kinase A (PKA) activation. Glucose readdition after glucose depletion activates PKA and alkalinizes the cytosol, which promotes V-ATPase reassembly. More assembled V-ATPase helps maintain alkalinized cytosol pH. The reassembled V-ATPase may activate PKA signaling, which enhances V-ATPase assembly, upregulates glycolysis, and mediates the rapid transition from respiratory to fermentative growth. Arrows and bars represent positive and negative interactions, respectively. Dashed lines represent putative or indirect interactions.

released from its rotor-locking inhibitory position during reassembly (Fig. 3) (7, 11, 12, 80).

YEAST V-ATPase: AT THE CROSSROADS OF MULTIPLE INTRACELLULAR SIGNALS

In support of the spring-loading hypothesis, there are no known chaperones that aid in V-ATPase disassembly; V-ATPase may be primed to disassemble (29). In addition to glucose depletion, exposure to less preferred carbon sources (galactose, glycerol/ethanol, and raffinose) causes disassembly (8, 19). These data further argue that little or no glucose is the driving signal of disassembly. There is evidence indicating that the Ras/cAMP/PKA pathway probably mediates reversible disassembly (18, 20). Ras/cAMP/PKA signaling controls metabolism in response to sudden availability of rapidly fermentable sugars (81), compatible with a role for Ras/cAMP/PKA during V_1V_o reassembly (Fig. 2). Constitutively active Ras and PKA suppress disassembly by glucose depletion (18). These studies suggest that the Ras/cAMP/PKA pathway acts upstream of V-ATPase. In an independent study linking V-ATPase reassembly to cAMP and PKA, reassembly appeared to be an upstream activator of PKA (20). That study suggested that alkalization of the cytosol after glucose readdition is the signal for reassembly. Although these results seem contradictory, the possibility that a positive feedback mechanism may regulate V-ATPase assembly cannot be excluded (Fig. 4). The reassembled V-ATPase may activate PKA signaling, which in turn enhances the V-ATPase assembly.

Cytosolic pH is emerging as a key regulator for various cellular functions (82), and V-ATPase affects cytosolic pH homeostasis (83). In addition to activating V-ATPase catalysis and proton transport, readdition of glucose activates the plasma membrane ATPase, Pma1p, which is the main efflux pump responsible for yeast cytosolic pH regulation (83, 84). V-ATPases are necessary for cytosolic pH homeostasis because (i) active V-ATPases are necessary for normal Pma1p levels to be present at the plasma membrane, and (ii) cytosolic pH homeostasis is maintained by the coordinated action of V-ATPase and Pma1p (83). In the evaluation of the signals for reassembly, the contribution of cytosolic pH merits additional investigation. Addressing whether glucose-dependent Pma1p activation precedes glucose-dependent V-ATPase activation may help clarify the role of cytosolic pH for reassembly.

Fungi grow more rapidly at acidic than neutral pH (85). It should come as no surprise that V_1V_o disassembly in response to glucose depletion is affected by environmental stress signals, such as elevated pH (86). At pH 7.0, V-ATPase disassembly is significantly suppressed compared to disassembly at pH 5.0, the optimal pH for yeast growth. Although the mechanisms involved in the prevention of disassembly by pH remain elusive, adaptation to high pH appears to have both $PI(3,5)P_2$-dependent and -independent components (16). Knowing whether glucose and pH use common mechanisms to regulate V_1V_o disassembly requires additional studies. Notably, it may help in the understanding of fungal pathogenicity; *Candida albicans* adaptation to neutral-to-alkaline pH environments in the host stimulates cellular signals that trigger its morphological change from the yeast form (nonpathogenic) to the hyphal form (pathogenic) (65, 68, 72, 87).

V-ATPase function is necessary for adaptation to stress condi-

tions. Vacuoles are yeast storage compartments and an important mechanism of protection against toxic metals and drugs (88). By modulating V-ATPase disassembly, yeast protects the vacuolar luminal pH and maintains secondary transport systems across the membrane. Exposure of yeast to osmotic shock increases the total pool of vacuolar V_1V_o assembled (89). This involves a mechanism that requires the signaling lipid PI(3,5)P_2 interacting with the V_o subunit a isoform Vph1p (16). Interestingly, PI(3,5)P_2 has little or no effect on glucose-dependent reversible disassembly of the V-ATPase, indicating that the cellular signals behind hyperosmotic stress- and glucose-induced V-ATPase reassembly are independent. High salts and high pH can increase V_1V_o assembly levels at steady state in the presence of glucose, when cellular energy is abundant and most V-ATPase complexes are assembled. How this may work is not clear. It suggests that vacuolar membranes may contain subpopulations of V-ATPases specialized to respond to different signals, adding a layer of complexity to this intricate regulatory event.

CONCLUDING REMARKS

Structural data are beginning to support a collection of studies investigating how glucose signals are communicated to V-ATPases. The new concept is that V_1V_o may be structurally built with an inherent facility to disassemble but that its reassembly imposes energetic constrains. This concept has reinforced our view of disassembly and reassembly as two independently controlled events. A variety of extracellular cues that control V-ATPase assembly and/or disassembly are emerging, although glucose is the main and strongest external stimulus. We do not know what is the glucose sensor or the mechanism involved in this communication. Our understanding of V-ATPase regulation by reversible disassembly is incomplete. The spring-loading hypothesis has not been experimentally tested. If all V-ATPases are structurally suited to reversibly disassemble, why do not all of them do so? Vph1p-containing V-ATPases disassemble and reassemble, but not Stv1p-containing V-ATPases. There are many questions that remain unanswered regarding the roles of glycolysis, RAS/cAMP/PKA, and V_1 catalysis. Some of these questions include the following: (i) do glycolytic enzymes and/or glycolysis control V-ATPase at steady state and during glucose depletion/readdition; (ii) are glycolysis and RAS/cAMP/PKA elements of a common pathway or different pathways that work in parallel to control V-ATPase assembly and function; (iii) is V-ATPase upstream of PKA or downstream; (iv) what is the yeast V-ATPase subunit that is phosphorylated, if any; and (v) what phosphatase enzyme is involved.

ACKNOWLEDGMENTS

We gratefully acknowledge support, in whole or in part, from the NIH grant R01GM086495 (to K.J.P.), AHA grant 14PRE19020015 (to C.-Y.C.), and the UNM Health Sciences Center RAC Award (to J.C.).

We thank Colleen Fordyce and David Vander Jagt for the helpful discussions and revisions. We also thank Jessica "DJ" Binder for assistance with the illustrations.

REFERENCES

1. **Kane PM.** 2006. The where, when, and how of organelle acidification by the yeast vacuolar H^+-ATPase. Microbiol. Mol. Biol. Rev. **70:**177–191. http://dx.doi.org/10.1128/MMBR.70.1.177-191.2006.
2. **Forgac M.** 2007. Vacuolar ATPases: rotary proton pumps in physiology and pathophysiology. Nat. Rev. Mol. Cell Biol. **8:**917–929. http://dx.doi.org/10.1038/nrm2272.
3. **Breton S, Brown D.** 2013. Regulation of luminal acidification by the V-ATPase. Physiology (Bethesda) **28:**318–329. http://dx.doi.org/10.1152/physiol.00007.2013.
4. **Sobacchi C, Frattini A, Orchard P, Porras O, Tezcan I, Andolina M, Babul-Hirji R, Baric I, Canham N, Chitayat D, Dupuis-Girod S, Ellis I, Etzioni A, Fasth A, Fisher A, Gerritsen B, Gulino V, Horwitz E, Klamroth V, Lanino E, Mirolo M, Musio A, Matthijs G, Nonomaya S, Notarangelo LD, Ochs HD, Superti Furga A, Valiaho J, van Hove JL, Vihinen M, Vujic D, Vezzoni P, Villa A.** 2001. The mutational spectrum of human malignant autosomal recessive osteopetrosis. Hum. Mol. Genet. **10:**1767–1773. http://dx.doi.org/10.1093/hmg/10.17.1767.
5. **Kane PM.** 2007. The long physiological reach of the yeast vacuolar H^+-ATPase. J. Bioenerg. Biomembr. **39:**415–421. http://dx.doi.org/10.1007/s10863-007-9112-z.
6. **Oot RA, Huang LS, Berry EA, Wilkens S.** 2012. Crystal structure of the yeast vacuolar ATPase heterotrimeric EGC(head) peripheral stalk complex. Structure **20:**1881–1892. http://dx.doi.org/10.1016/j.str.2012.08.020.
7. **Benlekbir S, Bueler SA, Rubinstein JL.** 2012. Structure of the vacuolar-type ATPase from Saccharomyces cerevisiae at 11-A resolution. Nat. Struct. Mol. Biol. **19:**1356–1362. http://dx.doi.org/10.1038/nsmb.2422.
8. **Kane PM.** 1995. Disassembly and reassembly of the yeast vacuolar H(+)-ATPase in vivo. J. Biol. Chem. **270:**17025–17032.
9. **Sumner JP, Dow JA, Earley FG, Klein U, Jager D, Wieczorek H.** 1995. Regulation of plasma membrane V-ATPase activity by dissociation of peripheral subunits. J. Biol. Chem. **270:**5649–5653. http://dx.doi.org/10.1074/jbc.270.10.5649.
10. **Kane PM, Parra KJ.** 2000. Assembly and regulation of the yeast vacuolar H(+)-ATPase. J. Exp. Biol. **203:**81–87.
11. **Parra KJ, Keenan KL, Kane PM.** 2000. The H subunit (Vma13p) of the yeast V-ATPase inhibits the ATPase activity of cytosolic V1 complexes. J. Biol. Chem. **275:**21761–21767. http://dx.doi.org/10.1074/jbc.M002305200.
12. **Jefferies KC, Forgac M.** 2008. Subunit H of the vacuolar (H+) ATPase inhibits ATP hydrolysis by the free V1 domain by interaction with the rotary subunit F. J. Biol. Chem. **283:**4512–4519. http://dx.doi.org/10.1074/jbc.M707144200.
13. **Diab H, Ohira M, Liu M, Cobb E, Kane PM.** 2009. Subunit interactions and requirements for inhibition of the yeast V1-ATPase. J. Biol. Chem. **284:**13316–13325. http://dx.doi.org/10.1074/jbc.M900475200.
14. **Wilkens S, Forgac M.** 2001. Three-dimensional structure of the vacuolar ATPase proton channel by electron microscopy. J. Biol. Chem. **276:**44064–44068. http://dx.doi.org/10.1074/jbc.M106579200.
15. **Ho MN, Hirata R, Umemoto N, Ohya Y, Takatsuki A, Stevens TH, Anraku Y.** 1993. VMA13 encodes a 54-kDa vacuolar H(+)-ATPase subunit required for activity but not assembly of the enzyme complex in Saccharomyces cerevisiae. J. Biol. Chem. **268:**18286–18292.
16. **Li SC, Diakov TT, Xu T, Tarsio M, Zhu W, Couoh-Cardel S, Weisman LS, Kane PM.** 2014. The signaling lipid PI(3,5)P2 stabilizes V1-Vo sector interactions and activates the V-ATPase. Mol. Biol. Cell **25:**1251–1262. http://dx.doi.org/10.1091/mbc.E13-10-0563.
17. **Smardon AM, Diab HI, Tarsio M, Diakov TT, Nasab ND, West RW, Kane PM.** 2014. The RAVE complex is an isoform-specific V-ATPase assembly factor in yeast. Mol. Biol. Cell **25:**356–367. http://dx.doi.org/10.1091/mbc.E13-05-0231.
18. **Bond S, Forgac M.** 2008. The Ras/cAMP/protein kinase A pathway regulates glucose-dependent assembly of the vacuolar (H+)-ATPase in yeast. J. Biol. Chem. **283:**36513–36521. http://dx.doi.org/10.1074/jbc.M805232200.
19. **Parra KJ, Kane PM.** 1998. Reversible association between the V1 and V0 domains of yeast vacuolar H^+-ATPase is an unconventional glucose-induced effect. Mol. Cell. Biol. **18:**7064–7074.
20. **Dechant R, Binda M, Lee SS, Pelet S, Winderickx J, Peter M.** 2010. Cytosolic pH is a second messenger for glucose and regulates the PKA pathway through V-ATPase. EMBO J. **29:**2515–2526. http://dx.doi.org/10.1038/emboj.2010.138.
21. **Lu M, Ammar D, Ives H, Albrecht F, Gluck SL.** 2007. Physical interaction between aldolase and vacuolar H^+-ATPase is essential for the assembly and activity of the proton pump. J. Biol. Chem. **282:**24495–24503. http://dx.doi.org/10.1074/jbc.M702598200.
22. **Tiburcy F, Beyenbach KW, Wieczorek H.** 2013. Protein kinase A-dependent and -independent activation of the V-ATPase in Malpighian tubules of Aedes aegypti. J. Exp. Biol. **216:**881–891. http://dx.doi.org/10.1242/jeb.078360.
23. **Voss M, Vitavska O, Walz B, Wieczorek H, Baumann O.** 2007. Stimulus-induced phosphorylation of vacuolar H(+)-ATPase by protein kinase

A. J. Biol. Chem. **282:**33735–33742. http://dx.doi.org/10.1074/jbc.M703368200.
24. **Su Y, Blake-Palmer KG, Sorrell S, Javid B, Bowers K, Zhou A, Chang SH, Qamar S, Karet FE.** 2008. Human H+ATPase a4 subunit mutations causing renal tubular acidosis reveal a role for interaction with phosphofructokinase-1. Am. J. Physiol. Renal Physiol. **295:**F950–F958. http://dx.doi.org/10.1152/ajprenal.90258.2008.
25. **Sautin YY, Lu M, Gaugler A, Zhang L, Gluck SL.** 2005. Phosphatidylinositol 3-kinase-mediated effects of glucose on vacuolar H^+-ATPase assembly, translocation, and acidification of intracellular compartments in renal epithelial cells. Mol. Cell. Biol. **25:**575–589. http://dx.doi.org/10.1128/MCB.25.2.575-589.2005.
26. **Trombetta ES, Ebersold M, Garrett W, Pypaert M, Mellman I.** 2003. Activation of lysosomal function during dendritic cell maturation. Science **299:**1400–1403. http://dx.doi.org/10.1126/science.1080106.
27. **Liberman R, Bond S, Shainheit MG, Stadecker MJ, Forgac M.** 2014. Regulated assembly of vacuolar ATPase is increased during cluster disruption-induced maturation of dendritic cells through a phosphatidylinositol 3-kinase/mTOR-dependent pathway. J. Biol. Chem. **289:**1355–1363. http://dx.doi.org/10.1074/jbc.M113.524561.
28. **Muench SP, Trinick J, Harrison MA.** 2011. Structural divergence of the rotary ATPases. Q. Rev. Biophys. **44:**311–356. http://dx.doi.org/10.1017/S0033583510000338.
29. **Stewart AG, Stock D.** 2012. Priming a molecular motor for disassembly. Structure **20:**1799–1800. http://dx.doi.org/10.1016/j.str.2012.10.003.
30. **Drory O, Frolow F, Nelson N.** 2004. Crystal structure of yeast V-ATPase subunit C reveals its stator function. EMBO Rep. **5:**1148–1152. http://dx.doi.org/10.1038/sj.embor.7400294.
31. **Oot RA, Wilkens S.** 2010. Domain characterization and interaction of the yeast vacuolar ATPase subunit C with the peripheral stator stalk subunits E and G. J. Biol. Chem. **285:**24654–24664. http://dx.doi.org/10.1074/jbc.M110.136960.
32. **Su Y, Zhou A, Al-Lamki RS, Karet FE.** 2003. The a-subunit of the V-type H_+-ATPase interacts with phosphofructokinase-1 in humans. J. Biol. Chem. **278:**20013–20018. http://dx.doi.org/10.1074/jbc.M210077200.
33. **Peters C, Bayer MJ, Buhler S, Andersen JS, Mann M, Mayer A.** 2001. Trans-complex formation by proteolipid channels in the terminal phase of membrane fusion. Nature **409:**581–588. http://dx.doi.org/10.1038/35054500.
34. **Lu M, Holliday LS, Zhang L, Dunn WA, Jr, Gluck SL.** 2001. Interaction between aldolase and vacuolar H^+-ATPase: evidence for direct coupling of glycolysis to the ATP-hydrolyzing proton pump. J. Biol. Chem. **276:**30407–30413. http://dx.doi.org/10.1074/jbc.M008768200.
35. **Kane PM.** 2006. The where, when, and how of organelle acidification by the yeast vacuolar H^+-ATPase. Microbiol. Mol. Biol. Rev. **70:**177–191. http://dx.doi.org/10.1128/MMBR.70.1.177-191.2006.
36. **Kane PM.** 2012. Targeting reversible disassembly as a mechanism of controlling V-ATPase activity. Curr. Protein Peptide Sci. **13:**117–123. http://dx.doi.org/10.2174/138920312800493142.
37. **Konishi H, Yamane H, Maeshima M, Komatsu S.** 2004. Characterization of fructose-bisphosphate aldolase regulated by gibberellin in roots of rice seedling. Plant Mol. Biol. **56:**839–848. http://dx.doi.org/10.1007/s11103-004-5920-2.
38. **Merkulova M, Hurtado-Lorenzo A, Hosokawa H, Zhuang Z, Brown D, Ausiello DA, Marshansky V.** 2011. Aldolase directly interacts with ARNO and modulates cell morphology and acidic vesicle distribution. Am. J. Physiol. Cell Physiol. **300:**C1442–C1455. http://dx.doi.org/10.1152/ajpcell.00076.2010.
39. **Nakamura S.** 2004. Glucose activates H(+)-ATPase in kidney epithelial cells. Am. J. Physiol. Cell Physiol. **287:**C97–C105. http://dx.doi.org/10.1152/ajpcell.00469.2003.
40. **Kohio HP, Adamson AL.** 2013. Glycolytic control of vacuolar-type ATPase activity: a mechanism to regulate influenza viral infection. Virology **444:**301–309. http://dx.doi.org/10.1016/j.virol.2013.06.026.
41. **Fogarty FM, O'Keeffe J, Zhadanov A, Papkovsky D, Ayllon V, O'Connor R.** 21 October 2013. HRG-1 enhances cancer cell invasive potential and couples glucose metabolism to cytosolic/extracellular pH gradient regulation by the vacuolar-H ATPase. Oncogene http://dx.doi.org/10.1038/onc.2013.403.
42. **Avnet S, Di Pompo G, Lemma S, Salerno M, Perut F, Bonuccelli G, Granchi D, Zini N, Baldini N.** 2013. V-ATPase is a candidate therapeutic target for Ewing sarcoma. Biochim. Biophys. Acta **1832:**1105–1116. http://dx.doi.org/10.1016/j.bbadis.2013.04.003.
43. **Lu M, Sautin YY, Holliday LS, Gluck SL.** 2004. The glycolytic enzyme aldolase mediates assembly, expression, and activity of vacuolar H+-ATPase. J. Biol. Chem. **279:**8732–8739. http://dx.doi.org/10.1074/jbc.M303871200.
44. **Ikemoto A, Bole DG, Ueda T.** 2003. Glycolysis and glutamate accumulation into synaptic vesicles. Role of glyceraldehyde phosphate dehydrogenase and 3-phosphoglycerate kinase. J. Biol. Chem. **278:**5929–5940. http://dx.doi.org/10.1074/jbc.M211617200.
45. **Shao E, Forgac M.** 2004. Involvement of the nonhomologous region of subunit A of the yeast V-ATPase in coupling and in vivo dissociation. J. Biol. Chem. **279:**48663–48670. http://dx.doi.org/10.1074/jbc.M408278200.
46. **Seol JH, Shevchenko A, Shevchenko A, Deshaies RJ.** 2001. Skp1 forms multiple protein complexes, including RAVE, a regulator of V-ATPase assembly. Nat. Cell Biol. **3:**384–391. http://dx.doi.org/10.1038/35070067.
47. **Smardon AM, Tarsio M, Kane PM.** 2002. The RAVE complex is essential for stable assembly of the yeast V-ATPase. J. Biol. Chem. **277:**13831–13839. http://dx.doi.org/10.1074/jbc.M200682200.
48. **Smardon AM, Kane PM.** 2007. RAVE is essential for the efficient assembly of the C subunit with the vacuolar H(+)-ATPase. J. Biol. Chem. **282:**26185–26194. http://dx.doi.org/10.1074/jbc.M703627200.
49. **Hirata R, Umemoto N, Ho MN, Ohya Y, Stevens TH, Anraku Y.** 1993. VMA12 is essential for assembly of the vacuolar H(+)-ATPase subunits onto the vacuolar membrane in Saccharomyces cerevisiae. J. Biol. Chem. **268:**961–967.
50. **Hill KJ, Stevens TH.** 1994. Vma21p is a yeast membrane protein retained in the endoplasmic reticulum by a di-lysine motif and is required for the assembly of the vacuolar H(+)-ATPase complex. Mol. Biol. Cell **5:**1039–1050. http://dx.doi.org/10.1091/mbc.5.9.1039.
51. **Hill KJ, Stevens TH.** 1995. Vma22p is a novel endoplasmic reticulum-associated protein required for assembly of the yeast vacuolar H(+)-ATPase complex. J. Biol. Chem. **270:**22329–22336. http://dx.doi.org/10.1074/jbc.270.38.22329.
52. **Ryan M, Graham LA, Stevens TH.** 2008. Voa1p functions in V-ATPase assembly in the yeast endoplasmic reticulum. Mol. Biol. Cell **19:**5131–5142. http://dx.doi.org/10.1091/mbc.E08-06-0629.
53. **Malkus P, Graham LA, Stevens TH, Schekman R.** 2004. Role of Vma21p in assembly and transport of the yeast vacuolar ATPase. Mol. Biol. Cell **15:**5075–5091. http://dx.doi.org/10.1091/mbc.E04-06-0514.
54. **Davis-Kaplan SR, Compton MA, Flannery AR, Ward DM, Kaplan J, Stevens TH, Graham LA.** 2006. PKR1 encodes an assembly factor for the yeast V-type ATPase. J. Biol. Chem. **281:**32025–32035. http://dx.doi.org/10.1074/jbc.M606451200.
55. **Kane PM, Tarsio M, Liu J.** 1999. Early steps in assembly of the yeast vacuolar H^+-ATPase. J. Biol. Chem. **274:**17275–17283. http://dx.doi.org/10.1074/jbc.274.24.17275.
56. **Manolson MF, Proteau D, Preston RA, Stenbit A, Roberts BT, Hoyt MA, Preuss D, Mulholland J, Botstein D, Jones EW.** 1992. The VPH1 gene encodes a 95-kDa integral membrane polypeptide required for in vivo assembly and activity of the yeast vacuolar H(+)-ATPase. J. Biol. Chem. **267:**14294–14303.
57. **Manolson MF, Wu B, Proteau D, Taillon BE, Roberts BT, Hoyt MA, Jones EW.** 1994. STV1 gene encodes functional homologue of 95-kDa yeast vacuolar H(+)-ATPase subunit Vph1p. J. Biol. Chem. **269:**14064–14074.
58. **Finnigan GC, Cronan GE, Park HJ, Srinivasan S, Quiocho FA, Stevens TH.** 2012. Sorting of the yeast vacuolar-type, proton-translocating ATPase enzyme complex (V-ATPase): identification of a necessary and sufficient Golgi/endosomal retention signal in Stv1p. J. Biol. Chem. **287:**19487–19500. http://dx.doi.org/10.1074/jbc.M112.343814.
59. **Coonrod EM, Stevens TH.** 2010. The yeast vps class E mutants: the beginning of the molecular genetic analysis of multivesicular body biogenesis. Mol. Biol. Cell **21:**4057–4060. http://dx.doi.org/10.1091/mbc.E09-07-0603.
60. **Kawasaki-Nishi S, Nishi T, Forgac M.** 2001. Yeast V-ATPase complexes containing different isoforms of the 100-kDa a-subunit differ in coupling efficiency and in vivo dissociation. J. Biol. Chem. **276:**17941–17948. http://dx.doi.org/10.1074/jbc.M010790200.
61. **Yan Y, Denef N, Schupbach T.** 2009. The vacuolar proton pump, V-ATPase, is required for notch signaling and endosomal trafficking in Drosophila. Dev. Cell **17:**387–402. http://dx.doi.org/10.1016/j.devcel.2009.07.001.
62. **Einhorn Z, Trapani JG, Liu Q, Nicolson T.** 2012. Rabconnectin3alpha promotes stable activity of the H+ pump on synaptic vesicles in hair cells.

J. Neurosci. **32:**11144–11156. http://dx.doi.org/10.1523/JNEUROSCI.1705-12.2012.
63. **Sethi N, Yan Y, Quek D, Schupbach T, Kang Y.** 2010. Rabconnectin-3 is a functional regulator of mammalian Notch signaling. J. Biol. Chem. **285:**34757–34764. http://dx.doi.org/10.1074/jbc.M110.158634.
64. **Toei M, Saum R, Forgac M.** 2010. Regulation and isoform function of the V-ATPases. Biochemistry **49:**4715–4723. http://dx.doi.org/10.1021/bi100397s.
65. **Hayek SR, Lee SA, Parra KJ.** 2014. Advances in targeting the vacuolar proton-translocating ATPase (V-ATPase) for anti-fungal therapy. Front. Pharmacol. **5:**4. http://dx.doi.org/10.3389/fphar.2014.00004.
66. **Raines SM, Rane HS, Bernardo SM, Binder JL, Lee SA, Parra KJ.** 2013. Deletion of vacuolar proton-translocating ATPase V(o)a isoforms clarifies the role of vacuolar pH as a determinant of virulence-associated traits in Candida albicans. J. Biol. Chem. **288:**6190–6201. http://dx.doi.org/10.1074/jbc.M112.426197.
67. **Rane HS, Bernardo SM, Raines SM, Binder JL, Parra KJ, Lee SA.** 2013. Candida albicans VMA3 is necessary for V-ATPase assembly and function and contributes to secretion and filamentation. Eukaryot. Cell **12:**1369–1382. http://dx.doi.org/10.1128/EC.00118-13.
68. **Patenaude C, Zhang Y, Cormack B, Kohler J, Rao R.** 2013. Essential role for vacuolar acidification in Candida albicans virulence. J. Biol. Chem. **288:**26256–26264. http://dx.doi.org/10.1074/jbc.M113.494815.
69. **Zhang YQ, Gamarra S, Garcia-Effron G, Park S, Perlin DS, Rao R.** 2010. Requirement for ergosterol in V-ATPase function underlies antifungal activity of azole drugs. PLoS Pathog. **6:**e1000939. http://dx.doi.org/10.1371/journal.ppat.1000939.
70. **Zhang YQ, Rao R.** 2010. Beyond ergosterol: linking pH to antifungal mechanisms. Virulence **1:**551–554. http://dx.doi.org/10.4161/viru.1.6.13802.
71. **Schachtschabel D, Arentshorst M, Lagendijk EL, Ram AF.** 2012. Vacuolar H(+)-ATPase plays a key role in cell wall biosynthesis of Aspergillus niger. Fungal Genet. Biol. **49:**284–293. http://dx.doi.org/10.1016/j.fgb.2011.12.008.
72. **Parra KJ.** 2012. Vacuolar ATPase (V-ATPase): a model proton pump for antifungal drug discovery, p 89–100. *In* Tegos G, Mylonakis E (ed), Antimicrobial drug discovery. Emerging strategies. Advances in molecular and cellular microbiology. CABI, Wallingford, Oxfordshire, United Kingdom.
73. **Parra KJ, Kane PM.** 1996. Wild-type and mutant vacuolar membranes support pH-dependent reassembly of the yeast vacuolar H^+-ATPase in vitro. J. Biol. Chem. **271:**19592–19598. http://dx.doi.org/10.1074/jbc.271.32.19592.
74. **Tomashek JJ, Garrison BS, Klionsky DJ.** 1997. Reconstitution in vitro of the V1 complex from the yeast vacuolar proton-translocating ATPase. Assembly recapitulates mechanism. J. Biol. Chem. **272:**16618–16623.
75. **Imamura H, Funamoto S, Yoshida M, Yokoyama K.** 2006. Reconstitution in vitro of V1 complex of Thermus thermophilus V-ATPase revealed that ATP binding to the A subunit is crucial for V1 formation. J. Biol. Chem. **281:**38582–38591. http://dx.doi.org/10.1074/jbc.M608253200.
76. **Okamoto-Terry H, Umeki K, Nakanishi-Matsui M, Futai M.** 2013. Glu-44 in the amino-terminal alpha-helix of yeast vacuolar ATPase E subunit (Vma4p) has a role for VoV1 assembly. J. Biol. Chem. **288:**36236–36243. http://dx.doi.org/10.1074/jbc.M113.506741.
77. **Owegi MA, Carenbauer AL, Wick NM, Brown JF, Terhune KL, Bilbo SA, Weaver RS, Shircliff R, Newcomb N, Parra-Belky KJ.** 2005. Mutational analysis of the stator subunit E of the yeast V-ATPase. J. Biol. Chem. **280:**18393–18402. http://dx.doi.org/10.1074/jbc.M412567200.
78. **Shao E, Nishi T, Kawasaki-Nishi S, Forgac M.** 2003. Mutational analysis of the non-homologous region of subunit A of the yeast V-ATPase. J. Biol. Chem. **278:**12985–12991. http://dx.doi.org/10.1074/jbc.M212096200.
79. **Charsky CM, Schumann NJ, Kane PM.** 2000. Mutational analysis of subunit G (Vma10p) of the yeast vacuolar H^+-ATPase. J. Biol. Chem. **275:**37232–37239. http://dx.doi.org/10.1074/jbc.M006640200.
80. **Rizzo JM, Tarsio M, Martinez-Munoz GA, Kane PM.** 2007. Diploids heterozygous for a vma13Delta mutation in Saccharomyces cerevisiae highlight the importance of V-ATPase subunit balance in supporting vacuolar acidification and silencing cytosolic V1-ATPase activity. J. Biol. Chem. **282:**8521–8532. http://dx.doi.org/10.1074/jbc.M607092200.
81. **Smets B, Ghillebert R, De Snijder P, Binda M, Swinnen E, De Virgilio C, Winderickx J.** 2010. Life in the midst of scarcity: adaptations to nutrient availability in Saccharomyces cerevisiae. Curr. Genet. **56:**1–32. http://dx.doi.org/10.1007/s00294-009-0287-1.
82. **Orij R, Urbanus ML, Vizeacoumar FJ, Giaever G, Boone C, Nislow C, Brul S, Smits GJ.** 2012. Genome-wide analysis of intracellular pH reveals quantitative control of cell division rate by pH(c) in Saccharomyces cerevisiae. Genome Biol. **13:**R80. http://dx.doi.org/10.1186/gb-2012-13-9-r80.
83. **Martinez-Munoz GA, Kane P.** 2008. Vacuolar and plasma membrane proton pumps collaborate to achieve cytosolic pH homeostasis in yeast. J. Biol. Chem. **283:**20309–20319. http://dx.doi.org/10.1074/jbc.M710470200.
84. **Rao R, Slayman CW.** 1993. Mutagenesis of conserved residues in the phosphorylation domain of the yeast plasma membrane H(+)-ATPase. Effects on structure and function. J. Biol. Chem. **268:**6708–6713.
85. **Blank LM, Sauer U.** 2004. TCA cycle activity in Saccharomyces cerevisiae is a function of the environmentally determined specific growth and glucose uptake rates. Microbiology **150:**1085–1093. http://dx.doi.org/10.1099/mic.0.26845-0.
86. **Diakov TT, Kane PM.** 2010. Regulation of vacuolar proton-translocating ATPase activity and assembly by extracellular pH. J. Biol. Chem. **285:**23771–23778. http://dx.doi.org/10.1074/jbc.M110.110122.
87. **Biswas S, Van Dijck P, Datta A.** 2007. Environmental sensing and signal transduction pathways regulating morphopathogenic determinants of *Candida albicans*. Microbiol. Mol. Biol. Rev. **71:**348–376. http://dx.doi.org/10.1128/MMBR.00009-06.
88. **Li SC, Kane PM.** 2009. The yeast lysosome-like vacuole: endpoint and crossroads. Biochim. Biophys. Acta **1793:**650–663. http://dx.doi.org/10.1016/j.bbamcr.2008.08.003.
89. **Li SC, Diakov TT, Rizzo JM, Kane PM.** 2012. Vacuolar H^+-ATPase works in parallel with the HOG pathway to adapt Saccharomyces cerevisiae cells to osmotic stress. Eukaryot. Cell **11:**282–291. http://dx.doi.org/10.1128/EC.05198-11.

Chapter VI

References

6. References

Alzamora, R., R. F. Thali, et al. (2010). "PKA regulates vacuolar H+-ATPase localization and activity via direct phosphorylation of the a subunit in kidney cells." J Biol Chem **285**(32): 24676-24685.

Ambesi, A., M. Miranda, et al. (2000). "Biogenesis and function of the yeast plasma-membrane H(+)-ATPase." J Exp Biol **203**(Pt 1): 155-160.

Arai, H., S. Pink, et al. (1989). "Interaction of anions and ATP with the coated vesicle proton pump." Biochemistry **28**(7): 3075-3082.

Arvanitidis, A. and J. J. Heinisch (1994). "Studies on the function of yeast phosphofructokinase subunits by in vitro mutagenesis." J Biol Chem **269**(12): 8911-8918.

Avnet, S., G. Di Pompo, et al. (2013). "V-ATPase is a candidate therapeutic target for Ewing sarcoma." Biochim Biophys Acta **1832**(8): 1105-1116.

Banaszak, K., I. Mechin, et al. (2011). "The crystal structures of eukaryotic phosphofructokinases from baker's yeast and rabbit skeletal muscle." J Mol Biol **407**(2): 284-297.

Bauerle, C., M. N. Ho, et al. (1993). "The Saccharomyces cerevisiae VMA6 gene encodes the 36-kDa subunit of the vacuolar H(+)-ATPase membrane sector." J Biol Chem **268**(17): 12749-12757.

Blander, J. M. and R. Medzhitov (2006). "On regulation of phagosome maturation and antigen presentation." Nat Immunol **7**(10): 1029-1035.

Bond, S. and M. Forgac (2008). "The Ras/cAMP/protein kinase A pathway regulates glucose-dependent assembly of the vacuolar (H+)-ATPase in yeast." J Biol Chem **283**(52): 36513-36521.

Bradford, M. M. (1976). "A rapid and sensitive method for the quantitation of microgram quantities of protein utilizing the principle of protein-dye binding." Anal Biochem **72**: 248-254.

Breton, S. and D. Brown (2007). "New insights into the regulation of V-ATPase-dependent proton secretion." Am J Physiol Renal Physiol **292**(1): F1-10.

Breton, S. and D. Brown (2013). "Regulation of luminal acidification by the V-ATPase." Physiology (Bethesda) **28**(5): 318-329.

Brett, C. L., D. N. Tukaye, et al. (2005). "The yeast endosomal Na+K+/H+ exchanger Nhx1 regulates cellular pH to control vesicle trafficking." Mol Biol Cell **16**(3): 1396-1405.

Brown, D. and S. Breton (2000). "H(+)V-ATPase-dependent luminal acidification in the kidney collecting duct and the epididymis/vas deferens: vesicle recycling and transcytotic pathways." J Exp Biol **203**(Pt 1): 137-145.

Chan, C. Y. and K. J. Parra (2014). "Yeast Phosphofructokinase-1 Subunit Pfk2p is Necessary for pH Homeostasis and Glucose-Dependent V-ATPase Reassembly." J Biol Chem.

Chan, C. Y., C. Prudom, et al. (2012). "Inhibitors of V-ATPase proton transport reveal uncoupling functions of tether linking cytosolic and membrane domains of V0 subunit a (Vph1p)." J Biol Chem **287**(13): 10236-10250.

DeCamilli, P., S. D. Emr, et al. (1996). "Phosphoinositides as regulators in membrane traffic." Science **271**(5255): 1533-1539.

Dechant, R., M. Binda, et al. (2010). "Cytosolic pH is a second messenger for glucose and regulates the PKA pathway through V-ATPase." EMBO J **29**(15): 2515-2526.
Dechant, R. and M. Peter (2011). "The N-terminal domain of the V-ATPase subunit 'a' is regulated by pH in vitro and in vivo." Channels (Austin) **5**(1): 4-8.
Dhar-Chowdhury, P., M. D. Harrell, et al. (2005). "The glycolytic enzymes, glyceraldehyde-3-phosphate dehydrogenase, triose-phosphate isomerase, and pyruvate kinase are components of the K(ATP) channel macromolecular complex and regulate its function." J Biol Chem **280**(46): 38464-38470.
Diakov, T. T. and P. M. Kane (2010). "Regulation of vacuolar proton-translocating ATPase activity and assembly by extracellular pH." J Biol Chem **285**(31): 23771-23778.
Doherty, R. D. and P. M. Kane (1993). "Partial assembly of the yeast vacuolar H(+)-ATPase in mutants lacking one subunit of the enzyme." J Biol Chem **268**(22): 16845-16851.
Drory, O., F. Frolow, et al. (2004). "Crystal structure of yeast V-ATPase subunit C reveals its stator function." EMBO Rep **5**(12): 1148-1152.
Ediger, B., S. D. Melman, et al. (2009). "The tether connecting cytosolic (N terminus) and membrane (C terminus) domains of yeast V-ATPase subunit a (Vph1) is required for assembly of V0 subunit d." J Biol Chem **284**(29): 19522-19532.
Efeyan, A., R. Zoncu, et al. (2012). "Amino acids and mTORC1: from lysosomes to disease." Trends Mol Med **18**(9): 524-533.
Elble, R. (1992). "A simple and efficient procedure for transformation of yeasts." Biotechniques **13**(1): 18-20.
Estruch, F. (2000). "Stress-controlled transcription factors, stress-induced genes and stress tolerance in budding yeast." FEMS Microbiol Rev **24**(4): 469-486.
Fan, S., Y. Niu, et al. (2012). "LASS2 enhances chemosensitivity of breast cancer by counteracting acidic tumor microenvironment through inhibiting activity of V-ATPase proton pump." Oncogene.
Farooqui, J., S. Kim, et al. (1980). "In vivo studies on yeast cytochrome c methylation in relation to protein synthesis." J Biol Chem **255**(10): 4468-4473.
Feng, Y. and M. Forgac (1992). "Cysteine 254 of the 73-kDa A subunit is responsible for inhibition of the coated vesicle (H+)-ATPase upon modification by sulfhydryl reagents." J Biol Chem **267**(9): 5817-5822.
Feng, Y. and M. Forgac (1992). "A novel mechanism for regulation of vacuolar acidification." J Biol Chem **267**(28): 19769-19772.
Feng, Y. and M. Forgac (1994). "Inhibition of vacuolar H(+)-ATPase by disulfide bond formation between cysteine 254 and cysteine 532 in subunit A." J Biol Chem **269**(18): 13224-13230.
Fogarty, F. M., J. O'Keeffe, et al. (2013). "HRG-1 enhances cancer cell invasive potential and couples glucose metabolism to cytosolic/extracellular pH gradient regulation by the vacuolar-H ATPase." Oncogene.
Forgac, M. (2007). "Vacuolar ATPases: rotary proton pumps in physiology and pathophysiology." Nat Rev Mol Cell Biol **8**(11): 917-929.
Forgac, M., L. Cantley, et al. (1983). "Clathrin-coated vesicles contain an ATP-dependent proton pump." Proc Natl Acad Sci U S A **80**(5): 1300-1303.

Garcia-Arranz, M., A. M. Maldonado, et al. (1994). "Transcriptional control of yeast plasma membrane H(+)-ATPase by glucose. Cloning and characterization of a new gene involved in this regulation." J Biol Chem **269**(27): 18076-18082.
Garcia-Garcia, A., M. Perez-Sayans Garcia, et al. (2012). "Immunohistochemical localization of C1 subunit of V-ATPase (ATPase C1) in oral squamous cell cancer and normal oral mucosa." Biotech Histochem **87**(2): 133-139.
Gruber, G., M. Radermacher, et al. (2000). "Three-dimensional structure and subunit topology of the V(1) ATPase from Manduca sexta midgut." Biochemistry **39**(29): 8609-8616.
Hayek, S. R., S. A. Lee, et al. (2014). "Advances in targeting the vacuolar proton-translocating ATPase (V-ATPase) for anti-fungal therapy." Front Pharmacol **5**: 4.
Heinisch, J. (1986). "Construction and physiological characterization of mutants disrupted in the phosphofructokinase genes of Saccharomyces cerevisiae." Curr Genet **11**(3): 227-234.
Heinisch, J. (1986). "Isolation and characterization of the two structural genes coding for phosphofructokinase in yeast." Mol Gen Genet **202**(1): 75-82.
Hinton, A., S. Bond, et al. (2009). "V-ATPase functions in normal and disease processes." Pflugers Arch **457**(3): 589-598.
Hsu, S. C. and R. S. Molday (1991). "Glycolytic enzymes and a GLUT-1 glucose transporter in the outer segments of rod and cone photoreceptor cells." J Biol Chem **266**(32): 21745-21752.
Huang, C. G., K. H. Tsai, et al. (2006). "Intestinal expression of H+ V-ATPase in the mosquito Aedes albopictus is tightly associated with gregarine infection." J Eukaryot Microbiol **53**(2): 127-135.
Hughes, A. L. and D. E. Gottschling (2012). "An early age increase in vacuolar pH limits mitochondrial function and lifespan in yeast." Nature **492**(7428): 261-265.
Ikemoto, A., D. G. Bole, et al. (2003). "Glycolysis and glutamate accumulation into synaptic vesicles. Role of glyceraldehyde phosphate dehydrogenase and 3-phosphoglycerate kinase." J Biol Chem **278**(8): 5929-5940.
Inoue, T. and M. Forgac (2005). "Cysteine-mediated cross-linking indicates that subunit C of the V-ATPase is in close proximity to subunits E and G of the V1 domain and subunit a of the V0 domain." J Biol Chem **280**(30): 27896-27903.
Jefferies, K. C. and M. Forgac (2008). "Subunit H of the vacuolar (H+) ATPase inhibits ATP hydrolysis by the free V1 domain by interaction with the rotary subunit F." J Biol Chem **283**(8): 4512-4519.
Jewell, J. L., R. C. Russell, et al. (2013). "Amino acid signalling upstream of mTOR." Nat Rev Mol Cell Biol **14**(3): 133-139.
Johnson, R. M., C. Allen, et al. (2010). "Identification of inhibitors of vacuolar proton-translocating ATPase pumps in yeast by high-throughput screening flow cytometry." Anal Biochem **398**(2): 203-211.
Kane, P. M. (1995). "Disassembly and reassembly of the yeast vacuolar H(+)-ATPase in vivo." J Biol Chem **270**(28): 17025-17032.
Kane, P. M. (2006). "The where, when, and how of organelle acidification by the yeast vacuolar H+-ATPase." Microbiol Mol Biol Rev **70**(1): 177-191.
Kane, P. M. (2012). "Targeting Reversible Disassembly as a Mechanism of Controlling V-ATPase Activity." Curr Protein Pept Sci **13**(2): 117-123.

Kane, P. M. and K. J. Parra (2000). "Assembly and regulation of the yeast vacuolar H(+)-ATPase." J Exp Biol **203**(Pt 1): 81-87.
Kane, P. M. and A. M. Smardon (2003). "Assembly and regulation of the yeast vacuolar H+-ATPase." J Bioenerg Biomembr **35**(4): 313-321.
Kawasaki-Nishi, S., T. Nishi, et al. (2001). "Yeast V-ATPase complexes containing different isoforms of the 100-kDa a-subunit differ in coupling efficiency and in vivo dissociation." J Biol Chem **276**(21): 17941-17948.
Keenan Curtis, K. and P. M. Kane (2002). "Novel vacuolar H+-ATPase complexes resulting from overproduction of Vma5p and Vma13p." J Biol Chem **277**(4): 2716-2724.
Klinder, A., J. Kirchberger, et al. (1998). "Assembly of phosphofructokinase-1 from Saccharomyces cerevisiae in extracts of single-deletion mutants." Yeast **14**(4): 323-334.
Kohio, H. P. and A. L. Adamson (2013). "Glycolytic control of vacuolar-type ATPase activity: a mechanism to regulate influenza viral infection." Virology **444**(1-2): 301-309.
Konishi, H., H. Yamane, et al. (2004). "Characterization of fructose-bisphosphate aldolase regulated by gibberellin in roots of rice seedling." Plant Mol Biol **56**(6): 839-848.
Kubisch, R., T. Frohlich, et al. (2014). "V-ATPase inhibition by archazolid leads to lysosomal dysfunction resulting in impaired cathepsin B activation in vivo." Int J Cancer **134**(10): 2478-2488.
Lau, W. C. and J. L. Rubinstein (2010). "Structure of intact Thermus thermophilus V-ATPase by cryo-EM reveals organization of the membrane-bound V(O) motor." Proc Natl Acad Sci U S A **107**(4): 1367-1372.
Lecchi, S., C. J. Nelson, et al. (2007). "Tandem phosphorylation of Ser-911 and Thr-912 at the C terminus of yeast plasma membrane H+-ATPase leads to glucose-dependent activation." J Biol Chem **282**(49): 35471-35481.
Lee, M. R., G. H. Lee, et al. (2014). "BAX inhibitor-1-associated V-ATPase glycosylation enhances collagen degradation in pulmonary fibrosis." Cell Death Dis **5**: e1113.
Leskovac, V., S. Trivic, et al. (2002). "The three zinc-containing alcohol dehydrogenases from baker's yeast, Saccharomyces cerevisiae." FEMS Yeast Res **2**(4): 481-494.
Li, S. C., T. T. Diakov, et al. (2012). "Vacuolar H+-ATPase works in parallel with the HOG pathway to adapt Saccharomyces cerevisiae cells to osmotic stress." Eukaryot Cell **11**(3): 282-291.
Li, S. C., T. T. Diakov, et al. (2014). "The signaling lipid PI(3,5)P2 stabilizes V1-Vo sector interactions and activates the V-ATPase." Mol Biol Cell **25**(8): 1251-1262.
Liberman, R., S. Bond, et al. (2014). "Regulated Assembly of Vacuolar ATPase Is Increased during Cluster Disruption-induced Maturation of Dendritic Cells through a Phosphatidylinositol 3-Kinase/mTOR-dependent Pathway." J Biol Chem **289**(3): 1355-1363.
Lu, M., D. Ammar, et al. (2007). "Physical interaction between aldolase and vacuolar H+-ATPase is essential for the assembly and activity of the proton pump." J Biol Chem **282**(34): 24495-24503.

Lu, M., L. S. Holliday, et al. (2001). "Interaction between aldolase and vacuolar H+-ATPase: evidence for direct coupling of glycolysis to the ATP-hydrolyzing proton pump." J Biol Chem **276**(32): 30407-30413.
Lu, M., Y. Y. Sautin, et al. (2004). "The glycolytic enzyme aldolase mediates assembly, expression, and activity of vacuolar H+-ATPase." J Biol Chem **279**(10): 8732-8739.
MacLeod, K. J., E. Vasilyeva, et al. (1999). "Photoaffinity labeling of wild-type and mutant forms of the yeast V-ATPase A subunit by 2-azido-[(32)P]ADP." J Biol Chem **274**(46): 32869-32874.
Martinez-Munoz, G. A. and P. Kane (2008). "Vacuolar and plasma membrane proton pumps collaborate to achieve cytosolic pH homeostasis in yeast." J Biol Chem **283**(29): 20309-20319.
Merkulova, M., A. Hurtado-Lorenzo, et al. (2011). "Aldolase directly interacts with ARNO and modulates cell morphology and acidic vesicle distribution." Am J Physiol Cell Physiol **300**(6): C1442-1455.
Michel, V., Y. Licon-Munoz, et al. (2013). "Inhibitors of vacuolar ATPase proton pumps inhibit human prostate cancer cell invasion and prostate-specific antigen expression and secretion." Int J Cancer **132**(2): E1-10.
Mijaljica, D., M. Prescott, et al. (2011). "V-ATPase engagement in autophagic processes." Autophagy **7**(6): 666-668.
Moriyama, Y. and N. Nelson (1988). "The vacuolar H+-ATPase, a proton pump controlled by a slip." Prog Clin Biol Res **273**: 387-394.
Morsomme, P., C. W. Slayman, et al. (2000). "Mutagenic study of the structure, function and biogenesis of the yeast plasma membrane H(+)-ATPase." Biochim Biophys Acta **1469**(3): 133-157.
Muench, S. P., J. Trinick, et al. (2011). "Structural divergence of the rotary ATPases." Q Rev Biophys **44**(3): 311-356.
Muller, M. L., M. Jensen, et al. (1999). "The vacuolar H+-ATPase of lemon fruits is regulated by variable H+/ATP coupling and slip." J Biol Chem **274**(16): 10706-10716.
Muller, M. L. and L. Taiz (2002). "Regulation of the lemon-fruit V-ATPase by variable stoichiometry and organic acids." J Membr Biol **185**(3): 209-220.
Muller, S., F. K. Zimmermann, et al. (1997). "Mutant studies of phosphofructo-2-kinases do not reveal an essential role of fructose-2,6-bisphosphate in the regulation of carbon fluxes in yeast cells." Microbiology **143 (Pt 9)**: 3055-3061.
Myers, M. and M. Forgac (1993). "Assembly of the peripheral domain of the bovine vacuolar H(+)-adenosine triphosphatase." J Cell Physiol **156**(1): 35-42.
Nakamura, S. (2004). "Glucose activates H(+)-ATPase in kidney epithelial cells." Am J Physiol Cell Physiol **287**(1): C97-105.
Nelson, H. and N. Nelson (1990). "Disruption of genes encoding subunits of yeast vacuolar H(+)-ATPase causes conditional lethality." Proc Natl Acad Sci U S A **87**(9): 3503-3507.
Nelson, N. (2003). "A journey from mammals to yeast with vacuolar H+-ATPase (V-ATPase)." J Bioenerg Biomembr **35**(4): 281-289.
Nishi, T. and M. Forgac (2002). "The vacuolar (H+)-ATPases--nature's most versatile proton pumps." Nat Rev Mol Cell Biol **3**(2): 94-103.

Norbeck, J. and A. Blomberg (2000). "The level of cAMP-dependent protein kinase A activity strongly affects osmotolerance and osmo-instigated gene expression changes in Saccharomyces cerevisiae." Yeast **16**(2): 121-137.
Ochotny, N., A. Van Vliet, et al. (2006). "Effects of human a3 and a4 mutations that result in osteopetrosis and distal renal tubular acidosis on yeast V-ATPase expression and activity." J Biol Chem **281**(36): 26102-26111.
Ohira, M., A. M. Smardon, et al. (2006). "The E and G subunits of the yeast V-ATPase interact tightly and are both present at more than one copy per V1 complex." J Biol Chem **281**(32): 22752-22760.
Ohya, Y., N. Umemoto, et al. (1991). "Calcium-sensitive cls mutants of Saccharomyces cerevisiae showing a Pet- phenotype are ascribable to defects of vacuolar membrane H(+)-ATPase activity." J Biol Chem **266**(21): 13971-13977.
Oluwatosin, Y. E. and P. M. Kane (1997). "Mutations in the CYS4 gene provide evidence for regulation of the yeast vacuolar H+-ATPase by oxidation and reduction in vivo." J Biol Chem **272**(44): 28149-28157.
Oot, R. A., L. S. Huang, et al. (2012). "Crystal structure of the yeast vacuolar ATPase heterotrimeric EGC(head) peripheral stalk complex." Structure **20**(11): 1881-1892.
Oot, R. A. and S. Wilkens (2010). "Domain characterization and interaction of the yeast vacuolar ATPase subunit C with the peripheral stator stalk subunits E and G." J Biol Chem **285**(32): 24654-24664.
Owegi, M. A., A. L. Carenbauer, et al. (2005). "Mutational analysis of the stator subunit E of the yeast V-ATPase." J Biol Chem **280**(18): 18393-18402.
Owegi, M. A., D. L. Pappas, et al. (2006). "Identification of a domain in the V0 subunit d that is critical for coupling of the yeast vacuolar proton-translocating ATPase." J Biol Chem **281**(40): 30001-30014.
Padilla-Lopez, S. and D. A. Pearce (2006). "Saccharomyces cerevisiae lacking Btn1p modulate vacuolar ATPase activity to regulate pH imbalance in the vacuole." J Biol Chem **281**(15): 10273-10280.
Parra, K., C. Y. Chan, et al. (2014). "Yeast V-ATPase Regulation by Disassembly and Re-Assembly: One Structure and Multiple Signals." Eukaryot Cell.
Parra, K. J. and P. M. Kane (1998). "Reversible association between the V1 and V0 domains of yeast vacuolar H+-ATPase is an unconventional glucose-induced effect." Mol Cell Biol **18**(12): 7064-7074.
Parra, K. J., K. L. Keenan, et al. (2000). "The H subunit (Vma13p) of the yeast V-ATPase inhibits the ATPase activity of cytosolic V1 complexes." J Biol Chem **275**(28): 21761-21767.
Perez-Sayans, M., J. M. Somoza-Martin, et al. (2009). "V-ATPase inhibitors and implication in cancer treatment." Cancer Treat Rev **35**(8): 707-713.
Peters, C., M. J. Bayer, et al. (2001). "Trans-complex formation by proteolipid channels in the terminal phase of membrane fusion." Nature **409**(6820): 581-588.
PM., K. (2006). "The where, when, and how of organelle acidification by the yeast vacuolar H+-ATPase." Microbiol Mol Biol Rev. **70**(1): 177-191.
Poulsen, A. K., A. Z. Andersen, et al. (2008). "Probing glycolytic and membrane potential oscillations in Saccharomyces cerevisiae." Biochemistry **47**(28): 7477-7484.

Qi, J. and M. Forgac (2008). "Function and subunit interactions of the N-terminal domain of subunit a (Vph1p) of the yeast V-ATPase." J Biol Chem **283**(28): 19274-19282.
Rane, H. S., S. M. Bernardo, et al. (2013). "Candida albicans VMA3 is necessary for V-ATPase assembly and function and contributes to secretion and filamentation." Eukaryot Cell **12**(10): 1369-1382.
Rao, R., D. Drummond-Barbosa, et al. (1993). "Transcriptional regulation by glucose of the yeast PMA1 gene encoding the plasma membrane H(+)-ATPase." Yeast **9**(10): 1075-1084.
Sambade, M. and P. M. Kane (2004). "The yeast vacuolar proton-translocating ATPase contains a subunit homologous to the Manduca sexta and bovine e subunits that is essential for function." J Biol Chem **279**(17): 17361-17365.
Santangelo, G. M. (2006). "Glucose signaling in Saccharomyces cerevisiae." Microbiol Mol Biol Rev **70**(1): 253-282.
Sautin, Y. Y., M. Lu, et al. (2005). "Phosphatidylinositol 3-kinase-mediated effects of glucose on vacuolar H+-ATPase assembly, translocation, and acidification of intracellular compartments in renal epithelial cells." Mol Cell Biol **25**(2): 575-589.
Schempp, C. M., K. von Schwarzenberg, et al. (2014). "V-ATPase Inhibition Regulates Anoikis Resistance and Metastasis of Cancer Cells." Mol Cancer Ther **13**(4): 926-937.
Schroder, T. D., V. C. Ozalp, et al. (2013). "An experimental study of the regulation of glycolytic oscillations in yeast." FEBS J **280**(23): 6033-6044.
Sennoune, S. R., K. Bakunts, et al. (2004). "Vacuolar H+-ATPase in human breast cancer cells with distinct metastatic potential: distribution and functional activity." Am J Physiol Cell Physiol **286**(6): C1443-1452.
Seol, J. H., A. Shevchenko, et al. (2001). "Skp1 forms multiple protein complexes, including RAVE, a regulator of V-ATPase assembly." Nat Cell Biol **3**(4): 384-391.
Seol, J. H., A. Shevchenko, et al. (2001). "Skp1 forms multiple protein complexes, including RAVE, a regulator of V-ATPase assembly." Nat Cell Biol **3**(4): 384-391.
Shao, E. and M. Forgac (2004). "Involvement of the nonhomologous region of subunit A of the yeast V-ATPase in coupling and in vivo dissociation." J Biol Chem **279**(47): 48663-48670.
Shao, E., T. Nishi, et al. (2003). "Mutational analysis of the non-homologous region of subunit A of the yeast V-ATPase." J Biol Chem **278**(15): 12985-12991.
Simonis, N., S. J. Wodak, et al. (2004). "Combining pattern discovery and discriminant analysis to predict gene co-regulation." Bioinformatics **20**(15): 2370-2379.
Smardon, A. M., H. I. Diab, et al. (2014). "The RAVE complex is an isoform-specific V-ATPase assembly factor in yeast." Mol Biol Cell **25**(3): 356-367.
Smardon, A. M. and P. M. Kane (2007). "RAVE is essential for the efficient assembly of the C subunit with the vacuolar H(+)-ATPase." J Biol Chem **282**(36): 26185-26194.
Smardon, A. M., M. Tarsio, et al. (2002). "The RAVE complex is essential for stable assembly of the yeast V-ATPase." J Biol Chem **277**(16): 13831-13839.
Sobacchi, C., A. Frattini, et al. (2001). "The mutational spectrum of human malignant autosomal recessive osteopetrosis." Hum Mol Genet **10**(17): 1767-1773.

Stehberger, P. A., N. Schulz, et al. (2003). "Localization and regulation of the ATP6V0A4 (a4) vacuolar H+-ATPase subunit defective in an inherited form of distal renal tubular acidosis." J Am Soc Nephrol **14**(12): 3027-3038.
Stewart, A. G. and D. Stock (2012). "Priming a molecular motor for disassembly." Structure **20**(11): 1799-1800.
Strahl, T. and J. Thorner (2007). "Synthesis and function of membrane phosphoinositides in budding yeast, Saccharomyces cerevisiae." Biochim Biophys Acta **1771**(3): 353-404.
Su, Y., K. G. Blake-Palmer, et al. (2008). "Human H+ATPase a4 subunit mutations causing renal tubular acidosis reveal a role for interaction with phosphofructokinase-1." Am J Physiol Renal Physiol **295**(4): F950-958.
Su, Y., A. Zhou, et al. (2003). "The a-subunit of the V-type H+-ATPase interacts with phosphofructokinase-1 in humans." J Biol Chem **278**(22): 20013-20018.
Sumner, J. P., J. A. Dow, et al. (1995). "Regulation of plasma membrane V-ATPase activity by dissociation of peripheral subunits." J Biol Chem **270**(10): 5649-5653.
Sun-Wada, G. H., Y. Wada, et al. (2003). "Vacuolar H+ pumping ATPases in luminal acidic organelles and extracellular compartments: common rotational mechanism and diverse physiological roles." J Bioenerg Biomembr **35**(4): 347-358.
Tarsio, M., H. Zheng, et al. (2011). "Consequences of loss of Vph1 protein-containing vacuolar ATPases (V-ATPases) for overall cellular pH homeostasis." J Biol Chem **286**(32): 28089-28096.
Thudium, C. S., V. K. Jensen, et al. (2012). "Disruption of the V-ATPase Functionality as a Way to Uncouple Bone Formation and Resorption - A Novel Target for Treatment of Osteoporosis." Curr Protein Pept Sci **13**(2): 141-151.
Tiburcy, F., K. W. Beyenbach, et al. (2013). "Protein kinase A-dependent and -independent activation of the V-ATPase in Malpighian tubules of Aedes aegypti." J Exp Biol **216**(Pt 5): 881-891.
Toei, M., C. Gerle, et al. (2007). "Dodecamer rotor ring defines H+/ATP ratio for ATP synthesis of prokaryotic V-ATPase from Thermus thermophilus." Proc Natl Acad Sci U S A **104**(51): 20256-20261.
Toei, M., R. Saum, et al. (2010). "Regulation and isoform function of the V-ATPases." Biochemistry **49**(23): 4715-4723.
Toyomura, T., Y. Murata, et al. (2003). "From lysosomes to the plasma membrane: localization of vacuolar-type H+ -ATPase with the a3 isoform during osteoclast differentiation." J Biol Chem **278**(24): 22023-22030.
Trombetta, E. S., M. Ebersold, et al. (2003). "Activation of lysosomal function during dendritic cell maturation." Science **299**(5611): 1400-1403.
Vasilyeva, E., Q. Liu, et al. (2000). "Cysteine scanning mutagenesis of the noncatalytic nucleotide binding site of the yeast V-ATPase." J Biol Chem **275**(1): 255-260.
von Schwarzenberg, K., T. Lajtos, et al. (2014). "V-ATPase inhibition overcomes trastuzumab resistance in breast cancer." Mol Oncol **8**(1): 9-19.
Voss, M., O. Vitavska, et al. (2007). "Stimulus-induced phosphorylation of vacuolar H(+)-ATPase by protein kinase A." J Biol Chem **282**(46): 33735-33742.
Wagner, C. A., K. E. Finberg, et al. (2004). "Renal vacuolar H+-ATPase." Physiol Rev **84**(4): 1263-1314.

Weisman, L. S. (2003). "Yeast vacuole inheritance and dynamics." Annu Rev Genet **37**: 435-460.
Weiss, J. N. and S. T. Lamp (1987). "Glycolysis preferentially inhibits ATP-sensitive K+ channels in isolated guinea pig cardiac myocytes." Science **238**(4823): 67-69.
Wick, A. N., D. R. Drury, et al. (1957). "Localization of the primary metabolic block produced by 2-deoxyglucose." J Biol Chem **224**(2): 963-969.
Wilkens, S. and M. Forgac (2001). "Three-dimensional structure of the vacuolar ATPase proton channel by electron microscopy." J Biol Chem **276**(47): 44064-44068.
Williamson, T., D. Adiamah, et al. (2012). "Exploring the genetic control of glycolytic oscillations in Saccharomyces cerevisiae." BMC Syst Biol **6**: 108.
Xu, T. and M. Forgac (2001). "Microtubules are involved in glucose-dependent dissociation of the yeast vacuolar [H+]-ATPase in vivo." J Biol Chem **276**(27): 24855-24861.
Yang, D. Q., S. Feng, et al. (2012). "V-ATPase subunit ATP6AP1 (Ac45) regulates osteoclast differentiation, extracellular acidification, lysosomal trafficking, and protease exocytosis in osteoclast-mediated bone resorption." J Bone Miner Res **27**(8): 1695-1707.
Yokoyama, K., M. Nakano, et al. (2003). "Rotation of the proteolipid ring in the V-ATPase." J Biol Chem **278**(27): 24255-24258.
Zhang, J., M. Myers, et al. (1992). "Characterization of the V0 domain of the coated vesicle (H+)-ATPase." J Biol Chem **267**(14): 9773-9778.
Zoncu, R., L. Bar-Peled, et al. (2011). "mTORC1 senses lysosomal amino acids through an inside-out mechanism that requires the vacuolar H(+)-ATPase." Science **334**(6056): 678-683.